VTT RESEARCH NOTES 2506

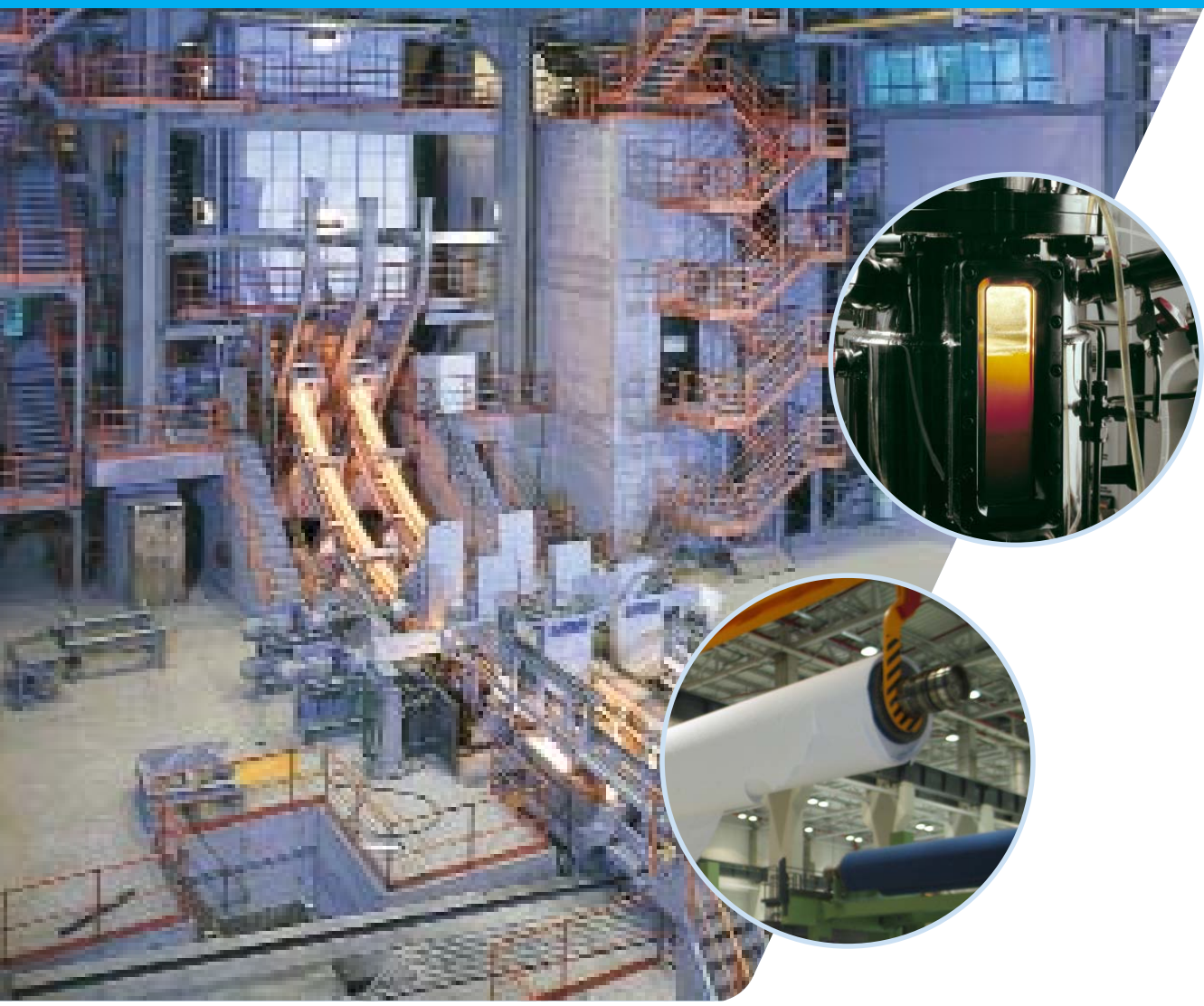

Pertti Koukkari (ed.)

Advanced Gibbs Energy Methods for Functional Materials and Processes

ChemSheet 1999–2009

VTT

VTT TIEDOTTEITA – RESEARCH NOTES 2506

Advanced Gibbs Energy Methods for Functional Materials and Processes

ChemSheet 1999–2009

Pertti Koukkari (ed.)

ISBN 978-951-38-7330-1 (soft back ed.)
ISSN 1235-0605 (soft back ed.)

ISBN 978-951-38-7331-8 (URL: http://www.vtt.fi/publications/index.jsp)
ISSN 1455-0865 (URL: http://www.vtt.fi/publications/index.jsp)

JULKAISIJA – UTGIVARE – PUBLISHER

VTT, Vuorimiehentie 5, PL 1000, 02044 VTT
puh. vaihde 020 722 111, faksi 020 722 4374

VTT, Bergsmansvägen 5, PB 1000, 02044 VTT
tel. växel 020 722 111, fax 020 722 4374

VTT Technical Research Centre of Finland, Vuorimiehentie 5, P.O. Box 1000, FI-02044 VTT, Finland
phone internat. +358 20 722 111, fax +358 20 722 4374

Text preparing Auli Rautakivi
Technical editing Mirjami Pullinen

Edita Prima Oy, Helsinki 2009

Pertti Koukkari (ed.). Advanced Gibbs Energy Methods for Functional Materials and Processes – ChemSheet 1999–2009. Espoo 2009. VTT Tiedotteita – Research Notes 2506. 146 p.

Keywords constrained Gibbs energy minimization, multi-phase systems, process simulation, reactor design, reaction rates, materials chemistry, fibre suspensions, surface energy, paraequilibrium, pathway energy diagrams

Abstract

ChemSheet is a thermochemical simulation tool, which combines the flexibility and practicality of spreadsheet operations with rigorous, multi-phase thermodynamic calculations. Customised applications are defined as independent worksheets in Excel® and simulations are run directly from the spreadsheet, taking advantage of its functional aspects and graphical features. A user-friendly dialog is available for model build-up.

ChemSheet was invented and published by VTT. It was commercialized in a joint venture with GTT Technologies GmbH of Herzogenrath, Germany. During the last decade, ChemSheet and its sister products have been adopted by both industrial users and active scientists worldwide. Due to the generic modelling principles based on Gibbs free energy minimization, the applications range from high temperature systems to biochemical analysis, including materials chemistry, corrosion, industrial reactor scale-up and process simulation. Practical models and expert systems have been developed e.g. in the chemical industry, pulp and paper, cement and lime manufacturing, metallurgy, steelmaking, power production and environmental technologies.

Within ChemSheet, the new Constrained Free Energy method allows immaterial constraints in the conservation matrix of the minimization problem, thereby enabling the association of constraint matrix properties with structural, physical, chemical or energetic attributes. Thus, the scope of free energy calculations can be extended well beyond the conventional studies of global chemical equilibria and phase diagrams. The most notable applications include surface and interfacial energies, electrochemical Donnan equilibria, calculation of paraequilibria and the introduction of mechanistic reaction kinetics to Gibbs'ian multiphase analysis. In biochemistry, the new method can be applied for efficient generation of energy diagrams for industrial production pathways within micro-organisms.

Preface

The computational approach with its ability to combine diverse quantitative methods to multi-disciplinary tools is a major trend in modern engineering science. This tendency has been particularly visible in the domain of chemical thermodynamics, which due to its systematic and quantitative structure is readily compliant with computer algorithms. The development has inspired experts throughout the world to innovate both new theory and practical applications to achieve new material and energy saving solutions.

VTT has become an active performer within the international community developing multiphase thermochemical simulation routines. The first multiphase algorithms for industrial process design were disclosed in 1995. ChemSheet was first announced in1999, and since then a number of both practical and scientific innovations have been developed and published. In 2007, the publication on the Constrained Free Energy method was given The 2006 Best Paper Award of the Calphad Journal[1].

The practical problems dealt with ChemSheet and its sister products range from the wet end of paper machines to inclusion control in the continuous casting of steel. Innovative expert systems have been developed both in academy and industry, the most recent example of the latter is SteaMax[2] for improved design of biofuel boilers. New application fields for the constrained free energy method are expected both in materials and interface science as well as in the analysis of biochemical pathways.

The development of ChemSheet applications has been an international joint venture, performed in close co-operation with many research colleagues and industrial customers both in Finland and abroad. ChemSheet was made to a

[1] Elsevier periodical: Computer Coupling of Phase Diagrams and Thermochemistry.
[2] SteaMax is a trademark of Metso Power Oyj.

commercial product by GTT Technologies GmbH of Germany already in 1999. Its joint marketing is further performed by VTT and GTT with active distributors e.g. in Japan and the U.S.

This booklet pursues to give a concise overview of Chemsheet and its related applications. It also serves as an acknowledgement to all contributors within this inspiring co-operation over the past ten years.

Contents

1. Advanced multiphase techniques open new frontiers for materials and process development

Pertti Koukkari, VTT

Development of functional materials and smart processes entails innovative links between physical, chemical and biological phenomena. The useful solution always benefits from such methods, which can bring together quantitative, interdisciplinary predictions of these topics. The thermodynamic free energy, commonly called the Gibbs energy, provides one such interdisciplinary concept. Particularly in macroscopic systems, where thermal, electrical or mechanical functions affect the chemical or biochemical phenomena, the Gibbs energy provides a general method to be applied for relationships between different properties. During the last decades, the thermodynamic science has united with advanced computational techniques, thus opening new frontiers to a wide field of applications.

The adaptation of the computational approach has created a completely new way of treating multicomponent and multi-phase problems in thermochemistry. The new opportunities offered by computers and data processing have encouraged both long-standing compilation of comprehensive databases and development of new thermodynamic algorithms. Concurrent thermodynamic databanks cover fields for many classes of substances ranging from organic and biochemical systems to various inorganic and metallurgical materials. The systematic data storage and management in connection with the increasing numerical capability of modern computers enables the treatment of the thermochemistry of complex systems as a whole. Thus, accurate theoretical studies of the phase stability and

equilibria of systems with a great number of chemical components can be made. Recent advancements also include introduction of such new algorithms, which facilitate modeling of time-dependent dynamic changes in multi-phase systems.

The thermodynamic research at VTT has been focused on developing such multiphase simulation routines which can be used for industrial applications. The first innovative solutions, such as the Ratemix® algorithm, which connects time dependent chemical reactions with equilibrium thermochemistry were developed and published in the 1990'ies. The Excel add-in program ChemSheet was introduced in 1999.

The basic feature of ChemSheet is that its user can work with multi-phase multi-component problems through the Microsoft Excel interface, familiar to engineers and scientists everywhere in the world. When developing applications, writing macro-code around the basic interface is helpful but for those who do not like programming, the custom made ChemSheet simulation model may appear as jus another spreadsheet file. ChemSheet was one pioneer of creating such a user-friendly interface to a scientific program, which since has become a must in the field.

Soon after its publication, ChemSheet was made to an international commercially available software by *GTT-Technologies* (Gesellschaft fur Technische Thermochemie und -physik mbH, Herzogenrath, Germany). The worldwide marketing of ChemSheet applications is organized jointly by VTT and GTT, the key additional partner being *RCCM* in Japan (Research Center of Calculational Mechanics, Tokyo). In the United States and Canada ChemSheet is represented by *The Spencer Group* (Trumansburg, New York) and *ThermFact* (Montreal). During the 10 years, VTT and its many international research partners have developed a family of new multidisciplinary methods, the application range of which covers both practical engineering solutions and new developments in frontier sciences. Successful scale-up projects, supported by ChemSheet, have been performed in the chemical industry. New chemistry concepts in process industries such as the neutral conversion of paper-machines have benefited from the use of ChemSheet. In steel-making new grades, new operational practices and inclusion control have been developed. ChemSheet and its sister programs have supported development of rotary drum processes such as lime kilns, cement production and waste incineration. In power production and environmental technology, the applications range from the chemical safety design of nuclear plants to modeling of fuel cell systems. A recent innovative

application is the STEAMAX expert system used in the design of bio- and mixed fuel boilers.

Due to their generic base in the second law of thermodynamics, the free energy methods are not only useful for macroscopic technologies. The utilization of the local chemical equilibrium concept as well as the immaterial (entity) constraints, so far uniquely applicable in ChemSheet, have led to new applications in materials science, particularly for interfacial and surface systems. In biotechnology, the thermodynamic free energy analysis can be applied to recognize promising reaction pathways in enzyme systems and for studies of local enzymatic conditions, thus reducing the need for elaborate kinetic experiments.

In this booklet a number of selected multiphase applications developed with ChemSheet and related software will be described. ChemSheet suits particularly well for the simulation of such processes, which include several chemically reacting components and phases. Its particular advantage is the coupled simulation of chemical and energetic changes. In addition, the multicomponent approach results with both bulk compositions and amounts of minor species, including monitoring of harmful impurities.

Well-defined thermodynamic quantities are constantly used, which enables good reproducibility and firm basis for model validation. The additional advantage is the systematic use of extensive state properties, which means that the model results, validated in a laboratory scale, are apt for direct scale-up to plant scale without costly pilot experiments. The use of established thermodynamic property data also facilitates straightforward interfacing with other simulation tools for multidisciplinary models. Novel applications with advanced contents and interfaces are constantly being developed in close co-operation with both Finnish and foreign colleagues and customers.

2. Use of ChemSheet as a modeling platform

Pertti Koukkari and Karri Penttilä, VTT
Daigen Fukayama, RCCM

Simulation by rigorous numerical methods has become an everyday necessity in process engineering and materials science. Few new processes or changes in their chemistry and materials are designed without computer models. Simulation focuses both the process design and experimental work on essentials, eliminates vain experimenting and enables economic choices of processes and materials. Recent developments in both computer efficiency and user-friendly interfaces has made it possible to combine rigorous multiphase methods with practical spreadsheet calculations.

2.1 Background

In a practical simulation project, with the thermochemical calculations executed, extensive work is yet needed to produce the critical evaluation of the simulation results. This must be done in terms of reaction conversions, energy consumption, alternative process conditions and choice of materials, including the cost factors. Often it is but here where the feasibility of the process is finally considered. The ChemSheet program links numerical thermodynamic calculation with the MS-Excel® worksheet, which allowing development of applications directly from the spreadsheet. The application data can accordingly be prepared by using the spreadsheet techniques.

2.2 Methods

2.2.1 Data-flow of ChemSheet

In ChemSheet the Gibbs energy minimization technique provided by the multi-phase program ChemApp has been dynamically linked to Excel's spreadsheet operations. The Gibbs energy solver used in ChemApp was originally developed by Eriksson [1]. It has been widely adopted to different applications, among those the commercial thermochemical software products of GTT Technologies of Aachen, Germany and ThermFact-Institute of Montreal, Canada [2].

ChemApp is a thermochemical program library with which application-specific thermodynamic calculations may be performed by using the ChemSage Gibbs energy minimisation procedure. ChemApp consists of a large number of subroutines, which allow for flexible definition of simulation inputs and outputs. Via ChemApp, the user defines the equilibrium conditions, the active phase constituents, properties for a thermochemical target calculations and chooses from the results those data he needs for further use. ChemApp is written in Fortran, but is available as a DLL-application for most programming environments. Since ChemSheet operates as an Add-in application in the Microsoft Excel®, the DLL form of ChemApp is that of Visual Basic.

The systematic approach of Gibbs energy minimisation in terms of the phases and their components bears the advantage that one needs not to work out stoichiometric reaction equations, which, for a multi-component system with increasing number of chemicals soon becomes elaborate and tedious to handle. Instead of equilibrium constants, the original thermodynamic data is used to derive the chemical potentials (partial molar Gibbs energies) of the chemical species, which may appear in the system. This data can be collected from several available data-bases. For example, in FactSage, there is a particular module which produces the application-specific data-files for various reaction mixtures extracting the relevant data from a larger data-base. The data-flow structure of ChemSheet is shown in figure 1.

The Gibbs energy data form the basis of the minimisation calculation. The application-specific data-files are generated from available databases such as those provided by SGTE and FACT [3, 4]. The data from other widely spread thermo-chemical sources, which are multi-phase oriented (such as Outotec's HSC® [5]) can usually be adopted with little modification. However, the data descending from the

conventional equation-of-state (EOS) thermodynamics is normally insufficient and need replenishment before adaptation to Gibbs'ian computations.

For pure substances and ideal mixtures, the primary standard data in terms of the standard enthalpies, entropies and heat capacities are needed. For mixtures the excess-Gibbs energies of the constituents are also required. For the moment, the non-ideality data cover extensively pyrometallurgical applications, incorporating molten slags and metals as well as a gas phase, but data are increasingly available for oxide and sulphide systems, ceramic materials, non-stoichiometric systems and concentrated aqueous solutions.

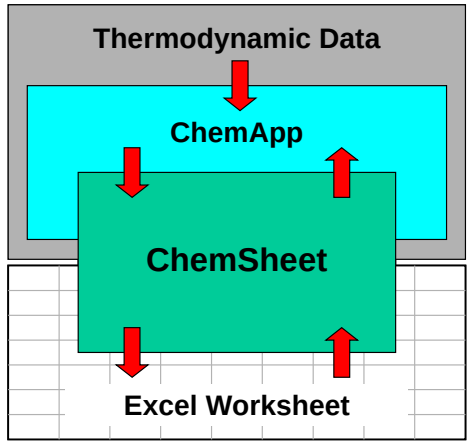

Figure 1. The data-flow structure of ChemSheet.

2.2.2 The thermochemical simulation method

The use of the Gibbs energy approach gives a possibility to utilize the driving force of a chemical system towards equilibrium in process models. In figure 2, a volume element of a continuous reaction system, interacting with its surroundings is shown. The system is affected by its thermal conditions (temperature and pressure) as well as by the chemical processes, which take place within the volume element. In addition, for a comprehensive thermochemical treatment of the system, the heat and mass transfer across the boundaries of the volume element need to be considered. The governing equations of the continuous thermochemical system are concisely presented in the chart.

When the process simulation is performed in terms of the chemical potentials of the constituents of the system (that is, in terms of minimum Gibbs energy),

the obvious advantage of the method is that one receives the results of the calculation in the form of the thermochemical state properties. Thus, instead of concentration-volume data, which is characteristic to the mechanistic models, one gets as a result a comprehensive set of both intensive and extensive state properties, by which the volume element becomes characterized. Thus, one may follow, as a result of the simulation e.g. the oxygen potential in terms of another intensive property, such as temperature.

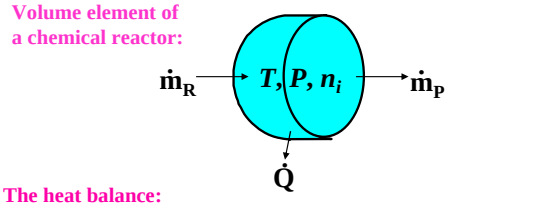

The heat balance:

$$-\text{div}\ \mathbf{J}_Q = \frac{C_P}{V}\left[\frac{\partial T}{\partial t} + \mathbf{v}\,\text{grad}\ T\right] + \sum_r \sum_k H_k\, \upsilon_{kr}\, b_r$$

The chemical reaction rate:

$$b_r = \frac{1}{V}\left[\frac{\mathrm{d}\xi_r}{\mathrm{d}t}\right] = k[A]^a[B]^b \ldots [M]^m$$

$$\text{where}\ \ \ln(k) = \ln(\mathbf{A}) - \frac{\mathbf{E}_a}{RT}$$

The Gibbs energy:

$$G = G\,(T, P, n_i)$$

$$G = \sum_\alpha \sum_i n_i^\alpha \left(\mu_i^{\circ\alpha}(T) + RT\ln a_i^\alpha\right)$$

$$\Longrightarrow \ \min(G)\ \text{ at equilibrium}$$

Result Option	Unit
Activity	
Amount	e.g. mol
Chemical potential	e.g. J/mol-K
Enthalpy	e.g. J
Entropy	e.g. J
Gibbs energy	e.g. J/K
Heat capacity	e.g. J/K
Volume change	e.g. dm3
Enthalpy/amount	e.g. J/mol
Entropy/amount	e.g. J/mol-K
Gibbs energy/amount	e.g. J/mol
Heat capacity/amount	e.g. J/mol-K
Incoming amount	e.g. mol
Pressure	e.g. bar
Temperature	e.g. K
Volume	e.g. dm3

Figure 2. The volume element of a thermochemical system with its governing equations. (see list of symbols in the end of the paper). The table gives a list of the state properties, which are calculated in ChemSheet simulations.

Modes of calculation in ChemSheet

The calculation in ChemSheet follows the convention adopted in the ChemApp library, which permits the calculation of thermochemical states in terms of their global conditions or in terms of incoming streams. When the global equilibrium mode is chosen, merely the composition of chemical inputs and the desired

equilibrium conditions, e.g. temperature and pressure need to be given for the program to calculate the composition of the chemical equilibrium state. Then, the state of the incoming substance is indifferent to the calculation and the amount of a substance may be given, for example, according to its elemental composition. The state properties given for the minimum Gibbs energy correspond to those of the global equilibrium, and are defined with respect to a reference state (typically 25 °C, 1 atm).

When instead the stream mode is used, one needs to specify the equilibrium condition and the chemical composition of the input streams, including their temperatures and pressures. In combination, the compositions of the input streams form the thermochemical system, for which the Gibbs energy is minimised. The changes of the extensive state properties between the final state and the input streams then become calculated. This can be done repetitively between states that follow each other in succession, and calculations of practical processes can then directly be executed.

The streams may be added or removed and one may choose whether the stream is taken as a simple mechanical mixture or whether it is equilibriated at a given temperature and pressure before it is introduced to the reaction. A specific reactor stream is defined in ChemSheet for a calculation of successive volume elements, consisting of the entire content of the previous volume element.

For both modes, thermochemical target calculations are also possible. A target calculation is an iterative procedure, where, under a given (equilibrium) condition a particular value of a (target) property is searched. The familiar example is the calculation of the adiabatic temperature of a combustion mixture. This is done in ChemSheet by defining the enthalpy target ($\Delta H = 0$) condition, while the algorithm searches for a temperature or a composition to fulfil that condition. It is also possible to use composition or total pressure as the search variables. In table 1, the present options for target calculations in ChemSheet are described such as they appear in the ChemApp library. The given combinations of conditions and target variables allow a number of different process problems to be solved. However, in practice it has proved to be straightforward to apply simple spreadsheet macros to provide such target calculations, which ChemApp does not include.

Table 1. State variables used for defining target properties in ChemSheet (as given by the program library ChemApp). The respective target conditions are selected from the equilibrium conditions.

Target property	**Equilibrium conditions**
Temperature	Heat Capacity
Pressure	Enthalpy
Incoming amount of substance	Entropy
Chemical potential	Gibbs Energy
Formation of phase	Volume
Precipitation of a phase from a given solution	Chemical potential
	Incoming amount
	Amount of phase
	Temperature
	Pressure

A particular application of target calculations is the possibility to use ChemSheet as a tool in phase-mapping. In this procedure, one follows a set of phases in a given system in terms of a single variable, e.g. temperature. By using the phase-mapping procedure one may search for all phase transitions within a given interval of the search variable. The search variable can be total pressure, temperature, or the composition of the mixture in terms of the incoming amount(s).

There are obvious advantages of the simultaneous calculation of the physical and chemical changes in the Gibbs energy minimisation method. Thence, an augmenting research effort has emerged to develop this method to include the necessary reaction kinetics and/or time-dependent heat or mass transfer in the calculations [6, 7, 8]. The overall scheme of the thermochemical simulation method is described in the simplified block diagram of figure 3. The time-dependent algorithms applicable in ChemSheet have been described in more detail in [6, 8, 10].

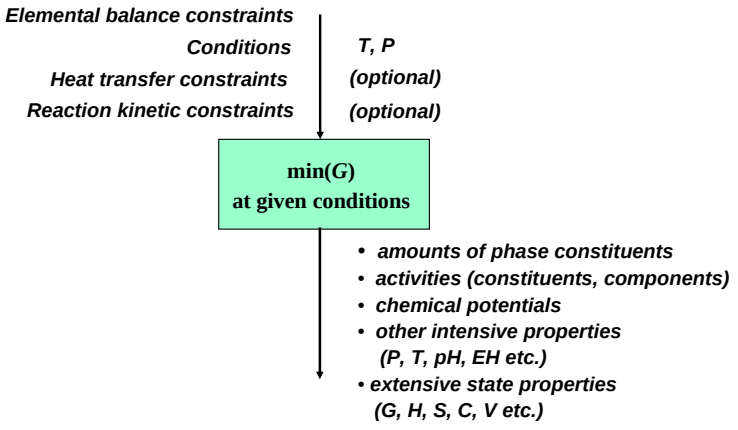

Figure 3. The block diagram for the Gibbsian thermochemical method. With the Gibbs energy simulation all the thermodynamic state quantities can be systematically derived from the calculated equilibrium state.

2.2.3 Use of ChemSheet

ChemSheet is operated as an add-in application within the Excel®-spreadsheet. The user needs merely the installed program and its activation as one of the add-in tools within the spreadsheet, and the thermodynamic data-file for source data. The operation of ChemSheet is done with a dialog control, which has been described e.g. in [8]. In figure 4, two excerpts of the ChemSheet-dialog used for the calculation of a slag window in a steelmaking process (see also figure 25) are shown.

From the dialog, the data-file is activated via a browser. The Options tab allows one to choose between the global, stream and phase-mapping modes. Export and Import features of the ChemSheet dialog allow the user to apply several model frames within a single Excel worksheet file. The Conditions tab includes the global input conditions (amounts of substances) as well as the desired equilibrium conditions. The properties are then chosen from control lists, which are based on the particular thermodynamic data file, and their values are given as Excel cell addresses. The Excel cell-editor may also be used to set the values for the active cells.

A separate tab is provided for setting targets in the ChemSheet dialog. In the Results tab, those results, which are selected to be shown in the worksheet, as well as their ranges in the worksheet are given. The Status tab is used to activate or de-activate phases or constituents in the thermodynamic system. Thus, while calculating metastable systems, phases more stable than a particular metastable

phase can be removed from the active calculation, so as to enable the screening of the circumstances producing the metastable phase.

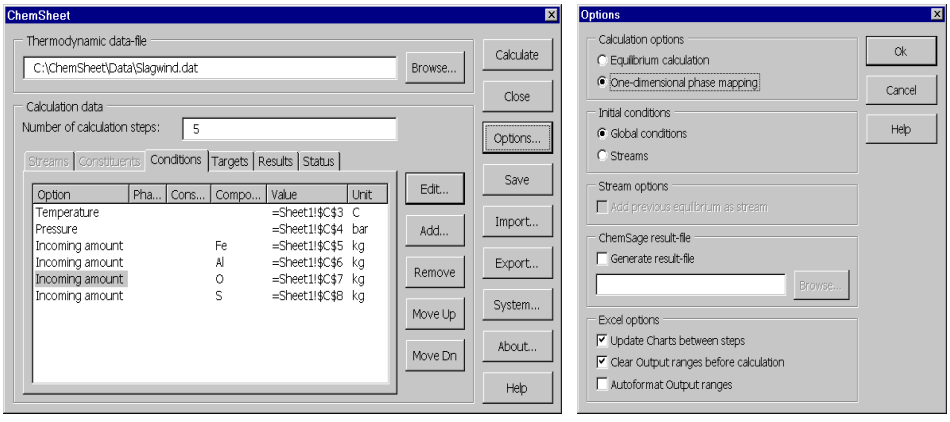

Figure 4. The ChemSheet-dialog is shown to the left. Here the user chooses the thermodynamic data-file and gives all the input parameters for the successive calculations steps and for the generation of results. The input parameters may contain references to worksheet cells and formulas that make use of Excel functions. Between the calculation steps the StepIndex-variable can be used to change any of the input parameters. The Options dialog is shown to the right.

The number of calculating steps is given in the middle section of the dialog box. In ChemSheet Excel-operations are performed between each step in a sequential calculation. All written Excel functions also become updated between each step and their effects may be introduced to the thermodynamic simulation. This enables a variety of changes to incoming streams, process conditions, and also to statuses of the phases within one calculation sequence.

The output range of a calculation can be a reference to a cell or range of cells or can refer to multiple areas. An area is a range of contiguous cells or a single cell. The values are stored to the areas from left to right and top to bottom. So the value for the first calculation step is stored to the first cell in the first area (upper left corner of the area) and the value for the last step is stored to the last cell in the last area (lower right corner of the area). The headers and units are automatically shown in the first two cells (rows) of a chosen range. Alternatively, the user may choose an option of not showing the header or unit, and just pick the desired value of a property for further use in the calculation. A comprehensive listing of the calculated results can be optionally written in a given directory. This appears as an ASCII file, using the ChemSage format for result tables.

The opening of a new ChemSheet model, exporting and importing the previously saved models and the actual calculation are initiated via a particular toolbar, which becomes activated in the Excel window during installation of the program (see figure 6).

2.2.4 Use of Excel features

ChemSheet is designed to take advantage of the features of the spreadsheet for thermochemical calculations. Thus, the sets of contiguous cells may be used to guide the inputs or calculation conditions and the results may be directly converted to indicate any quantity, which is used for further evaluation of process alternatives. The spreadsheet graphics can be used on-line to illustrate the effects of various conditions.

One key link to Excel properties when using ChemSheet is the utilization of the 2-dimensional cell structure of the spreadsheet with the *StepIndex* parameter. The *StepIndex* chronologically indicates the current step used in a multi-stage calculation. To its value, then, any discretisation or desired change in the amounts or conditions can be connected.

ChemSheet may also be used via customised worksheets, which allow the user to make variations of the inputs and conditions to the visible range of the worksheet. The result charts and the necessary cell addresses for the inputs and calculation conditions are set into the same spreadsheet. The operation of the model is at its simplest done with the ChemSheet toolbar within the Excel environment.

The graphical modules of the spreadsheet can be used for illustrations of the process to be calculated as well as for output of the calculations. Applying graphics ChemSheet can be operated as an illustrative screening tool, where the showing of the process conditions, incoming and exiting streams, essentials of reactor geometry etc. are outlined into the active calculation environment (cf., e.g. figure 5). Simultaneously, the output graphics can be used as real-time charts during the calculations.

2.2.5 Results: Examples of ChemSheet applications in process modeling

Due to its general thermochemical approach, ChemSheet is applicable for a diverse range of purposes in chemistry, metallurgy and materials science.

The most simple application example of ChemSheet is shown in figure 5. The reaction to be studied (in Gibbs'ian multi-component mode) is the thermal

decomposition of gaseous 3-chlorosilane ($SiHCl_3$), sometimes used to produce ultrapure silicon for electronic materials:

$$2SiHCl3 \leftrightarrow Si\downarrow + SiCl4 + 2\ HCl$$

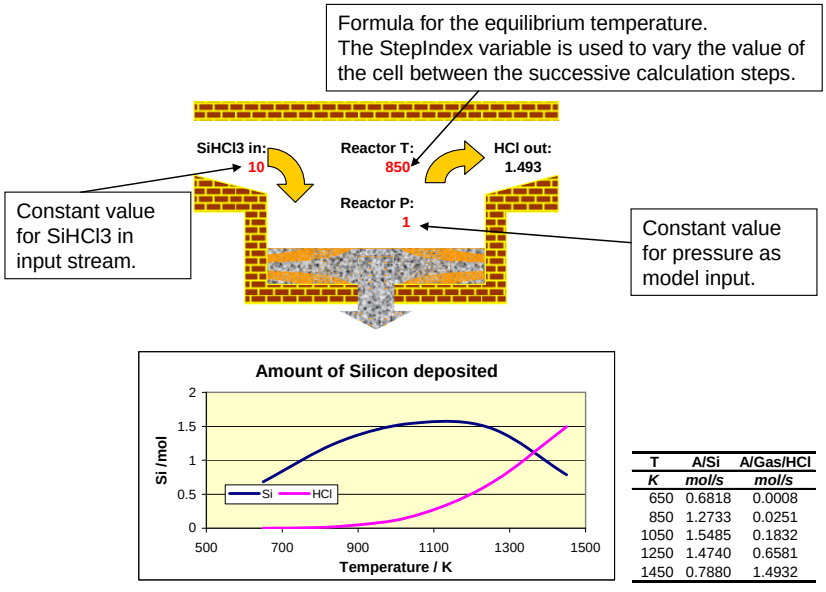

T	A/Si	A/Gas/HCl
K	*mol/s*	*mol/s*
650	0.6818	0.0008
850	1.2733	0.0251
1050	1.5485	0.1832
1250	1.4740	0.6581
1450	0.7880	1.4932

Figure 5. A simple thermal decomposition example which can be calculated with ChemSheet Light – the free demo version of ChemSheet. Model input cells are those with red figures. The graph indicates the Si yield maximum (numerical values given in the output table).

The reactor has been schematically drafted into the worksheet, and the input and output Excel shells are shown with explanations. The result indicates a maximum yield of silicon at ca. 1100 K temperature. Increasing the process temperature decreases Si-yield and produces more hydrochloric acid (HCl) and other side products.

It is straightforward to extend the model to include more realistic process configuration. In figure 6 the modeling of the growth rate of a silicon disk, as deposited from a $SiHCl_3$ – H_2 mixture by the thermally induced reaction is shown. Silicon is deposited and grown on the surface of a disk-like substrate that is heated by radiation through a quartz wall.

In the model the reactor is divided into two separate regions: the bulk region and the stagnant surface region. The deposition is to be controlled by the mass transfer from the bulk to the surface and the compositions of the bulk and the

surface are assumed to be in local equilibrium each. The variables in the model are the temperature of the bulk and the surface regions and the mole fractions of the elements in both regions. The variables are solved in a separate iteration loop and the local equilibria for the bulk and surface are calculated at given temperatures and initial compositions for each loop and the balance equations are then updated. In figure 7, the simulated growth rates of silicon have been compared with those measured by Habuka et al [9]. With the simple model, a fair agreement between the calculation and experiment was achieved.

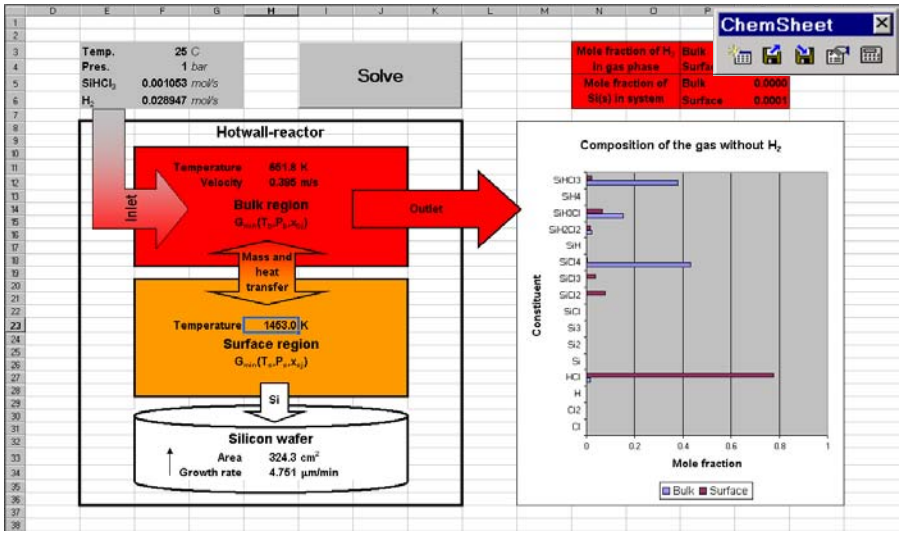

Figure 6. The ChemSheet simulation of a CVD-reactor with a known surface area, used in the production of polycrystalline silicon. The bar graph illustrates distribution of the various silicon compounds and HCl in the gas phase (neglecting hydrogen). ChemSheet toolbar is shown in the upper right corner.

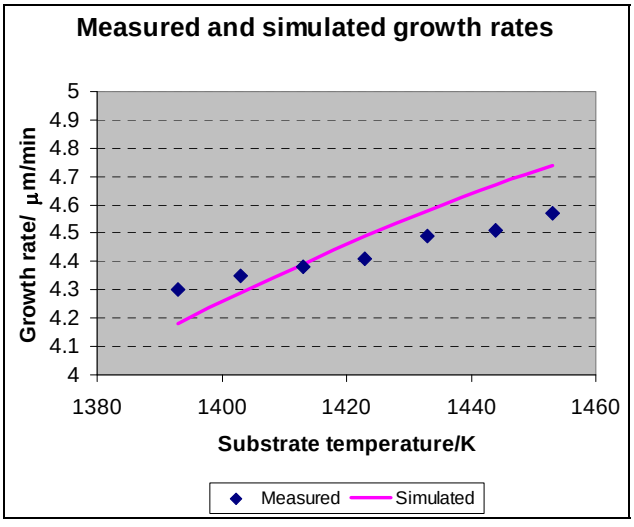

Figure 7. The measured and the simulated growth rates of the silicon wafer. The input conditions for the simulations and measured growth rates have been taken from Habuka et al. [9].

In figure 8, a schematic of a 'moving bed' reactor is shown (left) with its respective ChemSheet model scheme. Merely the model structure is indicated, without specification of the reactants and products.

The model construction in ChemSheet allows for changes both in axial and radial directions, while the model focus remains on the thermochemistry of the moving bed system. The ChemSheet input of the system includes functions for

- furnace dimensions
- feed conditions for both gas and bed (mass flows, temperature, pressure)
- heating power (temperature)
- heat transfer coefficient of heater and reactor walls
- thermal conductivities of bed and metal walls
- reaction rate parameters for constrained Gibbs energy calculations.

The kinetically restricted equilibrium calculation can be performed for each cell. The 2-dimensional profiles of the calculation are shown in figure 9. The advantage of the model is its easy construction in Excel, with both radial and axial profiles included.

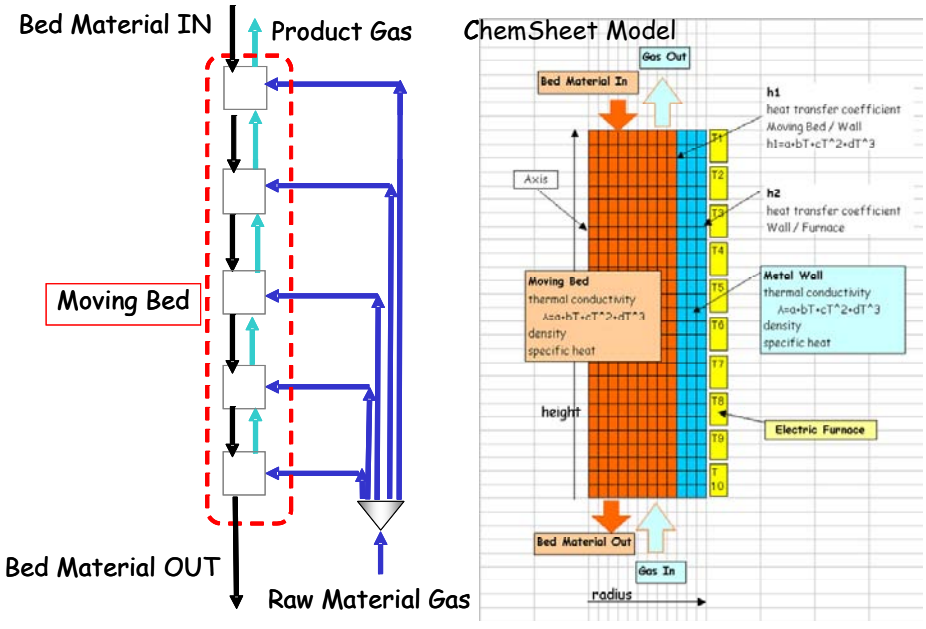

Figure 8. The schematic of a moving bed model in ChemSheet [10].

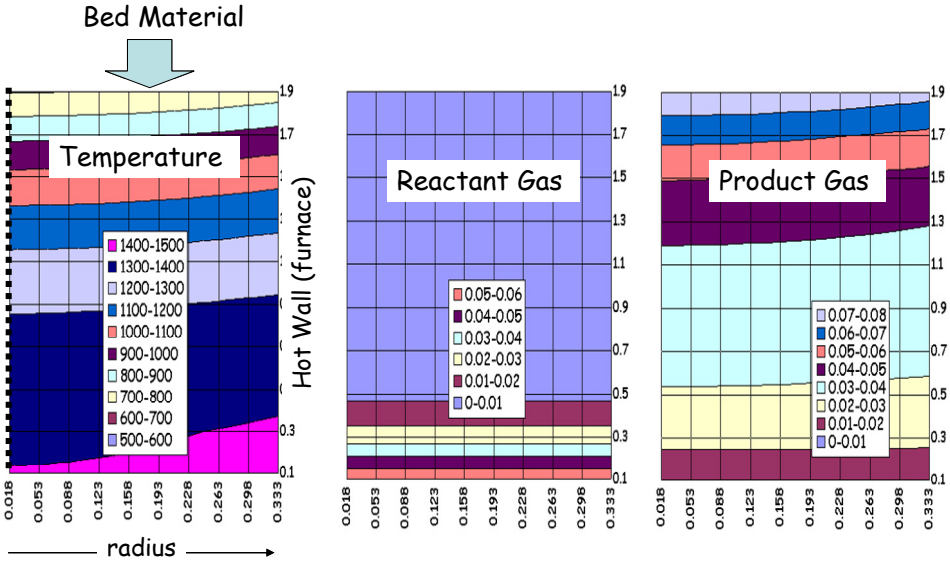

Figure 9. Temperature and concentration profiles of the moving bed reactor model.

2.3 Conclusions

ChemSheet, as an interface application of ChemApp is particularly well suited for the simulation of such processes, which include several chemically reacting components and phases. The particular advantage of the thermochemical method is the coupled simulation of chemical and energetic changes. In process simulation, the multicomponent approach results in both bulk compositions and amounts of minor species, including monitoring of often harmful impurities. Well-defined thermodynamic quantities are constantly used, which enables good reproducibility and firm basis for model validation. Processes ranging from high-temperature materials chemistry to aqueous suspensions at ambient conditions can be calculated with the same thermodynamic routines, provided that the appropriate Gibbs energy data is available.

Each application of ChemSheet can be made to a customised worksheet, and thus ready for a wide range of users. Also those who are less familiar with multi-phase thermodynamics will find the ChemSheet worksheet templates useful for both engineering purposes and research. For experts in multi-phase thermo-dynamics, ChemSheet provides a multi-disciplinary tool for a diverse range of applications.

2.4 List of symbols in figure 2

A	frequency factor of the reaction rate coefficient	n_i	amount of species I
[A],[B]	reactant concentration variables	P	pressure
b_r	chemical reaction rate of the reaction r	Q	heat
Cp	heat capacity of a system	R	gas constant, R = 8.314 J/mol-K
E_a	activation energy of a reaction	T	temperature
G	Gibbs energy	t	time
H	Enthalpy	V	volume
H_i	partial molar enthalpy of substance i	v	average velocity of the fluid
		α	superscript for region or phase
		υ_{ir}	stoichiometric constant of species i, reaction r

J_Q	heat current density for isotropic systems	μ_i	chemical potential of substance *i*
k_r	experimental rate constant of reaction *r*	ξ_r	extent of chemical reaction *r*

2.5 References

[1] Eriksson, G. and Hack, K. Met. Trans. B, 21B, December 1990, pp. 1013–1023.

[2] Eriksson, G., Hack, K. and Petersen, S. Werkstoffswoche '96, Symposium 8: Simulation Modellierung, Informationsysteme, 1997, 47, DGM Informationsgesellschaft, mbH, Frankfurt, Germany. ISBN 3-88355-236-4.

[3] FACT Manual, Edition 3.05, 1999, Montreal, Canada.

[4] Ansara, I. and Sundman, B. Computer handling and dissemination of data. T.S. Glaser (Ed.). Elsevier Science Publishers, CODATA, 1986, pp.154–158.

[5] http://www.hsc-chemistry.com/.

[6] Koukkari, P., Laukkanen, I. and Liukkonen, S. Fluid Phase Eq., 136, 1997, pp. 345–362.

[7] Koukkari, P. Computers Chem. Engng., No. 12, 1993, pp. 1157–1165.

[8] Koukkari P. et al. In: Y. Brechet (ed.). Microstructures, Mechanical Properties and Processes, Euromat 99 – Vol. 3, Wiley-VCH Publishers, Weinheim, 2000, pp. 323–330.

[9] Habuka, H., Katayama, M., Shimada, M. and Okuyama, K. Jpn. J. Appl. Phys., 33 (1994), pp. 1977–1985.

[10] Yokota, M. Moving bed reactor modelling by ChemSheet, 2007 RCCM Workshop, November 13–14, Tokyo.

3. ChemSheet – from computational thermodynamics to spreadsheet engineering

Pertti Koukkari, VTT
Stephan Petersen, GTT-Technologies

ChemSheet is one from the internationally renowned ChemSage/FactSage family of thermochemical calculation programs, which are extensively used in universities as well as in corporate and government laboratories. With its pioneering Excel interface, ChemSheet offers new possibilities and practical advantages to both scientists and engineers in the use of thermochemical calculations across a wide spectrum of applications by providing the easy-to-use spreadsheet approach towards complex thermodynamic multi-phase problems.

ChemSheet offers the same library of subroutines for data handling and phase equilibrium calculation purposes, which are included in the ChemApp Gibbs energy solver. In addition to the predetermined mass balance constraints, which are used for chemical and phase equilibria in Gibbs energy calculations, within the frame of ChemSheet it is easy to use dynamic and immaterial constraints. They allow for calculation of systems controlled by work factors (either systemic or externally induced) as well as of processes controlled by chemical reaction kinetics. Thus, solving e.g. surface and interface energies, Donnan potentials and simulation of chemical or biochemical reaction pathways can be performed.

3.1 Background

In macroscopic systems, where thermal, electrical and mechanical variables appear interconnected with chemistry the Gibbs free energy is the most general property to be applied for relationships between different quantities. With quantitative consideration of the Gibbs free energy, calculation methods have been developed for materials science and metallurgy, for chemical and process engineering as well as for energy and environmental technologies.

Thus, it is obvious that development of functional materials and innovative processes, so often asked in the contemporary society, interdisciplinary predictions between physical, chemical and even biological phenomena are often required on quantitative basis. The Gibbs free energy offers one such interdisciplinary concept and hence, several subject fields would benefit from the ability to perform Gibbs'ian calculations. However, substantial know-how in the field of computational thermochemistry is necessary to design such a code. On the other hand, the writing of own programs has become a less likely task for particularly the practical engineering experts working in the industry. Instead, the common expectation within industrial companies is that commercial software vendors will supply them with user-friendly software packages that require little or no programming skills[3]. A similar trend can be observed within universities and research institutes as well, in particular when highly specialized, modular software can be used compatibly with existing 'researcher code'.

ChemSheet, when introduced in 1999, was one of the software pioneers serving this general trend. During its 10-year history, ChemSheet has been adapted by the industrial user, particularly for such purposes where its easy inclusion of Excel features such as special functions, presentation graphics and use of customised spreadsheet interfaces have been beneficial. On the same terms, a number of scientists have adapted the spreadsheet based approach for their thermochemical problems, taking advantage of the advanced features

[3] In a fairly recent survey performed among young American chemical engineers it was concluded that computing in the workplace for entry-level experts is clearly on the rise (over two-thirds of the approximately 300 respondents spent at least one-half of their workday at their computer). Yet, it was found that most of the time spent working on the computer involved user-friendly commercial software packages, with the most common application being Microsoft Excel. Nearly three-quarters of the respondents were not expected by their employers to be competent in any programming language. See D. G. Coronell: Computer Science or Spreadsheet Engineering? An Excel A/BA-Based Programming and Problem Solving Course, *Chemical Engineering Education*, Vol. 39, No. 2, 2005, pp. 142–145.

implemented to ChemSheet, which allow for using the Gibbs'ian method for calculation of calculating local or partial equilibrium conditions within various kinetic models, computation of surface and interface energies and simulation of e.g. pulp suspension chemistry.

3.2 General features

3.2.1 Terminology

A thermodynamic system consists of a number of phases, where some may have a composition expressed as amounts of a number of phase constituents, and others can have an invariant composition. Descending from the classification of ChemApp, the phases are divided into three groups in ChemSheet – the gaseous phase, condensed mixtures, and condensed stoichiometric phases. For convenience, a condensed stoichiometric phase is considered to consist of a single phase constituent only.

Phases and phase constituents always have thermochemical properties (activities, chemical potentials, enthalpies, volumes, etc.). Phase constituents have compositions expressed as amounts of a number of components.

A component is a system-wide entity. Sometimes this is stressed by calling it a system component. In ChemApp, as well as in ChemSage, components are usually the elements, but they may also be composed of elements in any combination. In the latter case the stoichiometric formulae of the components must be linearly independent.

3.2.2 Thermochemical data and mixture models

The same comprehensive library of models for non-ideal solution phases available in ChemApp is also applicable in ChemSheet (see table 2). Thus, the wide range of existing thermochemical data for FactSage is available for ChemSheet. ChemSheet uses ChemSage datafiles.

Table 2. Solution models available in ChemApp/ChemSheet [5].

Model	**Application area**
Redlich-Kister-Muggianu Kohler-Toop	For general use with substitutional or associated solution phases
Compound energy formalism Two-sublattice order/disorder formalism* Species chemical potential/bond energy formalism* Extended compound energy formalism	Solid phases with sublattice descriptions
Two-sublattice ionic formalism*	Ionic liquids
Two-sublattice equivalent fraction formalism Two-sublattice equivalent fraction formalism as a polynomial Guts formalism	Molten salts
Gaye-Kapoor-Frohberg cell model* Modified quasichemical formalism*	Ionic oxidic mixtures with or without non-oxidic solutes
Quadruplet quasichemical model	Condensed non-aqueous solutions
Wagner	Metallic dilute solutions
Davies formalism* Helgeson-Tanger-Shock formalism (ideal)* Helgeson-Tanger-Shock formalism (Debye-Hückel)* Helgeson-Tanger-Shock formalism (Davies)*	Dilute aqueous solutions
Pitzer formalism* Pitzer formalism without E-theta and E-theta'* Specific ion-interaction formalism* Helgeson-Tanger-Shock formalism (Pitzer)*	Concentrated aqueous solutions
Revised Helgeson-Kirkham-Flowers (HKF) model*	Aqueous solutions up to 5 kbar and 1300 K
Virial equation with Tsonopoulos' second virial coefficient correlation*	Non-ideal gas

* Magnetic contributions are not permitted.

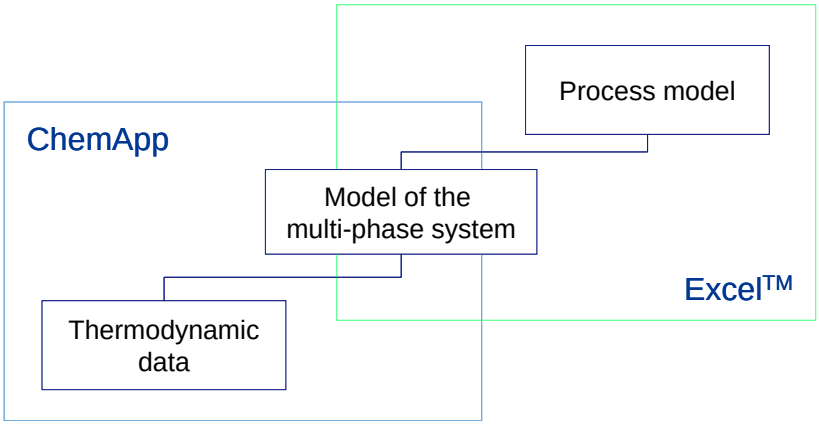

Figure 10. Modeling multi-phase systems and processes in ChemSheet (Excel is a trademark of Microsoft Corporation).

3.2.3 The constrained Gibbs energy method

As stated above, the particular advantage of the thermodynamic simulation is its ability to deal with the interdependence of chemical and physical changes. The conventional Gibbs energy minimisation method extensively used for calculation of complex chemical and phase equilibria, inherently accounts also for the energy changes these processes. Thus it would be lucrative to incorporate restrictions due to chemical kinetics or physical constraints into the calculation, as the technique then would be applicable to non-equilibrium processes and to various phenomena controlled by interior or exterior physical conditions.

The conventional Gibbs energy minimisation aiming at chemical and phase equilibria uses the Lagrange method with molar abundances (mass balance) as the sole necessary constraints. To incorporate the aforementioned additional phenomena, a new method with analogous immaterial constraints has been developed to be applicable particularly in ChemSheet, yet it can be adopted for most ChemApp applications, too [2].

When additional energy or work terms affect the Gibbs free energy, [$G = G(T,p,n_k)$] it is customary to transform the total differential of the Gibbs function to read as follows:

$$dG = -SdT + Vdp + \sum_{k=1}^{N} \mu_k \, dn_k + \sum_i F_i \, dx_i \qquad (1)$$

where *S* denotes the entropy and *V* the volume of the system, $\mu_k = \mu_k(T, p, n_k)$ is the chemical potential of the species (*k*), *T* is temperature, *p* is pressure and n_k refers to mole amounts of chemical substances. The last term ($F_i dx_i$) refers to additional generalised work effects.

The Gibbs energy minimisation requires the use of the chemical potentials μ_k (partial molar Gibbs energies) of the constituents of the system. If additional work terms are not included, the multi-phase chemical equilibrium is solved with the mass balance constraints as the necessary subsidiary conditions. In many physical circumstances the potentials appear constrained also by other, typically work-related factors. Then, immaterial constraints for chemical potentials can be applied together with the mass balance relations [3]. The additional conditions arise from the said work or energy effect or they are due to reaction kinetic condition [4]. In the Gibbs energy minimisation performed by the Lagrange method the new constraints are set with additional Lagrangian multipliers [2]. They assume the same mathematical form as the mass balance conditions. The equations governing the chemical potentials and their respective constraints in the multi-phase system can be derived as follows:

$$\mu_k = \sum_{j=1}^{l} a_{kj}\pi_j \quad (k = 1,2,...N) \tag{2}$$

$$\sum_{k=1}^{N} a_{kj} n_k - \beta_j = 0 \quad (j = 1,2,\ l) \tag{3}$$

where *N* is number of different chemical constituents as formed from *l* system components by means of a conservation matrix $\{a_{kj}\}$ (see e.g. [2] for details). The π_j's represent the chemical potentials of the components in the system and equation (3) includes in addition to the mass balance constraints the necessary immaterial conditions, such as electroneutrality, conservation of surface area, metastability of a given constituent etc.

Equations (2) and (3) can then be used to solve for the unknowns (n_k, π_j). For equilibrium problems, the Gibbs energy minimisation with given input amounts and the system temperature and pressure is sufficient to solve for the constraint potential and system composition. In non-equilibrium systems, an external algorithm of e.g. reaction kinetics can be additionally necessary to set the extent of change [4]. In Table 3 some examples of the constraints and their respective conjugate potentials have been listed.

The new method opens exciting possibilities to utilise and develop further the Gibbs energy calculations for materials and process research. The additional effects typically include surface deformation work (σdA), electric charge transport (φdq), electric or magnetic polarisation ($\boldsymbol{E}$d$\boldsymbol{D}$;$\boldsymbol{H}$d$\boldsymbol{B}$), linear elastic deformation ($\boldsymbol{F}_x$d$\boldsymbol{x}$) and for chemical kinetics in terms of extent of reaction ($\sum_k \nu_{kr}\,\mu_{kr}\,d\xi_r$).

The last mentioned effect relates to constraining by affinity that permits conditions to be set for chemical reaction kinetics and/or reaction selectivity. This enables the use of the Gibbs energy approach for time-dependent (dynamic) multi-phase problems.

Table 3. Thermodynamic properties received from constrained simulations.

System	Constraint	Conjugate potential	Practical examples
Chemical equilibrium systems	$\sum_{k=1}^{N} a_{kj} n_k = b_j$	$\pi_j = \frac{\partial G}{\partial b_j}$	Multi-phase chemical equilibria Phase diagrams
Systems with area constraints	$\sum_{k=1}^{N_s} A_k n_k^s = A$	$\pi_{area} = \frac{\partial G}{\partial b_{(area)}} = \sigma A_0$	Surface and interfacial tension, sorption phenomena surface compositions
Systems with volume constraints	$\sum_{k=1}^{N_F} V_k n_k^F = V_F$	$\pi_F = \frac{\partial G}{\partial b_{(V_F)}} = \Pi \overline{V}_F$	Swelling pressure of fibers and membranes
Electrochemical (Donnan) multi-phase systems	$\sum_{k=1}^{N_\alpha} z_k n_k^\alpha = 0$	$\pi_{(q^\alpha)} = \frac{\partial G}{\partial b_{(q^\alpha)}} = F\,\Delta\varphi^\alpha$	Process chemistry of fibres and pulps Multi-phase membrane systems
Rate-controlled complex systems	$\sum_{k=1}^{N} a_{kr} n_k = b_{(r_i)}$	$\pi_{(r_i)} = \frac{\partial G}{\partial b_{(r_i)}} = \frac{\partial G}{\partial \xi_i} = -Aff_i$	Metastable phases or constituents Multi-phase dynamics

a_{kj} = element of conservation matrix; N = nr. of constituents.; b_j = molar amount of component j^{th} component, $b_{(X)}$ = molar amount of component 'X';

π_i = Chemical potential of i^{th} component; $\pi_{(X)}$ = Chemical potential of component 'X'

A_k = molar area of constituent; σ = surface tension; A = total surface area; A_0 = normalisation constant

V_k = molar volume of constituent; Π = swelling pressure; V_F, $\overline{V}_F$ volume and molar volume of phase F

z_k = charge number of species; F = Faraday const.; $\Delta\varphi$ = electric potential difference between phases

Aff_i = Affinity of i^{th} reaction; indexes: s = surface, α = phase

3.3 Using the ChemSheet program

3.3.1 General

The features of ChemSheet, as well as some of its application examples are explained separately in this booklet. Thus only a brief outline of the major characteristics of the program is presented below.

ChemSheet provides (in Excel) an Add-in tablet which can be used to initialise the ChemApp interface and read the appropriate thermodynamic data-file. The thermochemical system of the user is adjusted with the dialog interface using Excel cell hierarchies. Similarly, the interface can be used to set the initial conditions for the Gibbs energy calculation, to perform the calculation and collect results to Excel cells. Between calculation sequences, Excel functions, indexes and graphics may be used. Visual Basic macros are an advantage to more experienced users.

3.3.2 Adjusting chemical equilibrium systems

Adjusting the chemical equilibrium system in thermodynamic calculations involves the identification of phases, their constituents, and the system components – all these must originally be present in the initial data-file. ChemSheet further allows for deleting or activating phases and/or constituents from a calculation.

The latter group of routines provide a very useful set of tools, since they allow the suppression of otherwise stable phases in order to calculate metastable conditions. This feature can also be utilised in the kinetically controlled calculations, where the introduction of a suppressed, auxiliary invariant phase may be used for unidirectional computation of the Gibbs energies beyond the equilibrium point (see e.g. the diagrams of figure 11). Also, by elimination of phases and/or constituents which are known not to be stable under the chosen conditions, considerable increase in computation speed can be gained.

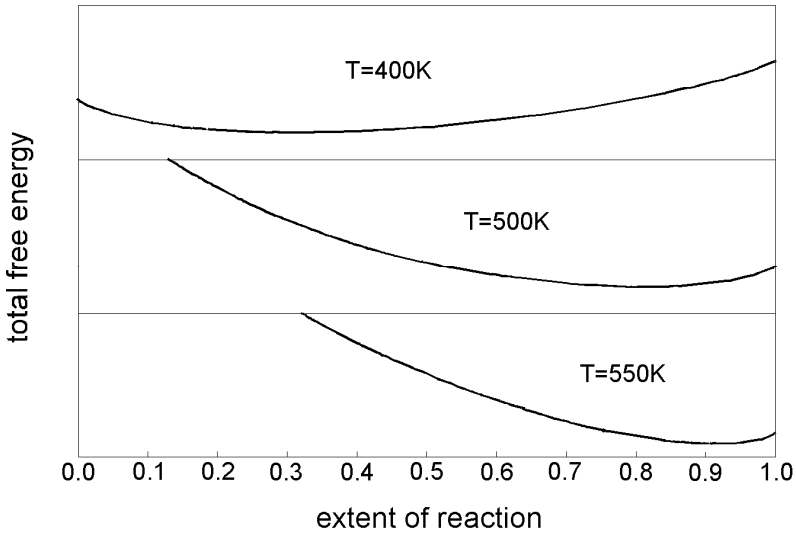

Figure 11. Gibbs energy as function of the extent of reaction for the reaction 2 NH_3 = N_2 + 3 H_2 at various temperatures.

3.3.3 Adjusting a system with immaterial constraints

Adjusting the system for constrained Gibbs energy calculations is basically very similar to the procedure involved in the conventional equilibrium calculation. The immaterial constraints must be defined beforehand and be included in the datafile, while in ChemSheet one may recognise them as system components and constituents, interpreted as parts of the conservation matrix. The necessary extension of the thermodynamic datafile (to introduce the immaterial constraints as bestowed in Table 1) were originally introduced by hand, but recently the program CSFAP has been available for this purpose [5].

For such systems as those including surface phases with their respective constituents and surface components and e.g. Donnan equilibria with two aqueous phases separated by a semi-permeable membrane, there is little or no difference at all in adjusting the system. The phases, phase constituents, and the particular system components are identified analogously with the bulk equilibrium systems.

For systems including reaction rate controls, the program CSFAP is first to be applied to select the kinetically controlled species. CSFAP creates the respective (immaterial) system component(s) and, corresponding to each reaction constraint, the auxiliary row constituents identified as R(IDENT)+ and R(IDENT)-, which can

be used for dynamic inputs for the forward and reverse reactions [3, 4]. The two constituents appear as 'virtual' phases of the system and by their usage for the dynamic input the advancement of the controlled reaction can be adjusted without interfering the mass and energy balances of the system. The input is typically derived from a known reaction rate, which can be formulated using features of Excel (or solved with another compatible subroutine).

The default state of the virtual phases R(IDENT)+ and R(IDENT)– is suppressed in ChemAPP, while their activation can be utilised to recognise the global equilibrium condition for the system [3].

3.3.4 Setting the initial conditions and performing the Gibbs energy calculations

ChemSheet offers the same features as ChemApp for performing the thermodynamic calculation. The two methods that will cover most cases experienced in practice are the one using global conditions of the system and the one by defining streams.

Using the method of global conditions, it is merely needed to set single conditions e.g. for pressure and temperature, and enter incoming species to define the composition of the system. Instead of temperature and pressure, other variables of state can be chosen too. The calculation is performed by using the reference state data as defined in the datafiles.

While the streams mode is used, the incoming flows are used as references. The input stream has constant temperature and pressure, and contains one or more phases of given composition. Hence, the conditions for the three variables – composition, temperature and pressure – need to be defined for one or more input streams. This method must be used for calculation of the extensive properties of reactions; for example, those involving the heat balance or the adiabatic temperature of a combustion process. It is also convenient to use the stream mode for process and reactor calculations, where it is known what is entering the system and it is desired to calculate results at various stages during and at the end of the process.

Calculation results for the following variables can be obtained

- total pressure, total volume, temperature
- equilibrium amount of phases, phase constituents, and system components
- chemical potential and activity

- heat capacity, enthalpy, entropy, and Gibbs energy of the equilibrium state
- mass or mole fraction of a system component or phase constituent.

From the results of ChemSheet, the thermodynamic properties, *Cp*, *H*, *S*, and *G* of a single phase and its constituents can also be received.

In addition to the aforementioned data, the Constrained Gibbs energy (CFE) calculation can be used to receive

- surface and interfacial energy (surface tension)
- equilibrium amount of surface and adsorption phases and their constituents
- equilibrium amounts of ionic species in Donnan equilibria
- the osmotic (swelling) pressure of Donnan systems
- affinity of irreversible non-equilibrium reactions (as function of time).

The results will be retrieved within Excel into the range specified by the user via the ChemSheet dialog. Excel graphics and all its postprocessing capabilities can of course be utilised. It is also expedient to an advanced user to work with Excel's programming tools (such as Visual Basic) to produce even multi-stage process models.

3.4 Applications of ChemSheet

ChemSheet has bee available as a stand-alone software product since 1999. Since then, a number of applications, both industrial and scientific have been developed. Brief descriptions of several projects employing ChemSheet can be found at GTT's Technical Thermochemistry Web Page (http://www.gtt-technologies.de), as well as at the VTT Web Page (http://www.vtt.fi).

ChemSheet applies to a wide variety of problems ranging from materials science to chemical and environmental processing. The applications in materials processing range from investigations of chemical and physical vapour deposition surface phase stabilities [6, 7] to thermodynamics of steelmaking, e.g. by Drozdz & coworkers in combining a metal bath mixing model with a thermodynamic model [8] and the modelling of inclusion formation by Holappa et al. [9].

Examples of high-temperature processes and equilibrium studies are those involved with the Åbo Black-Liquor Recovery Boiler Advisor [10]. This program, developed by the Åbo Akademi University is intended to provide information about the high-temperature ash and flue gas chemistry in black liquor recovery boilers of kraft pulp mills. There are also several modelling

projects involving flue gas and ash chemistry and their related aerosol formation with ChemSheet, see e.g. [11, 12]

The development of modelling tools for oxidation and high-temperature corrosion was performed in the EU-project OPTICORR (Optimisation of in-service performance of boiler steels by modelling high-temperature corrosion) [13]. With ChemSheet two key processes were treated: the internal corrosion of the metallic material by diffusion of gases and metals and local phase formation as well as the corrosion of heat exchanger material under a molten salt layer which is in contact with an outer gas phase, i.e. salt-induced hot corrosion.

ChemSheet has been used for solubility equilibria in hydrometallurgical processing e.g. by Koenigsberger [14], Kolhinen and Jalkanen, and Salminen et al.[15, 16]. A particular application, where the ability to calculate multi-phase Donnan equilibria is the modelling of aqueous fibre suspensions for pulp and papermaking industries has been intensively studied particularly in Finland and Sweden [17, 18, 19].

Combination of Reaction Kinetics with Gibbs Energy Minimization in ChemSheet is applied together with the RATEMIX® algorithm to calculate multicomponent chemical reaction mixtures as a series of sequential thermochemical states. The RATEMIX method applies the Constrained Gibbs energy approach in process simulation [20, 21, 22]. The calculation procedure combines chemical kinetics with multicomponent thermodynamics and may be used to simulate the multicomponent reactors as a thermochemical ’natural process’. The method is applicable in processes where the core thermodynamic and kinetic data of the system are known and the time-dependent heat transfer data can either be measured or estimated by calculation. The reactor simulations already performed using this method include high temperature aerosol reactors (e.g. $TiCl_4$ oxidation), zinc vapor oxidation during zinc condensation, counter-current rotary drums with chemical reactions, causticisation of aqueous (impure) sodium carbonate solution with lime.

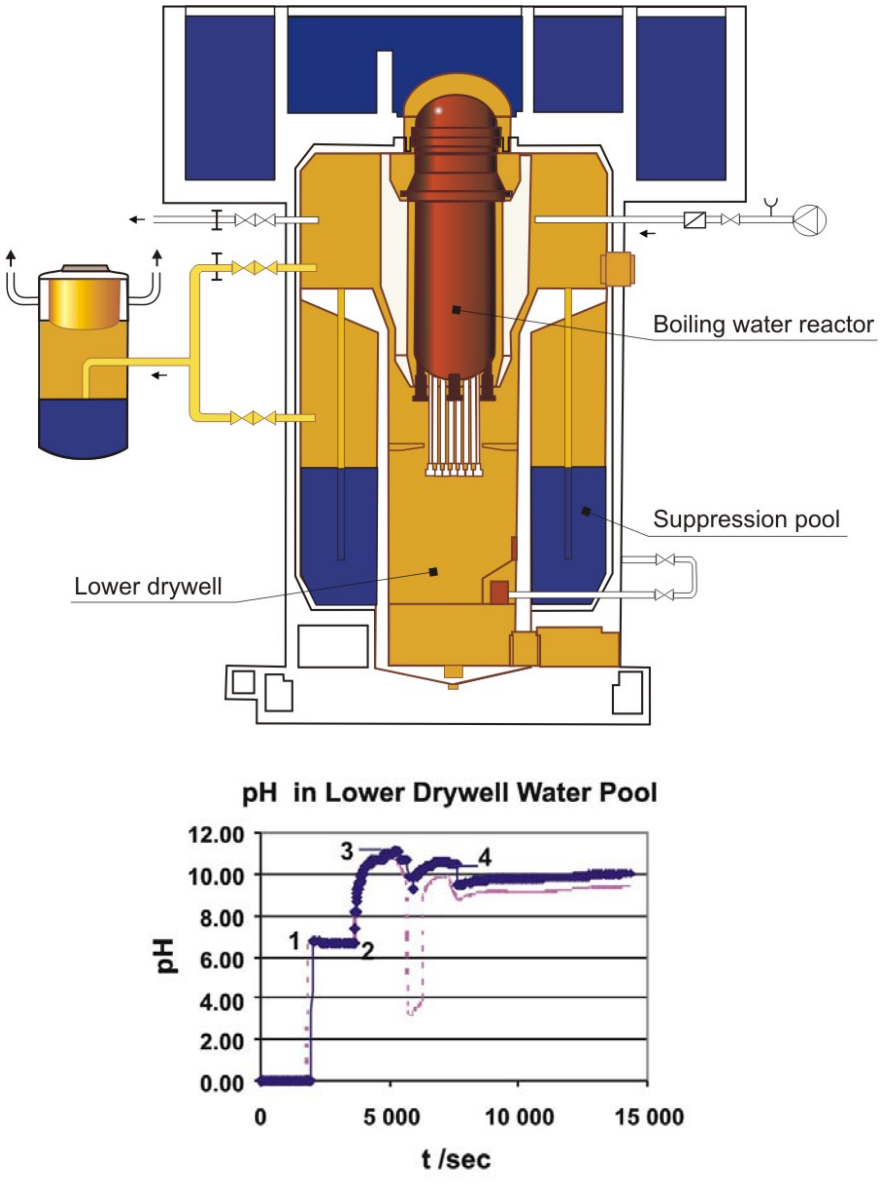

Figure 12. Olkiluoto BWR containment systems (above) and simulated pH in the lower drywell water pool (below) 1. Flooding of the lower drywell begins. 2. Water filling of the containment and supply of NaOH to the containment begin. 3. Vessel failure. Relocation of core debris to the lower drywell water pool. 4. Filtered venting begins. The dotted curve shows condition with the unwanted pH drop [23].

An interesting application of ChemSheet is its use in the accident management of nuclear plants in the field of reactor chemistry (figure 12). ChemSheet (and further ChemApp) was connected with the thermohydraulic program MELCOR to provide chemistry calculations for nuclear accident scenarios [23] During a severe accident at a Boiling Water Nuclear Reactor (BWR), a large amount of chlorine (Cl_2) and hydrochloric acid (HCl) might be released by irradiation and heating from the synthetic rubbers used as insulation material of the electrical cables. Most of the released chlorine hydrolyses within the water pools to hydrochloric and hypochlorous acid. However, pH of the water pools surrounding the reactor core must be kept non-acidic to prevent the release of radioactive gases, particularly iodine compounds. ChemSheet, in combination with MELCOR, was used for designing the necessary containment system and pumping rates to neutralize the generated acids with 50 % caustic soda.

The MELCOR combination has been further developed to a more generic method (CHEMPOOL), which is used for the pH calculations of nuclear accident scenarios. For such work, particular quality assurance protocols (QAP) for the verification and validation of the thermodynamic data and software are needed. The said QAP has in 2008 been approved as one part of work abiding the NRC 10CFR50 Appendix B (Nuclear Safety Related Work) [24] set by the Nuclear Regulatory Commission in the U.S.A.

An important feature of ChemSheet is its use within the industry for customised process and chemical dosage design, again ranging from chemical industry to pulp and paper and to metallurgy and steelmaking [25, 26, 27, 28, 29, 30, 31, 32]. For fuel cell development, both purification of liquid fuels, gas reforming and fuel cell operations have been simulated with ChemSheet [33, 34]. Some such applications have been further developed to Excel-based process models or expert systems. A recent example is the ChemSheet-based STEAMAX boiler design procedure, which was published by Metso Power in 2008. STEAMAX is a thermodynamically based ’expert system’, which is used for the design and material choice of bio- and mixed fuel boiler superheaters [35].

The latest interest in applying ChemSheet is in its ability to take advantage of the Constrained Gibbs energy calculations. The constraints can be applied to improve paraequilibrium calculations when studying the solidifying of steels and alloys [36], for interfacial energies and adsorption [37, 38] and even for analysing biochemical reaction pathways [39]. The diversity of the novel method will allow for additional interesting applications to emerge in the future.

3.5 References

[1] Koukkari, P., Penttilä, K., Hack, K. and Petersen, S. CHEMSHEET – An Efficient Worksheet Tool for Thermodynamic Process Simulation. In: Brechet, Y. (ed.). Microstructures, Mechanical Properties and Processes, Euromat 99 – Vol. 3, Wiley-VCH Publishers, Weinheim, 2000. Pp. 323–330. ISBN 3-527-30122-4.

[2] Koukkari, P. and Pajarre, R. Calculation of Constrained Equilibria by Gibbs Energy Minimization, Calphad, Vol. 30 (2006), pp. 18–26.

[3] Koukkari, P., Pajarre, R. and Hack, K.Constrained Gibbs energy minimisation, International Journal of Materials (former Z. Metallkd), 98 (2007) 10, pp. 926–934.

[4] Koukkari, P. and Pajarre, R. Introducing Mechanistic Kinetics to the Lagrangian Gibbs Energy Calculation, Computers and Chemical Engineering, Vol. 30 (2006), pp. 1189–1196.

[5] GTT Technologies Technical Product Information at http://www.exmente.co.za/ downloads/gtt/ techprodinfo.pdf, 2009-05-21.

[6] Fillot, F., Chenevier, B., Maîtrejean, S., Audier, M., Chaudouëtb, P., Bochu, B., Sénateur, J. P., Pisch, A., Mourier, T., Monchoix, H., Guillaumot, B. and Passemard, G. Investigations of the interface stability in HfO2–metal electrodes. Microelectronic Engineering, Vol. 70, Issues 2–4, November 2003. Pp. 384–391.

[7] Auvray, L., Chaussende, D., Baillet, F., Charpentier, L., Pons, M. and Madar, R. Comparison between various chemical systems for the CVD step in the CF-PVT crystal growth method. Materials for Advanced Metallization 2003, Materials Science Forum Vols. 457–460 (2004). Online at http://www.scientific.net, © (2004) Trans Tech Publications, Switzerland. Pp. 135–138.

[8] Drozdz, P. and Falkus, J. The modelling of vacuum steel refining in the RH degassing unit based on thermodynamic analysis of the system. Archives of Metallurgy and Materials, Vol. 52, 2007, Issue 4, pp. 585–591.

[9] Holappa, L., Hämäläinen, M., Liukkonen, M. and Lind, M. Thermodynamic Examination on Inclusion Modification and Precipitation from Calcium Treatment to Solidified Steel. 6th Int. Conf. on Clean Steel, Balatonfured, Hungary, 10–12 June 2002.

[10] Lindberg, D. and Backman, R. Thermochemical modelling of the inorganic reactions in pressurized black liquor gasification, May 13–16, 2003, Park City, UTAH.

[11] Jöller, M., Brunner T. and Obernberger, I. Modeling of aerosol formation during biomass combustion for various furnace and boiler types. Fuel Processing Technology, Vol. 88, Issues 11–12, December 2007, pp. 1136–1147.

[12] Mattenberger, H., Fraissler, G., Brunner, T., Herk, P., Hermann, L. and Obernberger, I. Sewage sludge ash to phosphorus fertiliser: Variables influencing heavy metal removal during thermochemical treatment. Waste Management, Vol. 28, Issue 12, December 2008, pp. 2709–2722.

[13] Heikinheimo, L., Baxter, D., Hack, K., Spiegel, M., Hämäläinen, M., Krupp, U., Penttilä, K. and Arponen, M. Optimisation of in-service performance of boiler steels by modelling high-temperature corrosion. Materials and Corrosion, Vol. 57, Issue 3, pp. 230–236.

[14] Koenigsberger, E. Solubility equilibria. From data optimization to process simulation. Pure Appl. Chem., Vol. 74, No. 10, 2002, pp. 1831–1841.

[15] Kolhinen, T. and Jalkanen, H. Thermodynamic modeling of ammoniacal nickel sulphate solutions. Scandinavian Journal of Metallurgy, Vol. 34, Issue 6, pp. 334–339.

[16] Salminen, J., Kobylin, P., Liukkonen, S. and Chiavone-Filho, O. Gibbs energy approach for aqueous processes with HF, HNO_3, and CO_2 $CaCO_3$. AIChE Journal, Vol. 50, Issue 8, pp. 1942–1947.

[17] Koukkari, P., Pajarre, R. and Pakarinen, H. Modeling of the ion exchange in pulp suspensions by Gibbs energy minimization. Journal of Solution Chemistry, Vol. 31 (2002) No. 8, pp. 627–638.

[18] Kalliola, A., Pajarre, R., Koukkari, P., Hakala, J., Rimpinen, O., Nuortila-Jokinen, J., Kukkamäki, E. Control of pH and calcium chemistry with multiphase modelling. In: Modelling and Simulation of Wet End Processes and Innovative Process Control. Kappen, J., Dietz, W. and Grenz, R. (eds.). Books on Demand GmBH, Munich, 2008. Pp. 77–88.

[19] Törngren, A. and Puukko, M. Process Chemistry simulation in Extend based programs, CheMac, FlowMac and KraftMac, http://www.aforsk.se/research_reports/forest-industry.php, 2007-12-17.

[20] Koukkari, P. A Physico-Chemical Method to Calculate Time-Dependent Reaction Mixtures. Computers & Chemical Engineering, Vol. 17, (1993) No. 12, pp. 1157–1165.

[21] Pajarre, R. Modelling of equilibrium and non-equilibrium systems by Gibbs energy minimisation. M.Sc. Thesis, Helsinki University of Technology, Department of Chemical Technology, Espoo, 2001.

[22] Koukkari, P., Pajarre, R. and Hack, K. Setting Kinetic Controls for Complex Equilibrium Calculations. In: Hack, K. (ed.). SGTE Casebook, Thermodynamics at Work, 2nd Ed., Woodhead Publishing, Cambridge, England, 2008. Pp. 359–367.

[23] Sjövall, H. Severe Accident Management in Olkiluoto 1 and 2, http://sacre.web.psi.ch/oecd-sami/Papers/p26-Sjoevall/oecdsampsiolkiluoto1and2sam.pdf, 2009-05-21.

[24] http://www.nrc.gov/reading-rm/doc-collections/cfr/part050/part050-appb.html, 2009-08-13.

[25] Yokota, M. Moving bed reactor modelling by ChemSheet, 2007 RCCM Workshop, November 13–14, Tokyo.

[26] Koukkari, P., Penttilä, K. and Keegel, M. Coupled Thermodynamic and Kinetic Models for High-Temperature Processes. Proceedings of the 10th International IUPAC Conference on High Temperature Materials Chemistry, Part I, Forscungszentrum Julich, 2000. Pp. 253–256.

[27] Kalliola, A. and Pakarinen, H. Experiences of pH buffering and calcium chemistry control in neutral papermaking. In: Chemical Technology of Papermaking, PTS Symposium, Munich, Germany, 2002. Pp. 5-1–5-11.

[28] Weaver, A., Kalliola, A. and Koukkari, P. A strategy for controlling pH and Ca hardness in paper making, Scientific and Technical Advances in Wet End Chemistry. Third Major Pira International Conference. Wien, 22–23 May 2002. Pira International (2002).

[29] Bruno, M. J. Aluminum Carbothermic Technology, DOE/ID/13900, December 31, 2004.

[30] Valovirta, E. Castability properties of resulfurised steels. (Master's thesis) Helsinki University of Technology, Department of Materials Science and Engineering, 2001.

[31] Miettinen, J., Louhenkilpi, S., Kytönen, H., Laine, J., Wang, S., Hätönen, T., Petäjäjärvi, M. and Hooli, P. IDS Tool – Theory And Applications for Continuous Casting and Including Modeling of Microstructure and Inclusions. 6th ECCC – 6th Europe, 3–6 June, 2008 Riccione, Italy.

[32] Rheinberg, O. van, Lucka, K., Köhne, H., Schade, T. and Andersson, J. T. Selective removal of sulphur in liquid fuels for fuel cell applications. Fuel, Vol. 87, Issues 13–14, October 2008, pp. 2988–2996.

[33] Yahagi, M. ChemSheet models for fuel cell applications. 2006 RCCM Workshop, November 13–14, Tokyo.

[34] Enestam, S., Niemi, J. and Mäkelä, K. STEAMAX – A novel approach for corrosion prediction, material selection and optimization of steam parameters for boilers

firing fuel and fuel mixtures derived from biomass and waste The Clearwater Coal Conference, Clearwater, Florida, June 2008.

[35] Koukkari, P., Pajarre, R., Kondratjev, A. and Hack, K. Calculation of back diffusion with the constrained Gibbs energy method. CALPHAD XXXVII, 15–20. June, 2008, Saariselkä, Finland.

[36] Shobu, K. CaTCalc: New thermodynamic equilibrium calculation software, CALPHAD Journal, in press.

[37] Pajarre, R., Koukkari, P., Tanaka, T. and Lee, Y. Computing Surface Tensions of Binary and Ternary Alloy Systems with the Gibbs'ian Method. Calphad, Vol. 30 (2006), pp. 196–200.

[38] Tang, K., Olsen, J., Johansen, S. and Kolbeinsen, L. Modelling of Surface/Interfacial Properties for the Ladle Refining Si Metal Processes, MOLTEN 2009 – International Conference on Molten Slags. Fluxes and Salts, Santiago de Chile, 18.–21.1.2009.

[39] Blomberg, P. and Koukkari, P. The Combination of Transformed and Constrained Gibbs Energies. Mathematical Biosciences 220 (2009), pp. 81–88.

4. Gas precipitation model for heat exchangers of power plants

Klaus Hack, GTT-Technologies

A thermodynamic model of flue gas deposits, potentially formed on the heat exchanger or duct surfaces in a power plant was constructed with ChemSheet. The spreadsheet interface allows for easy handling of model inputs and introduction of empirical parameters, which describe the initial aerosol freight in the gas or the degree of precipitate adhesion on the surfaces.

4.1 Background

Combustion of coal, wood, peat or mixed fuels in power plants releases flue gas with varying chemical composition. In addition to its major components the flue gas contains different amounts of minor species, some of which are condensed already on the heat exchanger and duct surfaces and appear potentially corrosive deposits [1]. The flue gas is in fact a gas-plus-aerosol two phase flow. A ChemSheet model has been set up which permits, on the basis of a given overall gas-plus-aerosol composition, investigation of the formation of precipitates from the combustion gas on cooling.

4.2 Methods

The model uses the internal “StepIndex” -variable of ChemSheet to set the gradual cooling of the flue gas. With the total number of steps defined prior to calculation the temperature in each step can be decreased using an Excel formula

(see figure 16). The user may furthermore influence the calculation by way of a “transfer coefficient” for the aerosols and of a “sticking factor” for the precipitates (figure 17). The former permits control of the amount of aerosols that is transferred from the combustion chamber by the gas phase (range: 0 to 1) while the latter permits in a course way to control the amount of precipitates extracted from the gas through sticking on the walls or pipes of the heat exchangers (range: 0 to 1). Thus the user can investigate the influence of the amount of carry-over dusts from the combustion chamber to the heat exchangers and the level of wall-sticking of precipitates in the higher temperature range on the precipitates in the lower temperature range.

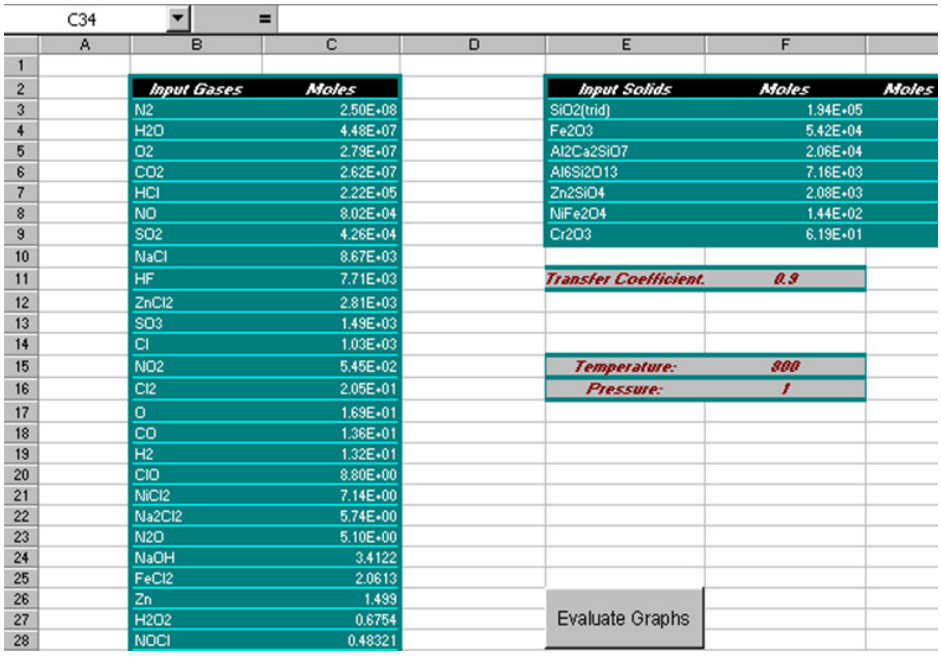

Input Gases	Moles
N2	2.50E+08
H2O	4.48E+07
O2	2.79E+07
CO2	2.62E+07
HCl	2.22E+05
NO	8.02E+04
SO2	4.26E+04
NaCl	8.67E+03
HF	7.71E+03
ZnCl2	2.81E+03
SO3	1.49E+03
Cl	1.03E+03
NO2	5.45E+02
Cl2	2.05E+01
O	1.69E+01
CO	1.36E+01
H2	1.32E+01
ClO	8.80E+00
NiCl2	7.14E+00
Na2Cl2	5.74E+00
N2O	5.10E+00
NaOH	3.4122
FeCl2	2.0613
Zn	1.499
H2O2	0.6754
NOCl	0.48321

Input Solids	Moles	Moles
SiO2(trid)	1.94E+05	
Fe2O3	5.42E+04	
Al2Ca2SiO7	2.06E+04	
Al6Si2O13	7.16E+03	
Zn2SiO4	2.08E+03	
NiFe2O4	1.44E+02	
Cr2O3	6.19E+01	

Transfer Coefficient.	0.3
Temperature:	800
Pressure:	1

Evaluate Graphs

Figure 13. The ChemSheet input screen for the gas precipitation model.

Input Gases	Moles
N2	2.50E+08
H2O	4.48E+07
O2	2.79E+07
CO2	2.62E+07
HCl	2.22E+05
NO	8.02E+04
SO2	4.26E+04
NaCl	8.67E+03
HF	7.71E+03
ZnCl2	2.81E+03
SO3	1.49E+03
Cl	1.03E+03
NO2	5.45E+02
Cl2	2.05E+01
O	1.69E+01
CO	1.36E+01
H2	1.32E+01
ClO	8.80E+00
NiCl2	7.14E+00
Na2Cl2	5.74E+00
N2O	5.10E+00
NaOH	3.4122
FeCl2	2.0613
Zn	1.499
H2O2	0.6754
NOCl	0.48321
NaF	0.40719
Na2SO4	0.19992
Fe(OH)2	0.18922
AlOH	0.16732

Figure 14. The composition of the combustion gas.

Input Solids	Moles	Moles transfer
SiO2(trid)	1.94E+05	1.94E+05
Fe2O3	5.42E+04	5.42E+04
Al2Ca2SiO7	2.06E+04	2.06E+04
Al6Si2O13	7.16E+03	7.16E+03
Zn2SiO4	2.08E+03	2.08E+03
NiFe2O4	1.44E+02	1.44E+02
Cr2O3	6.19E+01	6.19E+01

Figure 15. The composition of the aerosol.

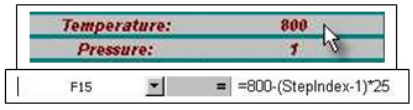

Figure 16. The temperature input box and the step formula using StepIndex.

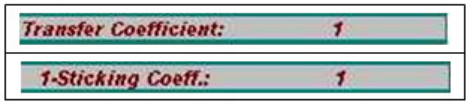

Figure 17. The input boxes for the Transfer Coefficient of the aerosol and the sticking coefficient (1-value).

Note: The values for the composition of the gas and the aerosol as shown in the spreadsheet interface in figure 13 and in figures 14 and 15 have been taken from a process model for a waste incinerator. (Courtesy of M. Modigel and D. Liebig, Institut für Verfahrenstechnik, RWTH Aachen.)

4.3 Results

The simple ChemSheet-based model has been used for parameter studies concerning the values of the “transfer coefficient” (initial aerosol freight) and the “sticking coefficient” (adhesion of precipitates on walls or pipes). The temperature range has been the same in all calculations assuming cooling between 800 and 300 K in steps of 25 K. The input composition of the gas and the aerosol are as introduced above. As the gas composition represents that of a waste incinerator, they could not as such be representative for a very wide range of combustion power plants. Nevertheless, the results of the simulation calculations

as shown below indicate what thermochemical modelling can do in complex cases such as those discussed here.

Figure 18 shows the result of a kind of reference calculation: this calculation contains all gas species and all condensed phases for each of the temperatures covered in the calculations. There are no material losses through sticking on the walls. Thus the chemical composition of the system is the same throughout the entire temperature range. Nevertheless, a first “feel” for the chemistry of such a complex system can be gained. Chlorides are formed at temperatures between 500 and 600 K, fluorides occur at temperatures below 550 K, while sulphates can be found in the entire range; at higher temperatures as a solid solution between Na_2SO_4 and $CaSO_4$, at lower temperatures as pure Na_2SO_4, $CaSO_4$ and also $NiSO_4$. Quartz, alumina, hematite, and Zn-aluminate are found at all temperatures, while mullite only occurs at high temperatures (775 to 800 K). These oxide phases are mainly due to the aerosol freight that is assumed at the start of the cooling sequence.

This first calculation cannot be related directly to the reality in a power station since it is known that some of the condensed matter transported by the gas and some of the condensed matter that precipitates from the gas on cooling sticks to the walls and heat exchanger pipes. Material has to be taken out of the calculation stepwise in order to simulate this behaviour. The following figures will give a first view on that situation.

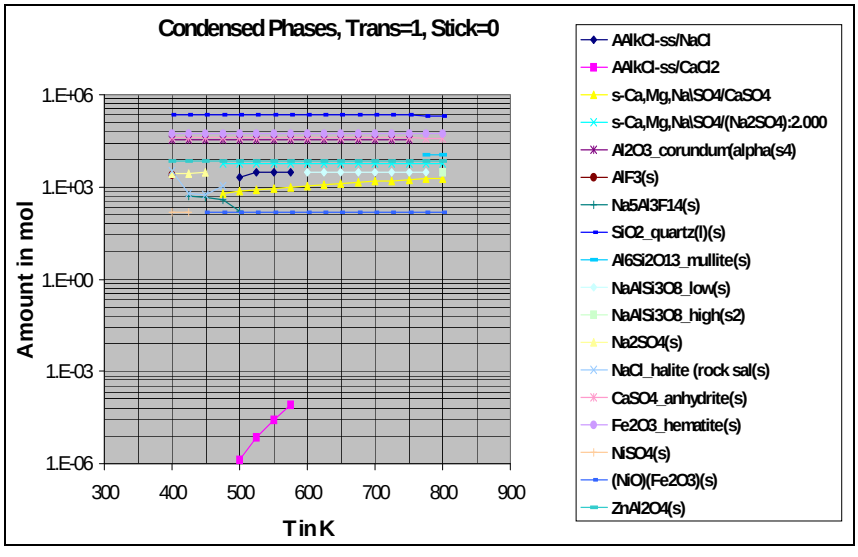

Figure 18. Condensed Phases for the case of full aerosol transfer and no wall sticking.

In figure 19 is shown how the condensed phases will behave if all matter that is in aerosol form in the combustion chamber is transferred to the cooling stages and if 10% of the condensed material that is formed at each temperature step is taken out of the calculation before the next step thus simulating wall sticking. The condensed phases formed are both salts and mineral oxides with the oxides occurring at all temperatures as in the first calculation, figure 18. Concerning the salts it can be seen that the sulphates form again the majority with a small temperature window between 575 and 525 K in which NaCl forms. The fluorites AlF_3 and $5NaF.3AlF_3$ are present again at low temperatures.

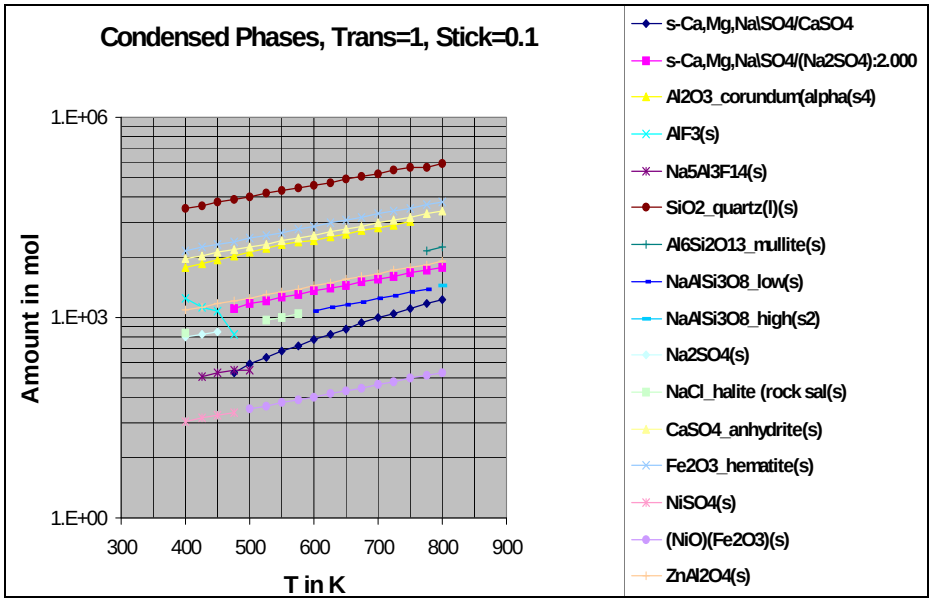

Figure 19. Condensed Phases for the case of full aerosol transfer and 10% wall sticking.

In figure 20 is shown a situation similar to that for figure 19, but with a slightly higher sticking coefficient and the additional assumption that not all aerosol is transferred to the cooling sequence, i.e. there is also some wall sticking already in the combustion chamber. It is interesting to note how much of a change in the phase constellation and also in the temperatures of stability is brought about by such a relatively small change in the sticking coefficient. No chloride formation is found in these calculations and the only fluoride is AlF_3 at low temperatures. In the other hand there is $ZnSO_4$ formation in an intermediate temperature range. This result, in comparison to that in figure 19, shows that the sticking factor

clearly has an influence on the results. It will therefore be very important for the future development of modelling of the heat exchanger processes to know in more detail the sticking behaviour of the condensed phases.

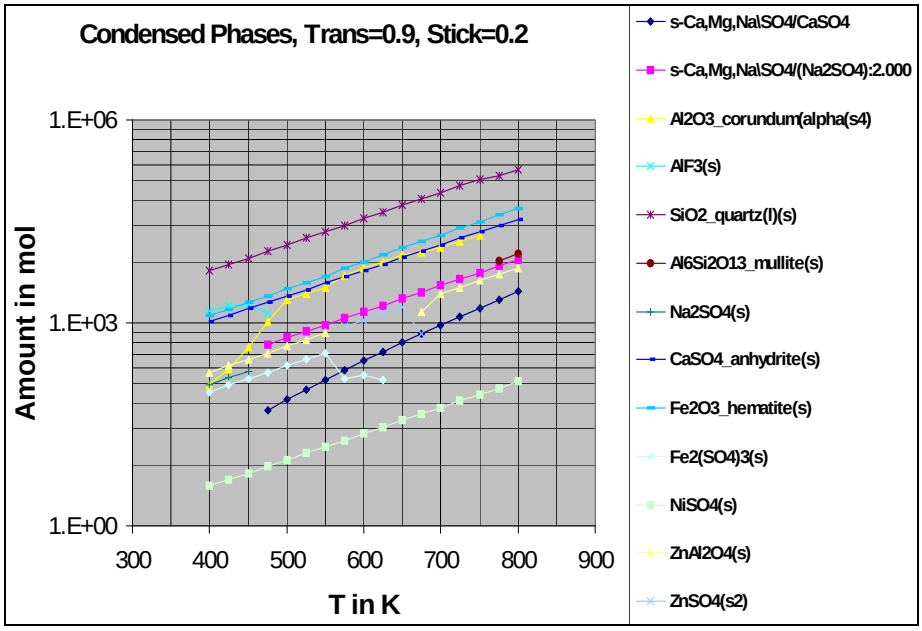

Figure 20. Condensed phases for restricted transfer (90%) and 20% sticking.

From figure 21 it is obvious (low transfer coefficient and low sticking factor) that a certain aerosol freight is necessary in order for some precipitation to occur. The precipitates are a mix of oxides (minerals) and salts with the salts being sulphates. It must be assumed that the chance to find salts from a mere condensation effect are small. They form mainly as a result of reactions with other solids already present as aerosols. This holds particularly for the chlorides which do not occur if the aerosol amount is assumed to be low.

Figure 22 has been generated for the very extreme case of almost no transfer of aerosol (10%) from the combustion chamber to the cooling sequence and for very high sticking (80%) of the precipitates formed. In contrast to all previous simulations there is now a strictly linear decrease of the amounts of precipitates with decreasing temperature. This is due to the extreme choice of the simulation parameters. This choice is not very likely to be close to the real case.

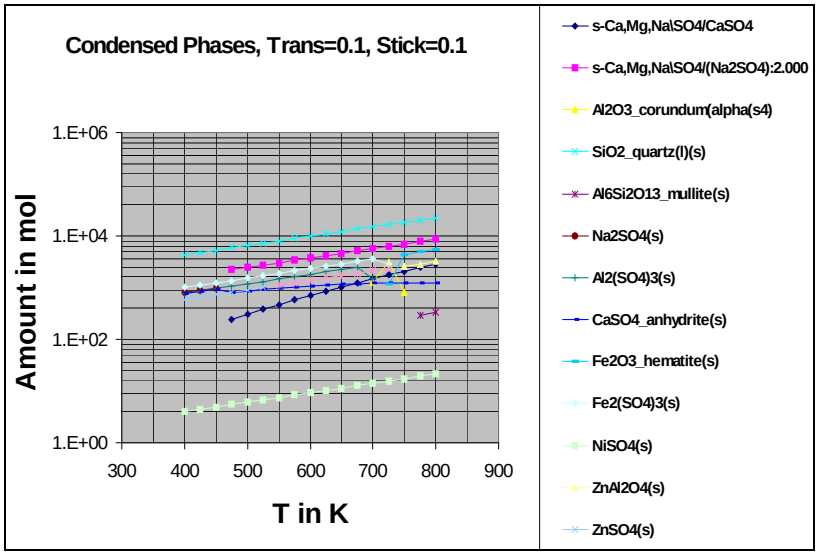

Figure 21. Condensed phases low transfer(10%) and low sticking (10%).

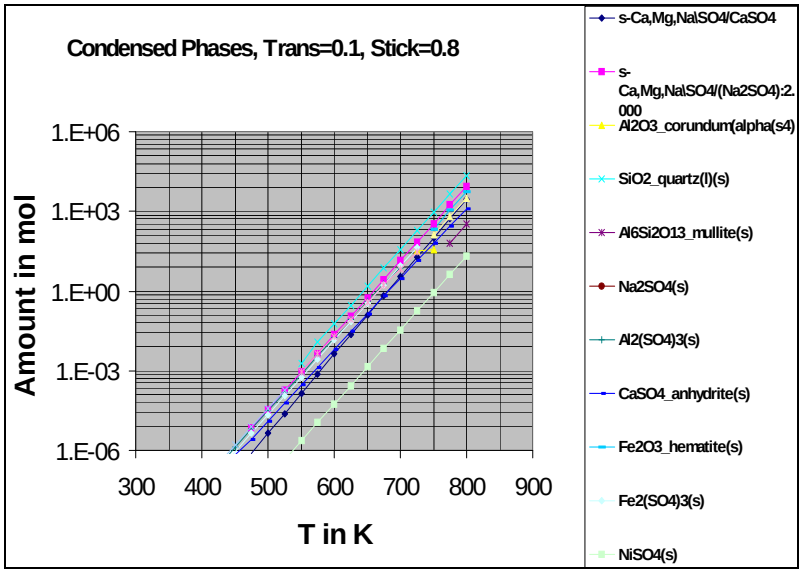

Figure 22. Condensed phases for very low transfer (10%) and very high sticking (80%).

4.4 References

[1] OptiCorr Guide Book, EUR 21736 EN, VTT Research Notes 2309.
http://www.vtt.fi/inf/pdf/tiedotteet/2005/T2309.pdf.

5. Calculation of slag windows in steelmaking

Matti Liukkonen, VTT

The presence of non-metallic elements in steel and alloy melts incorporate a number of effects, for which it is necessary to control the multicomponent chemistry in ladle processing as well as in casting. The non-metallic elements appear either as processing elements (oxygen, nitrogen) or they are deliberately added to the melt to improve the final product quality (e.g. sulphur to improve steel machinability). The formation of inclusions in the melts is then a process, where these non-metallic impurities will be reacting with various metallic components of the melt. In steels, different oxide nitride or sulphide based inclusions are characteristic.

5.1 Background

The inclusions incorporate inhomogeneity in the final steel product and thus are often held undesired. Typically they decrease the tensile strength and may also reduce surface and polishing properties. In machining, the oxide inclusions lead to increased wear of the tool edges. However, in chip machining, e.g. sulfide based inclusions can be beneficial, as the chip formation and lubrication properties of the preform may be improved. The inclusion content as well affects both the brittleness and hardness of the final product.

The control of inclusions and their formation has become one major issue in modern steelmaking. The addition or removal of inclusions, while performed in the melt refining stages, may yet lead to operational problems. For example, when the melt contains aluminium, oxygen and sulphur, calcium is added as a fluxing agent to prevent excessive formation of Al-oxide inclusions. The oxide

phases would solidify in higher temperatures than the Ca-aluminates, instigating clogging phenomena in the casting area. It is then imperative to remain alert on the multiple phases and constituents, which may form as function of temperature and composition in various steel melts.

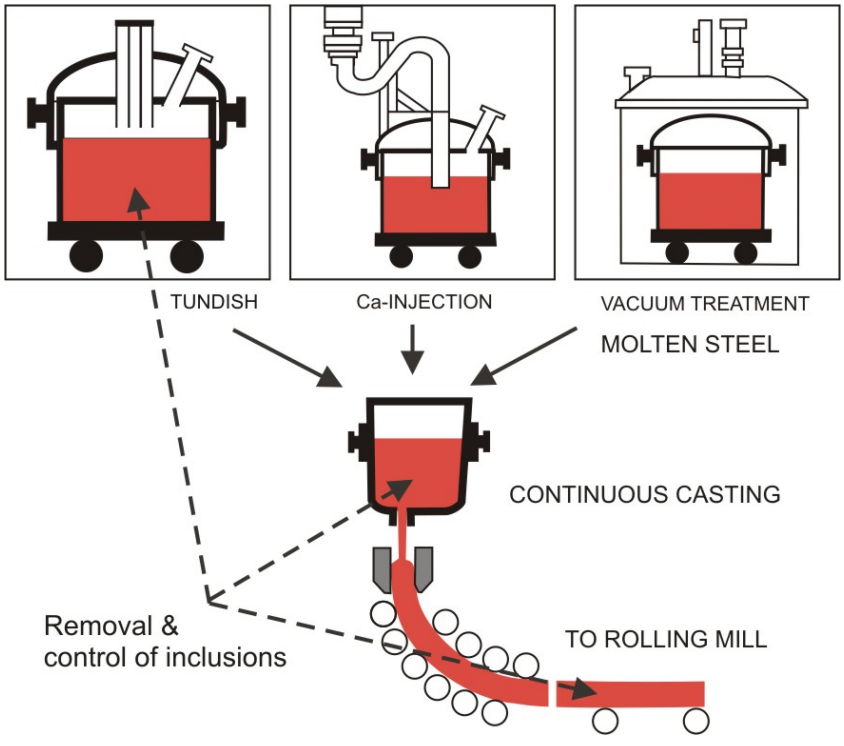

Figure 23. Continuous casting of steel with the preceding melt refining.

5.2 Methods

A characteristic multi-phase description of the steel melt containing manganese, calcium, sulphur, silicon and aluminium as additives is given in figure 24. The slag phase contains all major elements of the system and is described as a quasi-chemical oxide (slag-liquid) phase [2]. Similarly, the liquid iron contains all key elements, their interaction parameters are described with the thermodynamic Wagner model. In this somewhat schematic description, all solids are assumed as stoichiometric phases and no solid solutions are included.

The phase mapping was performed in ChemSheet by following the changes in phase composition in terms of oxygen and calcium content in the system. The

slag window calculation involves the mapping of such temperature-composition or composition-composition range (‘window’), where but negligible amount of solid inclusions are being formed from the point of view of the bloom operation in continuous casting.

Gas	Slag	Liquid	Stoichiometric	
..	Fe	Fe	C(s)	MnO(s)
	Mn	Mn	Al2O3(s)	MnO*SiO2(s)
	Ca	Ca	SiO2(s)	MnS(s)
	S	S	CaO(s)	Fe_bcc(s)
	Si	Si	CaO*Al2O3(s)	Fe_fcc(s)
	Al	Al	CaO*2Al2O3(s)	FeO(s)
	O	O	CaO*6Al2O3(s)	Fe2O3(s)
	C	C	3CaO*Al2O3(s)	Fe3O4(s)
			CaO*SiO2(s)	FeO*Al2O3(s)
			2CaO*SiO2(s)	2FeO*SiO2(s)
			CaO*2SiO2(s)	FeS(s)
...	...	...	CaS(s)	CaO*Fe2O3(s)

Figure 24.Typical multi-phase composition of steel melts.

5.3 Results

ChemSheet slag window models were developed to calculate injection doses for different grades of steel to ensure plant operation within the liquid slag range. In a system described in figure 23 one can find at a given temperature either solid aluminates, aluminates + liquid oxide, liquid oxide only, or liquid oxide + CaS-precipitate in equilibrium with the liquid steel. The composition depends on the O- and Ca-content of the steel. Figure 25 shows a typical example of a slag window calculation for steel-making. The white wedge-shaped area gives a melt range in terms of the [Ca] and [O] -content of the steel, with given amounts of sulphur and aluminium at 1600 °C. The ChemSheet dialog for defining conditions, operating on Excel is also shown.

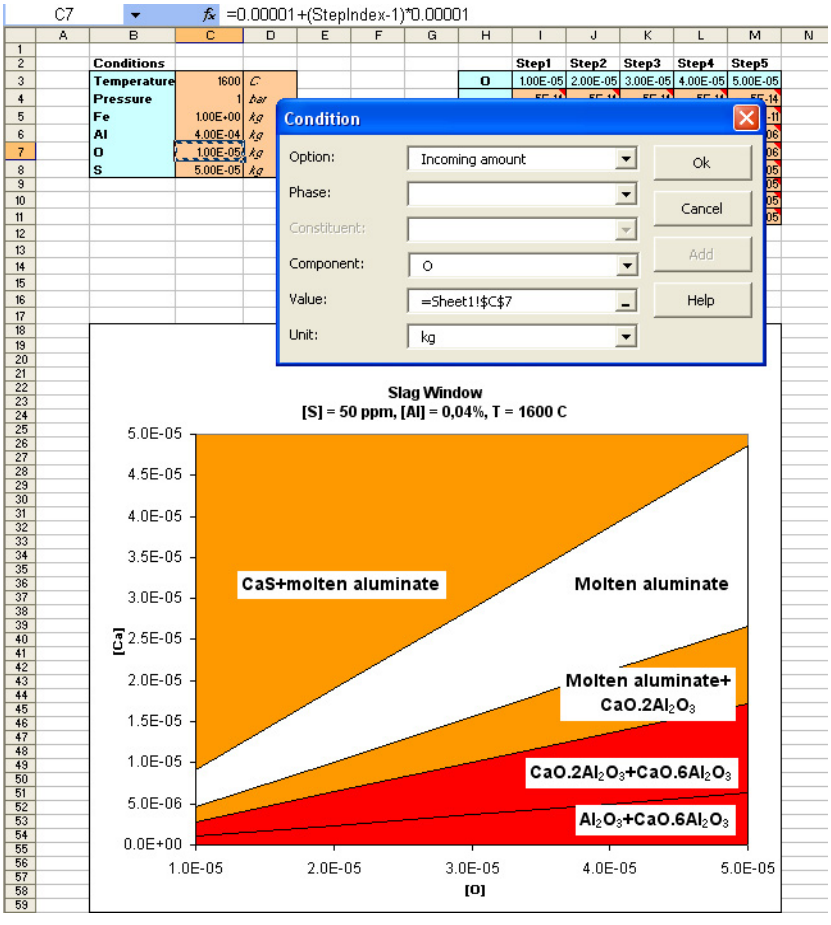

Figure 25. The ChemSheet slag window model.

A practical example of model-base inclusion control is given with the making of C09-grade steel in the Finnish Koverhar plant [1]. This particular grade was one of the new sulphurized steels, which were introduced as novel bar products. The target analysis of the grade C09 steel is given in table 4.

Table 4. Koverhar C09 -grade analysis.

	C	Si	Mn	P	S	Cr	V	Ti	Al	N
min.	0.08	0	0.25	0	0.02	0	0	0.0	0.03	0
target	0.09	0.03	0.29	0	0.025	0	0	0.02	0.03	0
max.	0.1	0.05	0.35	0.02	0.03	0.08	0.04	-	0.05	0.009

The castability requires that no solid inclusions be formed at temperatures of 1550 C. While the Ca-Al-O-interactions were known by experience, the addition of sulphur was new. Thus, slag window calculations were performed with Chemsheet to recognise the Ca-S-ratios at given levels of Al and oxygen in the system. In figure 26 the slag window calculation is shown together with the results from plant sample analysis. The slag window is formed between the saturation curves of Ca-sulfide and Ca-aluminates. The set points of Ca-injection (sample composition) in the plant appear close to the line of aluminate saturation [1].

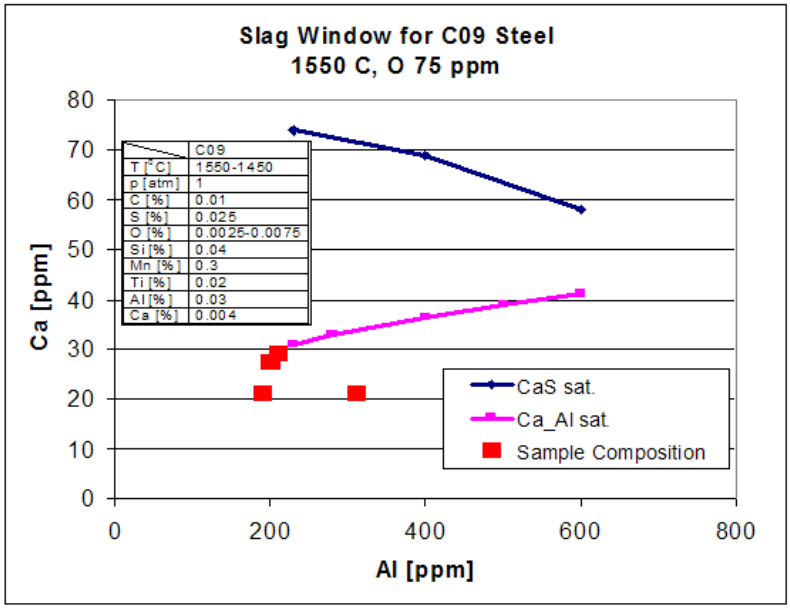

Figure 26. Ca-Al slag window in the C09 Ca-Al-O-S -system.

5.4 Conclusions

The multi-phase Gibbsian methods are practical in predicting the slag window conditions in alloy refining and steelmaking. Their flexibility to incorporate new elements into the system allows for assessment of new grades including e.g. boron or titanium as well as even rare earth components. The multiphase approach has been incorporated to an integrated steel solidification model [3], which can be used for consideration and optimisation of the conditions of continuous casting. Based on the slag window method, more sophisticated analysis on the kinetics of inclusion formation has also been made [4]. Future

work will cover increasingly the control of inclusion microstructures by combining the multiphase inclusion models with appropriate multi-scale calculations [5].

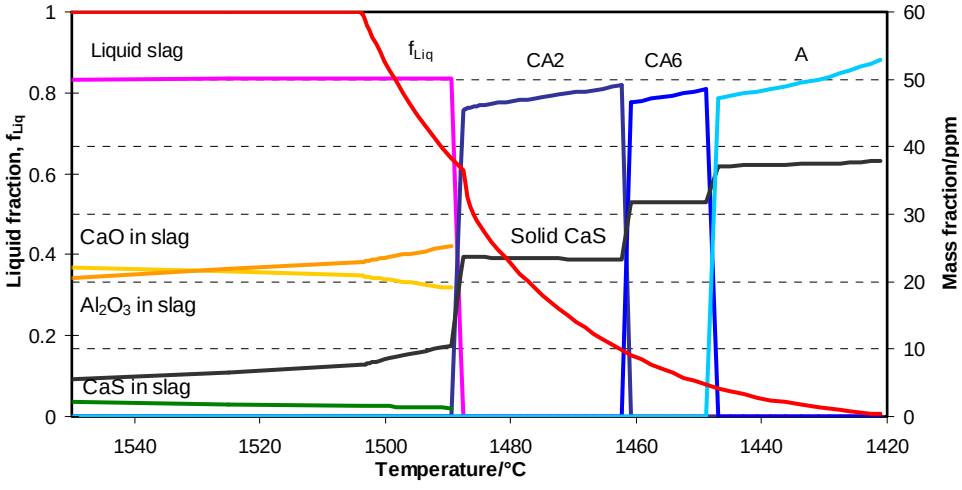

Figure 27. Formation of solid inclusion phases during steel solidification [1, 5].

5.5 References

[1] Valovirta, E. Castability properties of resulfurised steels. Helsinki University of Technology, Department of Materials Science and Engineering (Master's thesis) 2001.

[2] http://www.crct.polymtl.ca/fact/index.php. (FACT-Institute, Montreal, Canada).

[3] Holappa, L., Hämäläinen, M., Liukkonen, M. and Lind, M. Thermodynamic Examination on Inclusion Modification and Precipitation from Calcium Treatment to Solidified Steel. 6th Int. Conf. on Clean Steel, Balatonfured, Hungary, 10–12 June 2002.

[4] Lind, M. Mechanism and Kinetics of Transformation of Alumina-inclusions in Steel by Calcium Treatment. (Ph.D. Thesis), Helsinki University of Technology, Laboratory of Metallurgy, September 2006, TKK-MT-180.

[5] Miettinen, J., Louhenkilpi, S., Kytönen, H., Laine, J., Wang, S., Hätönen, T., Petäjäjärvi, M. and Hooli, P. IDS Tool – Theory And Applications for Continuous Casting and Including Modeling of Microstructure and Inclusions. 6th ECCC – 6th Europe, 3–6 June, 2008, Riccione, Italy.

6. Modelling partial equilibria during steel solidification

Klaus Hack, GTT-Technologies
Risto Pajarre and Pertti Koukkari, VTT

The back diffusion of a solidifying system under local equilibrium conditions can be simulated by using immaterial constraints as set to the (stoichiometric) conservation matrix of the alloy mixture. In a solidifying alloy, complete diffusion between the liquid and solid portions is often found for chemical components with small atoms which dissolve interstitially in the solid state. Carbon in steels is a classical example. The constrained Gibbs energy method appears to be a useful technique to incorporate the necessary restrictions for those components, which are not allowed to diffuse in the solidifying system, while the interstitial components can reach their partial equilibria.

6.1 Background

The phase composition of a solidifying alloy or steel is a key to the structural properties of the final solid product. The solidifying system is controlled by the thermodynamic properties and diffusion kinetics in the gradually solidifying system. Typically, one may distinguish between small interstitial atoms (non-metals such as carbon and nitrogen) and substitutional solids (the metal components of the alloy). The diffusion of the interstitial atoms is fast and may easily occur between the melt and solid portions of the alloy, while the diffusion of the substitutional components is slow or negligible.

To produce a meticulous model on a solidifying system, tedious and time-consuming kinetic calculations are needed, often to be performed with inadequate data on diffusion coefficients [1]. To avoid these difficulties, approximate

methods have been developed. By assuming that the system reaches sequential equilibria following a given time-dependent temperature profile the lever rule can be applied. Due to the rudeness of the equilibrium assumption, the predicted compositions thus received do not well match with observation. The conventional approach to improve this is to use the Scheil equation, which assumes solute redistribution during alloy solidification. This approach approximates the non-equilibrium solidification process by supposing a local equilibrium of the advancing solidification front for each infinitely small portion at the solid-liquid interface. These portions then retain the same composition through the solidification course. The advantage of the Scheil method is that it allows the use of equilibrium phase diagrams in solidification analysis.

The Scheil method often gives a reasonable approximation to the solidification behaviour of e.g. Al- and Ni-based alloys [1], but is not successful for such steels, where the back-diffusion of interstitial carbon must be taken into account. Thence, numerical methods for the partial equilibrium simulation of steels have been recently developed [1]. In ChemSheet, the method of kinetic constraints can be used to reach such partial equilibria by straightforward Gibbs energy minimisation. The method also serves to illustrate the role of immaterial constraints in the Gibbs'ian calculations.

6.2 Methods

In the constrained Gibbs energy method [2], the chemical state of the system is modeled by minimising the free energy function subject to elemental mass balances and additional immaterial constraints like surface areas, restricted extents of reactions and local charge balance or potential constraints. For back diffusion systems this includes setting constraints to those components in solid phases whose equilibration with the melt is to be restricted. The solidifying system is schematically illustrated in figure 28. The incremental solidifying portion is in complete equilibrium with the molten metal, while only a partial (constrained) equilibrium is allowed between the previously formed solid and the incrementally forming solid.

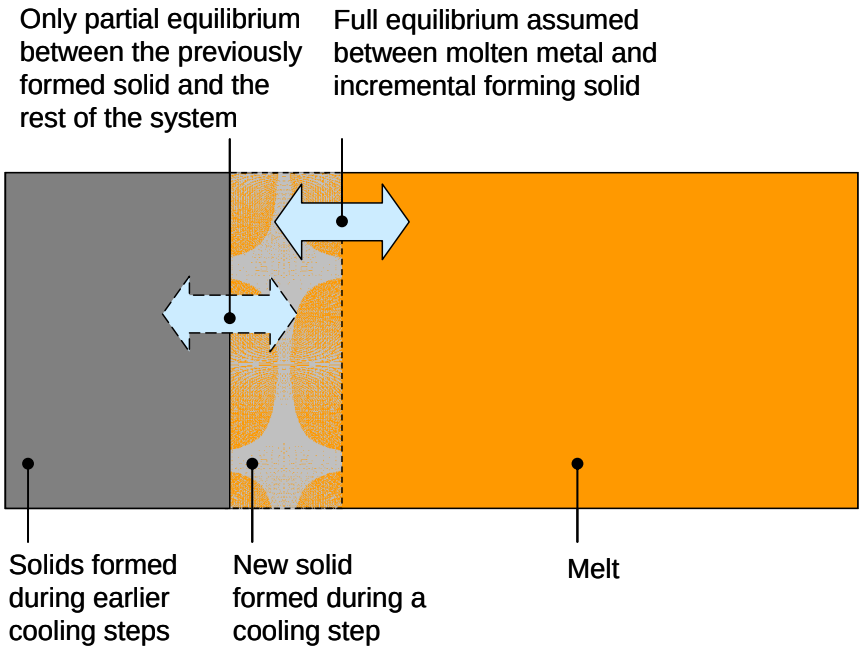

Figure 28. Scheme of the solidifying alloy.

Example of a constrained system structure description is given in table 5 (three elemental components, two solid phases). The atomic components are iron (Fe), chromium (Cr) and carbon (C), the stoichiometry of which in various phases is shown as the matrix elements of the three first columns. The phase description is read from the rows of the matrix, consisting of liquid iron with Cr and C as solutes and three solid phases, FCC-iron and 7:3 carbides of Fe and Cr. Both the FCC and the BCC are treated by sublattice models of the type (Fe,Cr,)x(Va,C)y with x = 1 and y = 1 or 3 respectively. The additional rows indicate the restricted phase copies, which are used to describe the solid formed during each cooling step. Adding an additional restriction component for the carbon in restricted FCC phase will lead to Scheil cooling behaviour. Free mass transfer of any of the restricted substances would be allowed by setting the chemical potential of the corresponding restrictive component to zero. Unlike equilibrium solidification, the solute (Cr) does not diffuse back into the solid and is rejected completely from diffusing into the liquid. Complete mixing of solutes in the liquid is also assumed.

Table 5. Phase composition of the Fe-Cr-C system. The restricted solids include stoichiometric constraints for the substitutional components Fe and Cr.

		Fe	Cr	C	*Fe_FCC	*Cr_FCC	*Fe_M7C3	*Cr_M7C3
Fe-Liquid	Fe	1						
	Cr		1					
	C			1				
FCC	Fe:C	1		1				
	Fe	1						
	Cr:C		1	1				
	Cr		1					
FCC-restricted	Fe:C	1		1	1			
	Fe	1			1			
	Cr:C		1	1		1		
	Cr		1			1		
M7C3	Fe:C	7		3				
	Cr:C		7	3				
M7C3-restricted	Fe:C	7		3			7	
	Cr:C		7	3				7

The calculation procedure is further shown in figure 29. The stepwise cooling and solidifying rates are deduced from experimental data [3]. While the incremental solidifying proceeds, the previous results are sequentially used as inputs for the next stage. The solids formed at each stage are added to the restricted phases, which are considered isotropic. Thus, the substitutional components (Fe and Cr) are accumulated in the solid phase according to the assumption of negligible diffusion, while the interstitial carbon is distributed according to its equilibrium chemical potential throughout the system.

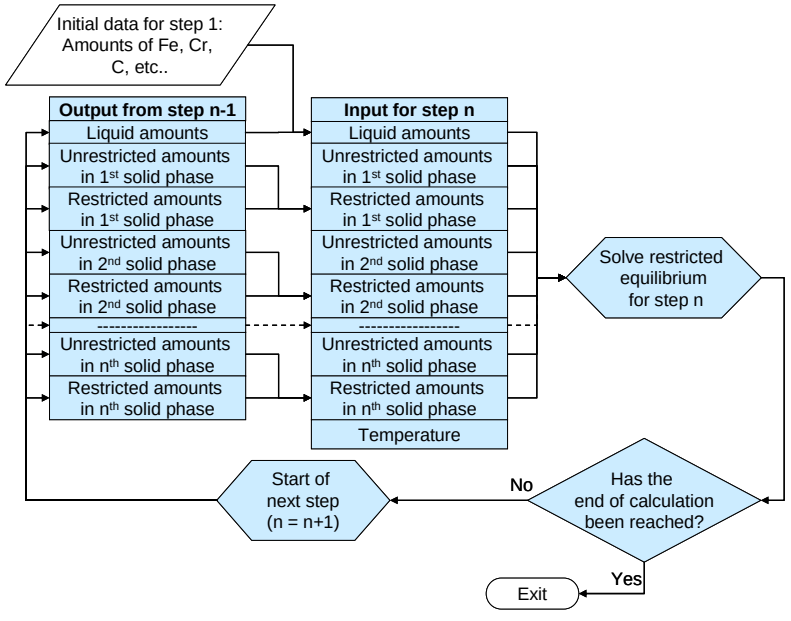

Figure 29. The calculation procedure for the restricted paraequilibria [4].

In addition ranges have been defined for the intermediate storage of the solids formed at one stage of the calculation. Then other ranges have been defined to store the full set of equilibrium amounts of all phases formed in any one calculational step. From these latter ranges the values for T and amount of liquid are taken to generate the fraction (%) solid plot and also the phase amounts plots.

In the first calculation liquid is equilibrated with the unrestricted solid at a temperature just below the liquidus curve. Then the entire amount of solid is transferred to the restricted solid by way of spreadsheet operations. The next equilibrium is calculated by reducing the temperature again and using the remaining amount of liquid of the previous calculation together with the amount (and composition) of the restricted solid as input. In this calculation unrestricted solid will form by precipitation from the liquid, but also the carbon of the restricted solid will equilibrate with this. After that the composition of the new free solid will be added to the restricted solid in order to prepare for step three of the calculations.

The procedure described last in the above paragraph is repeated until the final step of the calculation has been done. After that the plots indicated above can be generated.

6.3 Results

Three different options can be used for the simulation: 1) equilibrium solidification which is received by setting all the chemical potentials of the immaterial restriction components to zero 2) Scheil solidification, when constraints are applied to all solids 3) Partial equilibria with back diffusion of the interstitial atomic components (carbon). The results for each case are shown in figure 30.

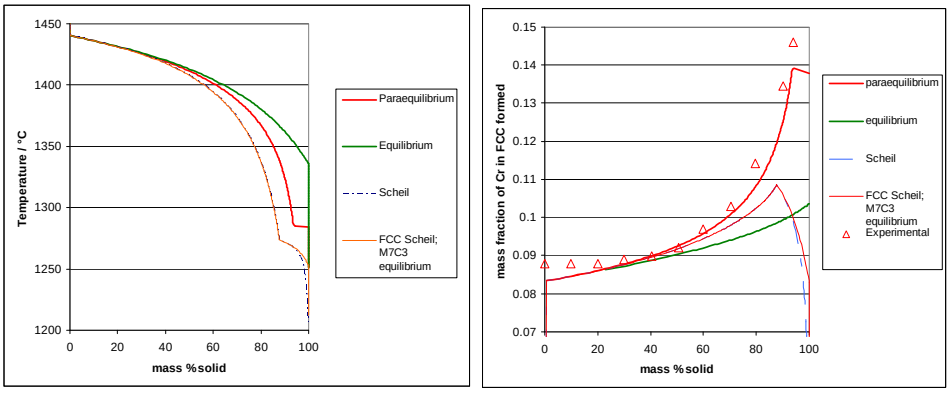

Figure 30. Solidification experiment of Fe-Cr-C-system with composition: 10.84% Cr, 0.95% C. Cooling rate in experiment 0.167K/s. Experimental data is from [3].

Obviously, the partial equilibrium (paraequilibrium) system is the closest approximation to observed data, when the Cr-content of the FCC-phase is used as a reference.

6.4 Conclusions

The Constrained Gibbs energies provide a practical approach for doing the Scheil-calculation for solidifying steels and alloys. A particular advantage of the CFE-ChemSheet technique is that by using the same simulation system, the respective equilibrium and paraequilibrium curves can also be calculated. When the system consists of both substitutional and interstitial components, the paraequilibrium generally is in best agreement with experiment. The method thus provides a good approximation for predictive calculations while elaborating kinetic inhibitions can be avoided.

6.5 References

[1] Chen, Q. and Sundman, B. Materials Transactions, 43 (2002), pp. 551–559.

[2] Koukkari, P. and Pajarre, R. Calphad, 30 (2006), pp. 18–26.

[3] Ono, Y., Takechi, T. and Ogi, K. J. Japan. Inst. Metals 57 (1993), pp. 432–439.

[4] Pajarre, R., Koukkari, P., Hack, K. and Kondratjev, A. Calculation of Back Diffusion with the Constrained Gibbs Energy Method. CALPHAD XXXVII, June 15.–20., 2008 Saariselkä, Finland (poster).

7. Improving the chemistry control of paper-making furnishes with multiphase modelling

Anna Kalliola, Risto Pajarre, Pertti Koukkari and Juha Hakala, VTT
Esko Kukkamäki, UPM Kymmene Oy

This paper presents a nearly ten years history of multiphase modelling of pH and calcium chemistry in neutral papermaking. Initially the multiphase modelling was focused on pulp acidification and pH buffering concepts, and the unit operation models were used to define the dosages of acidification chemicals and buffering aids at certain stages of the process.

Multiphase chemistry calculation can be appended to process simulation, thus enabling the monitoring of chemistry of large-scale processes. Recently a pioneering chemistry simulation of a process integrate consisting of two paper machine lines with both mechanical and deinked feed stocks was performed. In this integrate difficulties were often experienced when the dosage of bleaching chemicals was increased while maintaining the high brightness target of the paper product. The simulation of the large integrate could be used to quantify the calcium carbonate losses at selected process units and to improve understanding of the bleaching practices in neutral papermaking.

7.1 Background

Papermaking chemistry is vulnerable to changes in pH, temperature and ion concentrations as the behaviour of inorganic compounds and organic wood based compounds depend on these properties. One of the challenges in neutral papermaking is that the acid conditions accelerate the dissolution of calcium

carbonate, $CaCO_3$. This leads to pigment loss, raises the amount of dissolved calcium and increases foaming. Fluctuating concentration of dissolved calcium induces unwanted inorganic and organic precipitation which can abate the production efficiency.

Innovation of carbon dioxide acidification of de-inked pulp (patented by UPM and Linde gas, former AGA) [5, 8] evoked the curiosity for deeper understanding of neutral papermaking chemistry. Also, in that time, calcium carbonate became a more common raw material in the production of mechanical pulp dominating paper grades. At UPM it was concluded that improved pH control was needed to tackle the problems of neutral papermaking chemistry, and thermodynamic multiphase modelling provided by the ChemSheet program could be of help.

The objective of this paper is to review the studies performed with multiphase models for improving the control practices of neutral papermaking chemistry and to present the some of the latest work done in this field.

A general multiphase model for pulp suspension combining the solubility equilibria with both solids and gas phase and the ion exchange equilibria between the pulp fibres and the surrounding aqueous liquid was developed in the early 2000's [4]. At first, the multiphase modelling was focused in pulp acidification and pH buffering concepts, and the models were used to quantify the acidification chemical and buffering aid at different stages of the process [11, 7, 1]. Also, the coming neutral conversions were simulated in terms of pH and dissolved calcium levels [10]. The models were initially produced with the ChemSheet program, which proved to be practical due to its multicomponent thermodynamic base and easy-to-use spreadsheet interface. During the last decade, in addition to UPM also other pulp and papermaking companies and chemical suppliers have participated in a number of projects developing multiphase models for pulp suspensions. The general aim has been to improve control practices in neutral papermaking. Simultaneously, the modelling base has extended to coupling of the multiphase subroutine to process simulation programs.

The latest simulation study was performed to find out those process stages, which would have the major effect on $CaCO_3$ dissolution in a large-scale papermaking integrate. Difficulties were often experienced when the bleaching dosages increased greatly while the high brightness target of the paper was maintained. The integrate consisted of two neutral paper machines, TMP department and deinking plant. Sodium dithionite, $Na_2S_2O_4$ was used in pulp bleaching. The study focused on comparing $CaCO_3$ and sulphur chemistry in the

production of low versus high brightness grades. In addition, the quantitative loss of $CaCO_3$ was determined for these production conditions.

7.2 Methods

7.2.1 Multiphase modelling of pulp suspensions

In the papermaking furnish, which is an aqueous suspension with pulp fibres and inorganic pigments, there are at least four different phases and tens of different chemical constituents. The salient feature is that the fibre itself forms a chemically active component, as fibres from different sources hold different acidity. Thus, a separate fibre phase can be assumed, consisting of these fibre-bound acidic groups and the water absorbed by the fibre. This property leads to the so called Donnan equilibrium between the fibre and its surrounding filtrate phase [9] and will strongly affect any simulation, which pursues to master the chemical state of fibre suspensions.

The ion exchange and ionic equilibria in pulp–water systems can be described quantitatively when the overall ionic composition accounting for anions, cations, ionic species and fibre charge are known. The nature of cellulose fibre wall in ionic media as a negatively charged polyelectrolyte phase determines the equilibrium ion distribution. The amount of the fibre-bound water is conventionally known as the water retention value (WRV). The characterisation of the charge properties is performed by potentiometric or conductometric titration methods. Together with the electroneutrality condition, this information can be combined with multicomponent equilibrium data of the suspension. The data accounts for possible precipitates as well as the effect of the gaseous phase. Thus, a multiphase equilibrium theory of the suspension is received. The theory applies to charge properties of different fibres, their ion exchange behaviour in terms of pH and ionic composition of the suspension. The chemical state, i.e. the ionic composition of the two aqueous phases, solubilities of various compounds and pH of solutions can be determined either by equilibrium constant or Gibbs energy data [2, 4]. For practical simulation tasks, the Gibbs'ian approach has proven to be numerically most practicable. The compatibility of the thermodynamic Gibbs energy solvers also allows for their combination with other simulation programs, such as BALAS® [3].

7.2.2 Multiphase calculation in process simulation

Concept development, studies of scenarios, process and automation design and operator training are typical uses for large-scale process simulation. In recent years the multiphase chemistry calculation has been appended to process simulators such as APROS® (vtt.apros.fi) and BALAS® (vtt.balas.fi), thus enabling the monitoring of chemistry of large-scale processes. BALAS® can be used for any mass or energy balance calculations within the pulp and paper industry. Its extension with multiphase reactor modules provides an efficient tool for extensive and diversified process studies, which take into account the process chemistry.

7.2.3 Building the model

Initially, several unit operation studies had been performed for various paper machines as well as for de-inking and mechanical pulping processes. The multiphase chemistry models were generally made with ChemSheet. The most common process stages modelled were machine chest, broke chest or tower, pulp bleaching and acidification. The validation of the model was done with all known chemicals, acids or bases, entering the process stage. Fibre charge properties were determined and included in the model. The validation data included also fibre consistency and a typical water retention value (WRV) of the fibre species.

The integrate of two paper machines (PMA and PMB), deinking plant and TMP department was modelled with BALAS®, to which again the multiphase chemistry model was appended. Mass and energy balances were validated in the process model prior to the extension of the multiphase reactor modules. The process chemistry was evaluated by using the low brightness case as a reference. The amounts of all known chemicals, acids or bases, entering the integrate plant while the low brightness target was active on both PM lines were then used as model input. Fibre acids were included in the multiphase reactor modules according to the charge determination of fibres. Due to the dithionite bleaching at five different stages in the integrated process (in pulp departments as well as in PMs) particular attention was laid on the sulphur chemistry. The molar proportions of species (Na^+, HSO_3^-, HSO_4^-) formed from the dosed dithionite [6] and the oxidation reactions of sulphite to sulphate were applied in the model.

The concentrations of the most typical metal cations present in the raw materials (TMP chips, fresh water, DIPulp) were set in the model according to

ICP-AES and CE (capillary electrophoresis) measurements. The amount of $CaCO_3$ and clay (considered as inert pigment) were set according to 525 & 925 ^oC ash determinations. A schematic model of the integrated process and the most important phenomena in terms of combined $CaCO_3$ and sulphur chemistry are shown in figure 31.

In addition to the measured and analysed values, experience and literature based assumptions were also needed. These include e.g. furnish aging induced formation of acids (CH_3COOH) in broke circulations, formation of dissolved material (CO_2(aq), CH_3COOH and HCOOH) in peroxide bleaching in the deinking drum, the formation of calcium oxalate in the TMP refining as well as in the peroxide bleaching. Release of CO_2(aq) in certain process points (e.g. in defoamer) was also considered.

Some chemicals appearing in minor amounts were excluded from the model. Those were typically retention aids, fixatives, antifoaming agents, biocides, chelate, gaseous air, $NaBO_2$ in the dithionite liquor (the amount was replaced with NaOH). Dissolution kinetics of solid compounds (e.g. $CaCO_3$) was not considered as equilibrium state calculation was applied in every multiphase reactor module.

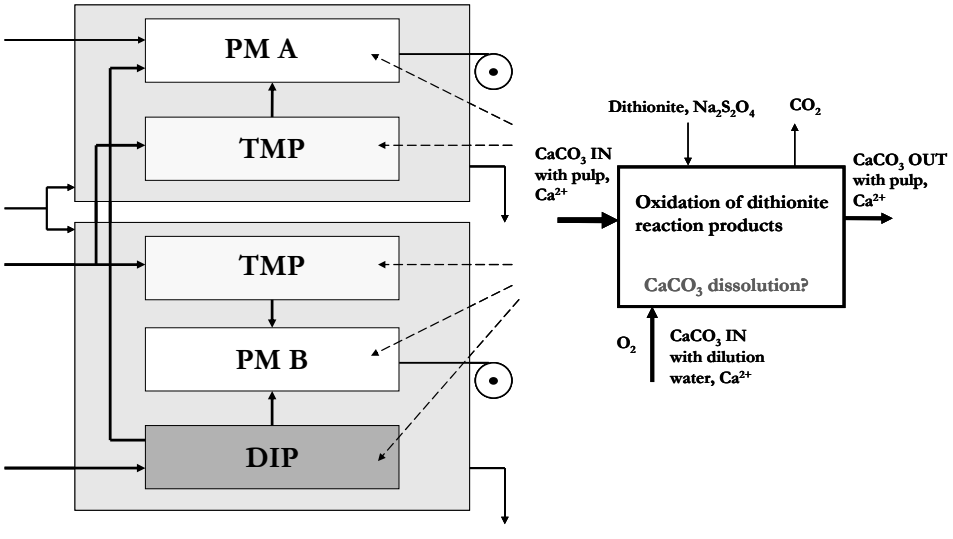

Figure 31. A schematic process model and the basics of the combined $CaCO_3$ and sulphur chemistry effecting the chemical state of the process.

7.2.4 Case for simulation

The process model was validated against the data measured during the production of paper grades with low brightness target at both PM lines. The simulated case was the simultaneous production of high brightness grades at both PMs. The process simulation was done using the steady state mode. For the low brightness grades the minimum dithionite dose (of the six different bleaching stages) was 0% and the maximum 0.38%. During the production of high brightness grades the minimum was 0.12% and the maximum 0.80%. Proportion of DIP and TMP pulps used at the paper production varied with the brightness target of the paper.

7.2.5 Determination of the calcium carbonate loss

Eight small-scale areas of the process model were selected for the $CaCO_3$ balance study. The selected areas were the surroundings of bleaching stages (altogether six), broke circulations and short circulations of both PMs. The amount of $CaCO_3$ entering and leaving each of the areas were calculated. As a result the amount of dissolved $CaCO_3$ i.e. the pigment losses were gained. The quantities were conducted for unit of kg/day. A simplified presentation of the observation is shown in the figure 31 (right).

7.3 Results

7.3.1 Unit operations models

ChemSheet models for unit operations have been used to quantify chemical dosages for pH buffering test runs. Figure 32 presents calculated values of pH and HCO_3^- ion concentration, used for choosing the proper $NaHCO_3$ dose for the pH adjustment of bleached kraft [11]. With these results on pulp acidification it has been shown that when aiming to minimise $CaCO_3$ dissolution, carbon dioxide (CO_2) is a fair choice, if pulp contains much $CaCO_3$, as is the case i.e. with de-inked pulp [7, 11].

Figure 33 presents an example study on the neutral conversion of LWC producing PM [10]. In this case the modelling was used to define the mass percentage of the feed of coated broke for maintaining neutral pH in the short circulation. The results show that the proportions of 10%, 15% and 26% consisting respectively minimum 40, 27 and 17 parts of $CaCO_3$ in the coating

colour should maintain the machine chest pH at ca. 7.4. Usually, as the runnability of the PM is good, the coated broke dosage can be less than 10%. However, as long as there is solid $CaCO_3$ or buffering capacity (e.g. HCO_3^- ions) in the circulation water, the process pH at PM side would not decrease sharply.

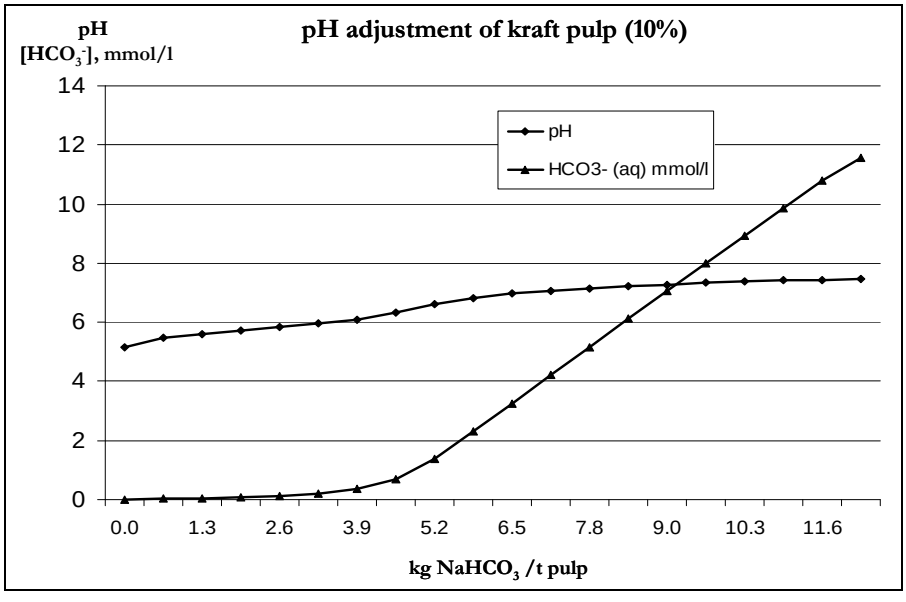

Figure 32. pH and the buffering capacity, $[HCO_3^-]$ as a function of dosed $NaHCO_3$ [11].

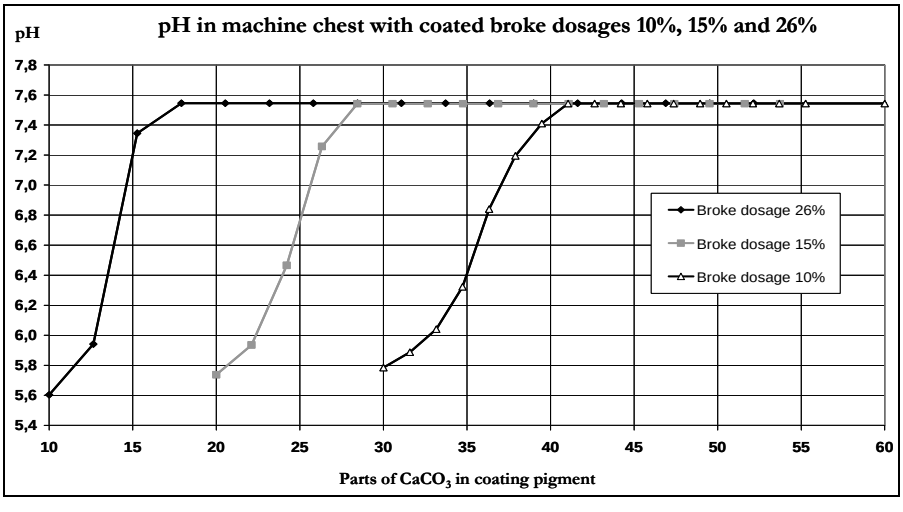

Figure 33. pH in machine chest as a function of coated broke proportions of 10%, 15% and 26% of the total furnish [10].

7.3.2 Process integrate

Figure 34 presents the modelled and measured values of calcium ion concentration and pH (DIP, PM A, TMP). The model validation was done against the measured process chemistry during the production of grades with low brightness target. In general, the validation succeeded satisfyingly in terms of the all modelled concentrations of metal cations and anions with the exception of sulphate ion, which appeared in a lower level than the measured values near in every process point of the model.

Figure 35 presents the simulated values of calcium ion concentration and pH (production of grades with high brightness target). The single point measurements of calcium ion concentration and pH are also presented.

The applicability of the model proved to be satisfactory in terms of its correspondence with the measured values of calcium ion concentration and pH (figure 34). It has been observed in practice that the more dithionite is used the more $CaCO_3$ is dissolved and the higher the amount of free calcium ions in the process [1]. The simulated calcium chemistry of the production of high brightness grades agrees with the practice. However, at certain process points the measured values of calcium ion concentration were more than double when comparing to the simulated values (these points are marked with arrows in figure 35). Increase in the dithionite dosing decreases the process pH. There is a good correspondence with the simulated and measured pH values at PM A, but not as good in deinking plant and TMP department (figure 35).

While troubleshooting of a process, the deviation between model and measurement typically gives valuable clues to recognise unwanted chemical behaviour, or, like in the case of figure 35 to identify previously unknown sources of surplus ionic strength affecting the process. The model also can be used to locate areas, where the gain-% of PCC could be improved by reducing the $CaCO_3$ dissolution.

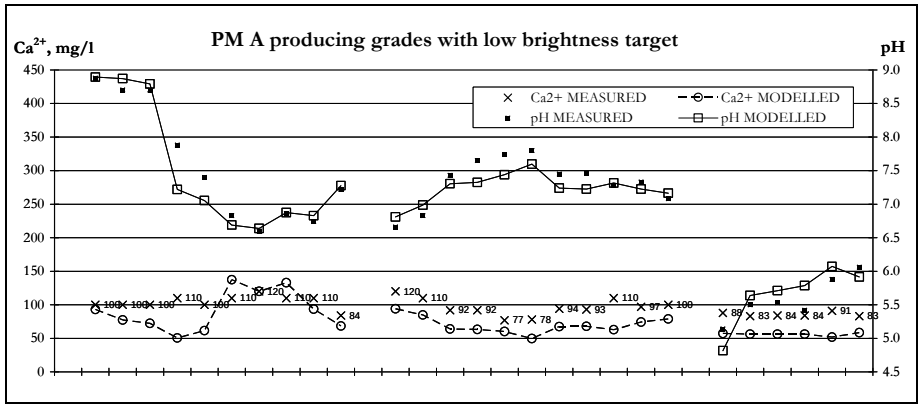

Figure 34. Modelled and measured calcium ion concentration and pH in the PM A line (x-axis corresponds the process points at deinking plant, PM A and TMP department).

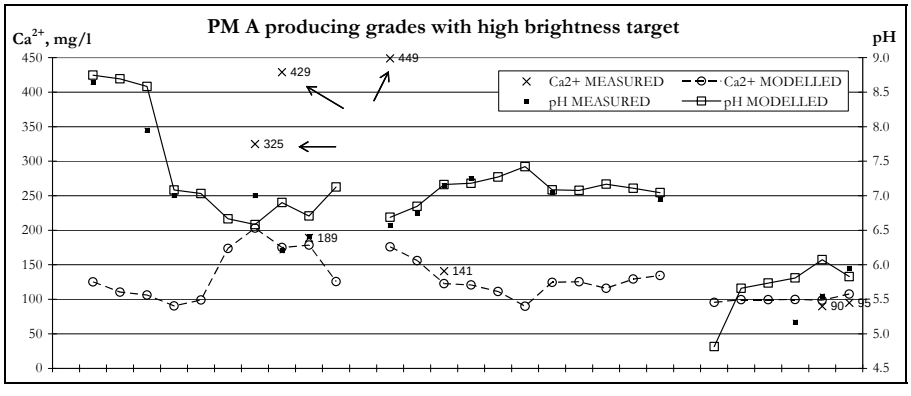

Figure 35. Simulated and measured (single points) calcium ion concentration and pH in the PM A line (x-axis corresponds the process points at deinking plant, PM A and TMP department). Greatly deviating simulated vs. measured values are marked with arrows.

7.4 Discussion

The chemistry model of the studied process integrate included altogether ca. 200 multiphase reactor modules. With such an extensive model, the chemical system needs to be held concise, as any additional constituent is a new variable, and the computational load increases respectively.

Deviation from the measurements is interpreted as inaccuracy of model information, i.e. the input data for an extensive process is not comprehensive in terms of the chemical inputs, another obvious source of disagreement again being the basic assumption of chemical equilibria in the chemistry units of the

model. The simulation yet gives a quantitative agreement for the expected pH and concentration values.

Discrepancies between the model and measurement can be used to interpret unexpected operational practices as well as to detect unknown 'chemistry sources'. For example, one may conclude that both calcium and sulphur (e.g. as form of gypsum pigment) are entering the process with recycled paper to some extent, which can not be quantified as model input. Also, sulphate anions tend to concentrate in the process circuits and metals cations in the fibres in their order of increasing valence.

Improved pH and calcium control may lead to substantial savings e.g. as remedy of $CaCO_3$ losses. A further advantage is explanation of process chemistry variations when different grades are produced.

There are also some drawbacks in such a large-scale process simulation. While the agreement between the model and mill data remains satisfactory, the model validation yet requires extensive measurements at the mill. Updating the model after optional process changes may become an arduous task during the course of active renovation. The substantial computation time required by the multi-reactor system may also appear as a retarding factor in development work.

7.5 Conclusions

The unit operation models have been useful in comparing different chemicals in pulp acidification and have supported e.g. the replacement of H_2SO_4 with CO_2. With the model quantification of pH buffering aid dosage, the number of test runs has been minimized. Also, with models, a deeper understanding of the chemistry involved in each impending neutral conversion has been gained.

The modelling and simulation quantified the $CaCO_3$ losses at selected process stages of the papermaking integrate and could be used to renew some of the bleaching practices.

Multiphase chemistry models can be successfully used for pulp and papermaking simulation in development of new chemistry concepts, extensive chemical balance analysis, design tool for chemical dosages, troubleshooting and operational changes support of process control and measurement. Usually, simplified models containing only the most important chemical phenomena are sufficient enough to support thought and can be used for control or decision-making processes. The extension of multiphase chemistry model within the calculation frame of a process simulator will provide an effective tool for extensive and diversified process studies performed by researchers, industrial

experts and process consultants in pulp and paper industries as well as in development of new generation concepts.

7.6 References

[1] Kalliola, A. and Pakarinen, H. Experiences of pH buffering and calcium chemistry control in neutral papermaking. In: 15th PTS Symposium: Chemical Technology of Papermaking, Munich (2002).

[2] Kangas, P. Multi-phase chemistry in process simulation, In: Paper Research Symposium, Kuopio (2009).

[3] Koukkari, P., Pajarre, R., Kaijaluoto, S. and Molin, U. Control of Wet End Chemistry with Multiphase Models. Scientific and Technical Advances in Wet End Chemistry. In: 4th Major Pira International Conference, Nice (2003).

[4] Koukkari, P., Pajarre, R. and Pakarinen, H. Modelling of the Ion Exchange in Pulp Suspensions by Gibbs Energy Minimisation. J. Soln Chem., 21(8)2002, pp. 623–634.

[5] Laurila-Lumme, A., Pakarinen, H. and Leino, H. U.S. Patent 6540870: Process for substantially retarding dissolution of calcium carbonate in a papermaking system.

[6] Malkavaara, P., Isoaho, J. P., Alen, R. and Soininen, J. Dithionite bleaching of thermomechanical pulp: factors having effects on bleaching efficiency. J. Chemometrics, 14, (2000), pp. 1–6.

[7] Pajarre, R., Kalliola, A., Koukkari, P. and Räsänen, E. Thermodynamic modelling of wet end chemistry. In: PIRA Conference: Scientific and Technical Advances in Wet End Chemistry, Vienna (2002).

[8] Pakarinen, H. and Leino, H. Benefits of using carbon dioxide in the production of DIP containing newsprint. In: 9th PTS Deinking Symposium, Munich (2000).

[9] Towers, M. and Scallan, A. M. Predicting the ion-exchange of kraft pulps using Donnan Theory. J. Pulp Pap. Sci., 22(9), 1996, pp. J332–J337.

[10] Viitikko, K. and Kalliola, A. Simulation of neutral conversion and water management in LWC paper making. In: Scandinavian Paper Symposium: Wet End Technology, Helsinki (2002).

[11] Weaver, A., Kalliola, A. and Koukkari, P. A strategy to control pH and calcium hardness in papermaking. In: Slides of the Oral Presentation at PIRA conference: Scientific and Technical Advances in Wet End Chemistry, Vienna (2002).

8. Multi-phase thermodynamics in process simulation

Petteri Kangas and Pertti Koukkari, VTT

The feasibility of using multi-phase chemistry as part of the large-scale process simulation was evaluated. Three methods for calculating thermodynamic equilibrium were studied: equilibrium constants, Gibbs' energy minimization and neural networks. These methods were tested in three different process models: pulp suspension in the short circulation of paper machine, boiler water of power plants and pulp suspension in the pulp bleaching line. The Gibbs'ian method appears as the best option for the calculation of equilibrium in multi-phase systems. However, the computational speed required for dynamic problems is yet not sufficient. Additional studies should be made to optimize the present calculation routines and to exploit possibilities of parallel computing in order to fully utilize the multi-phase chemistry approach in process simulation.

8.1 Background

Multi-phase chemistry has been successfully utilized in several problems in the pulp and paper industry. Examples range from the neutral conversion of paper machines [7, 12] to bleaching chemistry of pulp suspensions [9] and operations of lime kilns [8]. However these solutions have focused only on single reactors or on small parts of the process.

During the last decade, several large-scale process models of pulp and paper processes have been published. They seldom include rigorous multi-phase chemistry as a part of the full-scale process simulation. [4]. The applicability of models on recovery boilers, pulp washing and bleaching, mechanical pulp processes and

approach systems of board and paper machines remains limited if little or no chemistry is included. Thus there is an apparent need for implementing precise chemistry into these simulation tools. The aim of this study was to evaluate the feasibility of applying multi-phase chemistry as part of large scale process simulation.

8.1.1 The multi-phase systems

A typical multi-phase system is presented schematically in figure 36. The number of compounds or constituents in each phase in not limited. Gas phase is practically always present but there may be several liquid and solid phases, which form, vanish and re-form based on the process conditions (temperature, pressure and composition of system).

A typical pulp suspension can contain following phases and compounds:

- Gas phase: O_2(g), N_2(g), H_20(g) and CO_2(g)
- Aqueous phase: H_2O(aq), H+(aq), OH-(aq), Ca+2(aq), $CaCO_3$(aq), CH_3COO-(aq), CH_3COO-(aq), CH_3COOH(aq), Cl-(aq), CO_2(aq), CO_3-2(aq), HCO_3-(aq), HSO_3-(aq), HSO_4-(aq), Na+(aq), SO_2(aq), SO_3-2(aq), SO_4-2(aq), AcidFree7.2-(aq) and AcidFree7.2H(aq)
- Fibre phase: H_2O(f), H+(f), OH-(f), Ca+2(f), $CaCO_3$(f), CH_3COO-(f), CH_3COOH(f), Cl-(f), CO_2(f), CO_3-2(f), HCO_3-(f), HSO_3-(f), HSO_4-(f), Na+(f), SO_2(f), SO_3-2(f), SO_4-2(f), AcidFree7.2-(f), AcidFree7.2H(f), Acid2.1-(f), Acid2.1H(f), Acid4.8-(f) and Acid4.8H(f)
- Solid phase: $CaCO_3$.

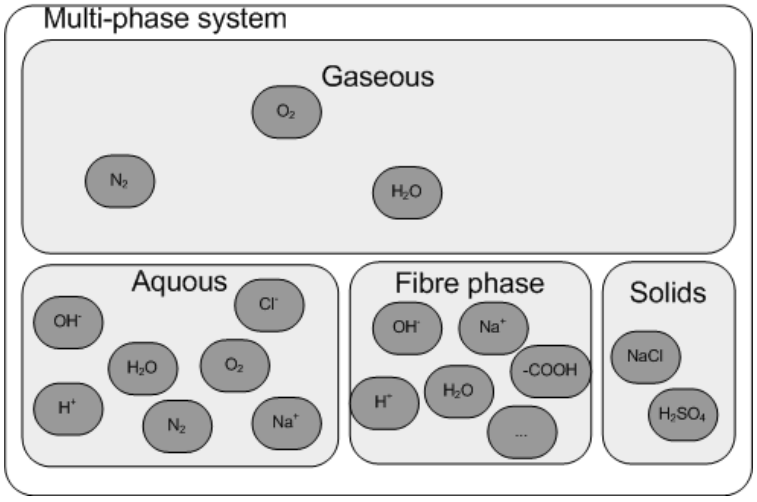

Figure 36. A typical multi-phase system with four separate phases and many different compounds [5].

8.1.2 Large-scale process simulation

Concept development, studies of scenarios, process and automation design and operator training are typical uses for large scale process simulation. For these purposes the unit operations, streams and even automation must be included in the models. The modeling scope thus varies from parts of production line, such as approach system of paper machine, to full-scope simulation of the entire plant, such as a power plant or a paper mill.

Both steady-state and dynamic simulation are used in these large-scale studies. Steady-state simulation is well suited for new concept development and optimizing mass and energy usage. Dynamic process simulation is applied for automation tuning and operator training.

In both cases there remain dozens of calculation volumes, unit operations and streams which should be calculated during every simulation step. For such engineering tools, fast (real-time) calculation is a necessity.

Figure 37 shows three typical processes, which are used as test-beds in this study. Each of these processes is wide enough for large-scale simulation. In addition, the multi-phase chemistry is an essential part of the observed processes. It was assumed that computational power has reached such magnitude that rigorous multi-phase chemistry can be implemented in the large-scale process simulation.

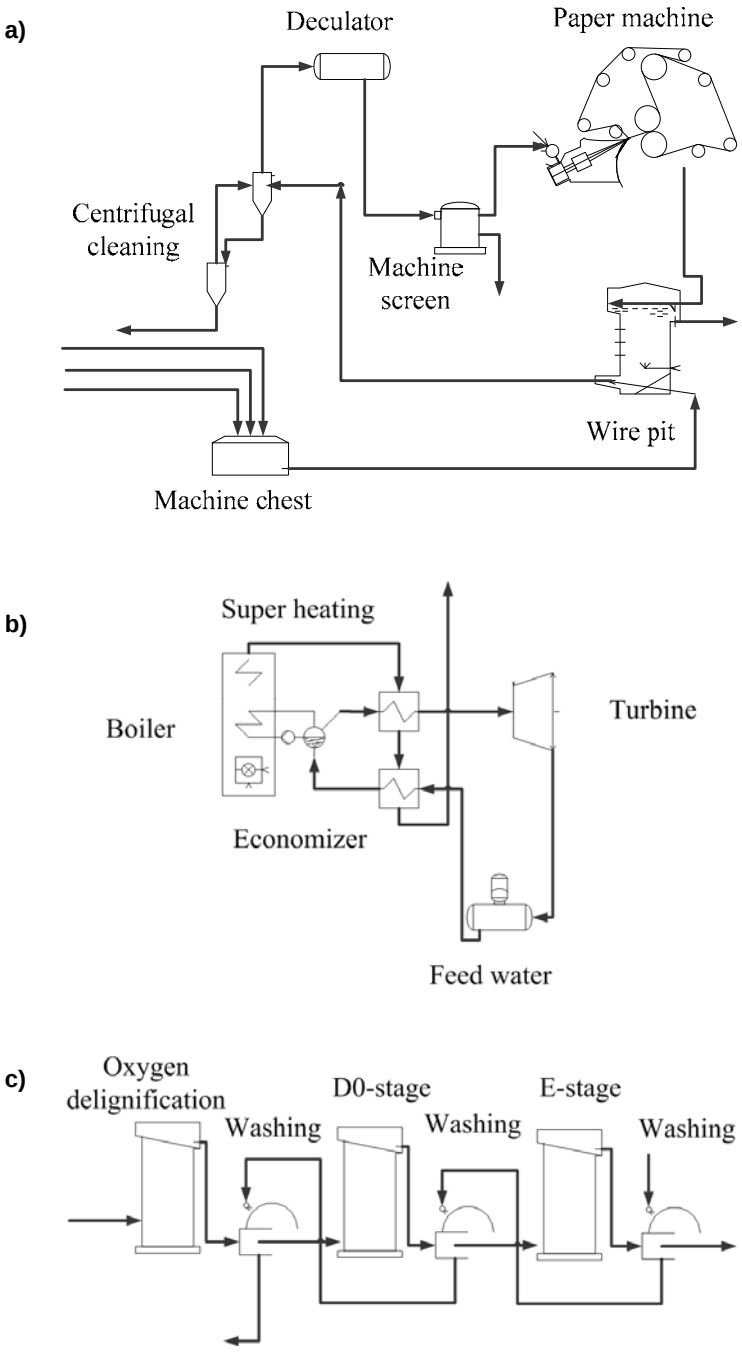

Figure 37. Three example cases for implementing multi-phase chemistry in the large scale process simulation. a) Short circulation of paper machine, b) the boiler and c) the bleaching sequence. [5]

8.2 Methods

Three different approaches to calculate thermodynamic equilibrium of multi-phase systems were evaluated. Equilibrium constants, Gibbs' free energy minimization technique and neural networks were studied. The aim was to find an applicable method to be used as part of the comprehensive process simulation.

A dynamic simulator was used for process modeling. Mass and energy balances, all the unit operations and streams were defined inside the simulator, which also included the necessary automation procedures.

8.2.1 Equilibrium constants

The obvious method for calculating the chemical equilibrium is based on the equilibrium constants, *K*. These constants can be used to determine equilibrium concentrations of compounds of specific reaction:

$$a_1 A_1 + a_2 A_2 + \ldots \leftrightarrow a_{n+1} A_{n+1} + a_{n+2} A_{n+2} + \ldots \tag{1}$$

$$K = \frac{\hat{a}_{n+1}^{\,a_{n+1}} \hat{a}_{n+2}^{\,a_{n+2}} \ldots}{\hat{a}_1^{\,a_1} \hat{a}_2^{\,a_2} \ldots} \tag{2}$$

where A_i is compound i, a_i is stoichiometric factor, $\hat{a}_i$ is activity.

The equilibrium constants should be defined for all reactions in the multi-phase system. Constants are temperature dependent and adjustments are needed, if the temperature is changed. When a complicated multi-phase system is considered, the equilibrium concentration can not be calculated analytically but iterative solutions are needed.

Two equilibrium constant based descriptions of pulp suspensions were used in this study. The first one was used for modeling the approach system of paper machine [11] and the second one for modeling the pulp bleaching [9]. The latter was wrapped as a software component called ChemCLL.

8.2.2 The Gibb's free energy method

Gibbs' free energy minimization is the second technique, which was tested. It can be regarded as a generalization of the equilibrium constant technique. The main benefit of this approach when compared with the equilibrium constant

method is that individual reactions do not need to be defined separately. Instead the multi-phase system is treated as whole:

$$A = \begin{bmatrix} a_{11} & a_{12} & . & . & a_{1J} \\ a_{21} & a_{22} & . & . & a_{2J} \\ . & . & & & . \\ . & . & & & . \\ a_{I1} & a_{I2} & . & . & a_{IJ} \end{bmatrix} \tag{3}$$

where A is the stoichimetric matrix of multi-phase system and a_{ij} is stoichiometric factor of j:th element of compound i.

To reach the thermodynamic equilibrium, the Gibb's energy of this closed isothermal system is minimized using the Lagrange method:

$$L = G - \lambda\Psi = \sum_{i=1}^{I} n_i \mu_i - \sum_{j=1}^{J} \lambda_j \left(\sum_{i=1}^{I} a_{ij} n_i - b_j \right) \tag{4}$$

where G is the Gibbs' energy of the system, λ is Lagrange multiplier, Ψ is mass balance of different elements in each compound, n_i amount of compound i, μ_i is chemical potential of compound i and b_j is the amount of element j.

Partial differentiation and linearization eventually leads to presentation for different phases. Equation 5 is for gaseous phase, Equation 6 is for mixed phases (such as aqueous or fibre phases) and Equation 7 is for solid phases [2]:

$$\sum_{j=1}^{J} \lambda_j a_{ij} - RT \frac{n_i}{n_i^0} = \mu_i^0 + RT \left[\ln\left(\frac{P}{P^0} \right) + \ln\left(\frac{n_i^0}{N_{gas}^0} \right) - 1 \right] \tag{5}$$

$$\sum_{j=1}^{J} \lambda_j a_{ij} - RT \frac{n_i}{n_i^0} = \mu_i^0 + RT \left[\ln\left(f_i \right) + \ln\left(\frac{n_i^0}{N_{mix}^0} \right) - 1 \right] \tag{6}$$

$$\sum_{j=1}^{J} \lambda_j a_{ij} = \mu_i^0 \tag{7}$$

where J number of compounds, λ is Lagrange multiplier, a_{ij} is stoichiometric factor, R is gas constant, T is temperature, n_i is amount of substance, n^0_i is

amount of substance in previous iteration, μ^0_i is chemical potential at reference point, P is pressure, P^0 is pressure at reference point, $N^0_{gas/mix}$ is total amount of substance in gas/mix phases and f_i is activity.

Equations 5–7 are arranged in matrix form and a group of linearized equations is solved. An iterative calculation is needed until convergence is reached [2].

In this study, Gibbs' energy minimization technique was used for calculating thermodynamic equilibrium of pulp suspension in short circulation and for boiler water. A commercial software component, ChemApp, was used for the Gibb's energy minimization calculations [3].

8.2.3 Neural networks

Neural networks were considered as a fast alternative for multi-phase chemistry calculation. Both equilibrium constants and Gibbs' energy minimization techniques lead to slower iterative routines, which can be a drawback when large-scale process simulation is considered. An example of a neural network used in this study is shown in figure 38.

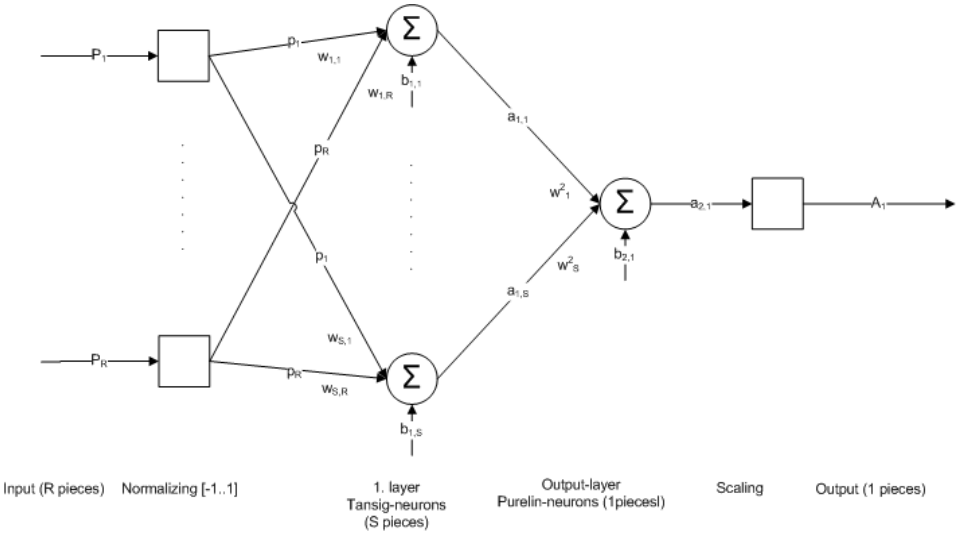

Figure 38. Schematics of two-layer neural networks.

First inputs, P_1 to $P_{R,}$ of neural network are normalized between -1 and 1, as seen in figure 38. Each of the neurons is calculated [6]:

$$n = w_{1,1} p_1 + \cdots + w_{1,R} p_R \tag{8}$$

where n neuron input, $w_{i,j}$ is weight of $_i$:th neurons $_j$:th input and p_j is j:th input.

The first layer of neural network is based on the Tansig-neurons, Equation 9, and second layer on Purelin-neurons, Equation 10. Output, a, is calculated as [6]:

$$a = \frac{2}{1 + e^{-2n}} - 1 \tag{9}$$

$$a = n \tag{10}$$

Neural network is taught using backpropagation algorithm [6]:

$$x_{k+1} = x_k - \alpha_k g_k \tag{11}$$

where x_k is a vector of current weights and biases, g_k is the current gradient and α_k is learning rate.

Neural networks were used for calculating the equilibrium of pulp suspension in the short circulation of paper machine. In this study, commercial software Matlab was used for developing the neural networks.

8.2.4 The process models

Three different cases, as described in figure 37, were modelled using a dynamic process simulator. Pulp suspensions in the short circulation of the paper machine and in the pulp bleaching were studied. A separate study was made for the chemistry of boiler water. When successful these models could be used for automation testing and operator training. All process models included several tens of calculation volumes, for which the pressure and enthalpies as well as mass fractions were solved.

A typical calculation step for this kind of process is 0.2 seconds. During every calculation step there can be one or several iterations, when the thermodynamic equilibrium is calculated. This leads to hundreds or thousands of equilibrium calculations during every second. For the automation tuning and training purposes, the process simulator should run at least real time. This requires high efficiency of calculations.

In this study, a commercial process simulator, APROS, was used for evaluating the feasibility of using multi-phase chemistry as a part of large-scale process simulation [4].

8.3 Results and discussion

8.3.1 Combining multi-phase chemistry and process simulation

The multi-phase systems modelled in the three different cases were quite extensive. The chemistry of pulp suspension used in the short circulation of paper machine contains 46 different compounds in four different phases. The chemistry of boiler water is based on 59 different compounds in 25 different phases. (This is due to 23 invariant phases, which appear as precipitated solids). The chemistry of pulp suspension in the bleaching line included 18 different compounds in four different phases.

When these large multi-phase systems are compared to the streams and sections, which are available in a typical large scale process simulator, it is readily seen that the simulator does not support chemical systems of this kind. The bare minimum used in process simulators can be just two phases: liquid and gas. The increasing amount of included compounds could also effect on the convergence of mass balances in the simulators. Usually the number of flowing compounds is limited. It is essential to either develop process simulators to support more phases and compounds or to reduce and simplify the multi-phase system.

It was also noticed that the interfaces between legacy software need additional development. Each software item tested here, APROS, ChemApp, ChemCll and Matlab provide their own unique interface, which must be used. In practise, there is always a need for a special wrapper when process simulator and multi-phase routines are combined. Multi-phase chemistry can be implemented using different approaches: it can be calculated as part of the material properties calculation or in separate reactors or reaction volumes.

The future standards, such as Cape-Open [1] could provide advanced solutions for combining process simulator and multi-phase solvers, but the performance of these interfaces were not evaluated.

8.3.2 Calculating the thermodynamic equilibrium

At the early stages of the modelling of pulp suspension chemistry, the focus was in pulp acidification and pH buffering, e.g. in CO_2 acidification and introduction of sodium carbonates to the feed stocks or to the short circulation of a papermaking process. When the use of calcium carbonate (chalk, precipitated or ground Ca-carbonates, PCC and GCC) became more common in the production of mechanical pulp dominating grades, the need for the pH and calcium chemistry control in neutral papermaking increased. Unit operation studies could be performed by using the ChemSheet multiphase program and were performed for several paper machines as well as for de-inking and mechanical pulping. These off-line simulations could be extensively applied for the comparison of the acidifying techniques, to determine chemical dosages, broke circulation ratios etc. An example of a mill test for pH buffering is presented in figure 39. The test was performed to stabilise the furnish pH, which under non-buffered conditions varied greatly while both pine and birch pulps were being used (see [13] for details). The dosage of the non-stoichiometric NaOH-CO_2 buffering solution was calculated with ChemSheet for the test. As the result showed good pH stability and no detrimental effects on product paper quality were observed, they were used to design permanent alkalinity controlling units to the mill.

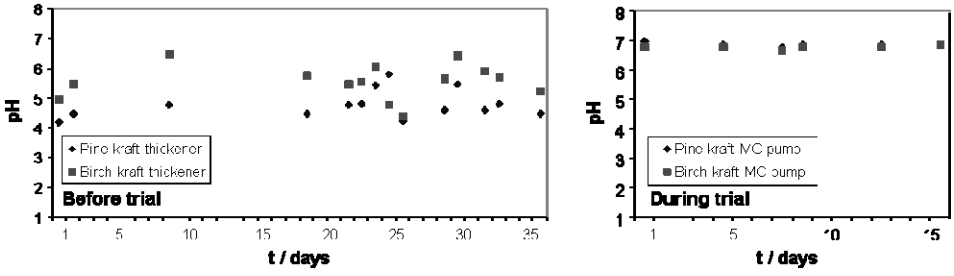

Figure 39. A mill test run of pH buffering at a fine paper producing mill. The dosage of the buffer mixture (non-stoichiometric NaOH-CO2-solution) was calculated with ChemSheet [13].

When these steady-state calculation methods were proven to work well, the focus was transferred to the dynamic modeling of the multi-phase thermodynamics of pulp suspensions. The aim was to model the transient phenomena, such as release of carbon dioxide and precipitation of calcium carbonate. The time constants of these events are relevant when the operation of a paper machine is considered.

The first approach was to use a constrained thermodynamic equilibrium [16]. The release of carbon dioxide and precipitation of calcium carbonate were excluded from the calculation of the thermodynamic equilibrium. For these compound the following differential equations were used [15]:

$$\frac{d\left[Ca^{2+}\right]}{dt} = k_1\left[H^+\right] + k_2 \tag{12}$$

$$\frac{d\left[CO_2\right]}{dt} = k_3\left\{a^*\left(CO_2{}^g\right) - a\left(CO_2{}^g\right)\right\} \tag{13}$$

where $k_1 = 2.925$ min^{-1}, $k_2 = 0.000225$ mol·(l·min)$^{-1}$, $k_3 = 0.0047$ mol·(l·min)$^{-1}$, $a^*(CO_2)$ is activity over saturated carbon dioxide and $a(CO_2{}^g)$ is activity of carbon dioxide in gas phase.

The result of this constrained thermodynamic equilibrium model and validation data can be seen in the figure 40.

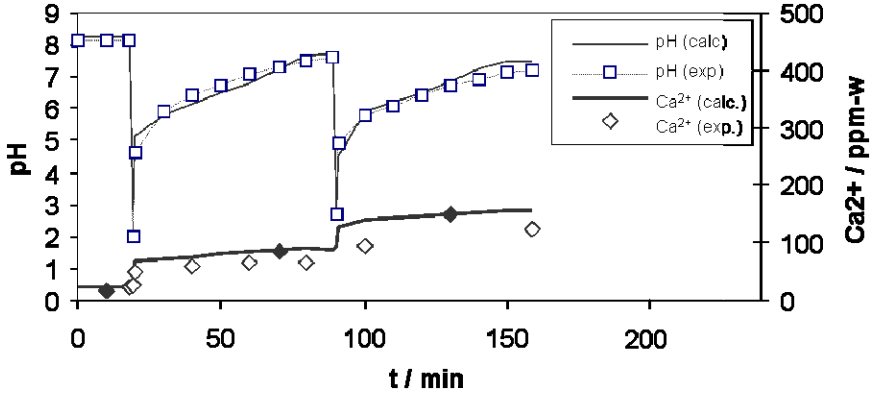

Figure 40. A dynamic constrained multi-phase thermodynamic equilibrium. Concentration of dissolved calcium is measured with ion selective electrode and AAS (dark dots). Model was calculated with ChemSheet [15].

The results of the simple dynamic models also for pulp suspension chemistry were promising. Yet the calculation speed appeared inadequate for larger scale process simulation. For this reason a much faster approach, neural network, was tested to model the pulp suspension chemistry in the approach system of paper machines. The training data was generated using the same rigorous multi-phase model as explained previously. ChemSheet was again used theses pre-calculations.

The aim in using neural networks was to remove time consuming iteration from the solutions. Neural network was used to estimate the pH of the suspension. After that it was possible to calculate the concentrations of all ions analytically based on the equilibrium constants. The slow phenomena were taken into account as presented in Equations 12 and 13.

This model was validated against a parallel model calculation, explained in more detail by Ylen [see 11]. The results of the two calculations can be seen in figure 41.

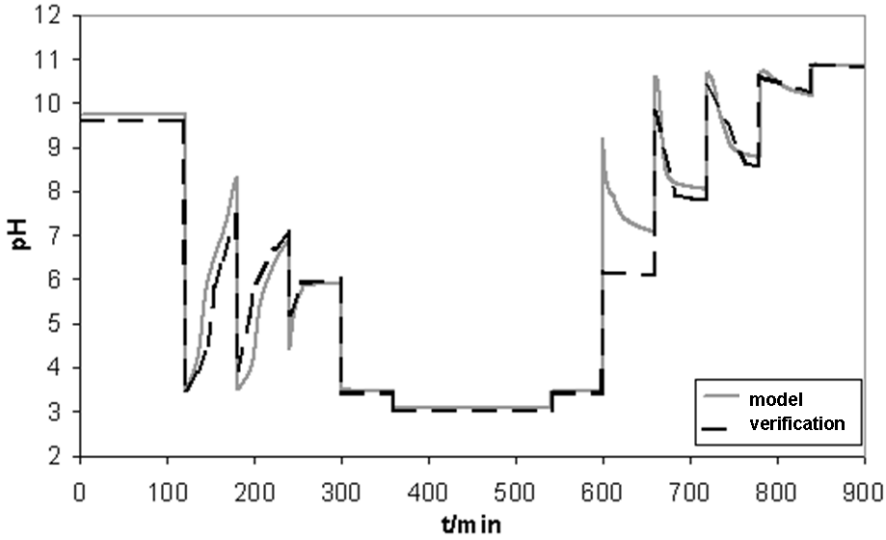

Figure 41. A dynamic model of the multi-phase chemistry of a pulp suspension. The model is based on neural networks and equilibrium constants [14] and verified against the results of Ylen [11].

Neural networks were applicable when a simplified model of the suspension was considered: the fibre phase was neglected. When more comprehensive models were introduced, the training of neural networks appeared to be too laborious. In some cases it is viable to simplify the multi-phase system by excluding the effect of the fibre phase, but if a reliable pH and solubility model of an arbitrary pulp suspension is needed, this phase has to be included.

Later on the equilibrium constants were also used to model the pulp suspension chemistry for a pulp bleaching line. In this case the more comprehensive model with fibre phase was used [9]. Then consequently the ion exchange between the bulk water and fibre phases was included by the Donnan

approach [10]. The multiphase Gibbs'ian technique was further applied for the chemistry of boiler waters. The pH values in different locations were calculated as well as the fractionation of different compounds between the gas and liquid phases in the drum of the boiler.

It was concluded that the Gibbs energy minimization was the most general method for calculation of the multi-phase chemistry as part of the large-scale process simulation. Equilibrium constants are applicable when the temperature dependence of these constants is included in the model. Neural network could provide an alternative fast solution for the calculations. However, neural networks are best to be applied as smart sensors, but cannot be utilized for direct calculation of equilibrium compositions in complex systems.

8.3.3 The computational power

Algorithms based on the equilibrium constants and Gibbs' Energy minimization are iterative when complex multi-phase systems are considered. Additional computational difficulties may occur in such process conditions where phases are formed or removed from the system. Due these factors, the calculation of multi-phase chemistry was often not fast enough to be used as part of large dynamic process simulation with concurrent standard desktop computers.

In the model of the approach system of a paper machine, the simplified chemical system was modelled using the equilibrium constants. This simplified model was practicable, but when Gibbs energy minimization was used, the increase of the number of the calculation steps was unavoidable. In practice the multi-phase chemistry was only calculated using a time step of five seconds when the material properties were calculated by the simulator itself using a time step of 0.2 seconds.

If real-time or faster than real-time computation speeds were needed in the Gibbsian boiler water calculation, it was necessary to reduce the amount of control volumes to five. Multi-phase chemistry was only calculated in those places, where pH measurements were done in the real processes. In addition the thermodynamic equilibrium was calculated in the drum of the boiler. With these simplifications, the real-time simulation speed was achieved.

The chemistry of pulp bleaching line was modelled by using equilibrium constants. The same calculation engine was used to calculate the equilibrium constants and the reactions within the unit operations of the bleaching line, such as washers and bleaching stages. The original calculation speed was too slow,

but it appeared possible to tune the code. After optimization of the code, the calculation speed was nearly 60 times faster than that of the original version. Even with this optimization it was possible to simulate only a single stage of a bleaching line, if real-time simulation speed was desired.

Neural networks represent a very fast method. This technique has been successfully used for estimating the material properties in process simulation of power plants [4]. In this study, neural networks were tested in modelling of the multi-phase chemistry of the short circulation of a paper machine. This proved applicable only for reduced systems, to which the fibre phase was not introduced. If accurate neural networks could be trained for example for the comprehensive pH calculation, this method would provide fast enough calculation for the large-scale process simulation.

8.4 Conclusions

It was possible to use multi-phase chemistry as part of the large-scale process simulation particularly for off-line purposes. However, concurrent dynamic process simulators seldom support the concept of multi-phase chemistry. Multiple phases are not included in their standard architecture. Thus, the number of flowing compounds is often too low for the modelling of a rigorous multi-phase system. This necessitates either simplification of the chemical systems or development of novel simulation software. As well, the interfaces between dynamic simulators and multi-phase solvers need to be improved. Currently there exist different legacy standards which are not compatible with each other.

The Gibbs energy minimization seems to provide the most universal approach for calculating the thermodynamic equilibrium as part of a large-scale dynamic process simulator. Equilibrium constants can be used if their temperature dependence is covered. Neural networks can be used in some special circumstances. They are optimal for soft-sensor type applications.

The calculation speed further remains a limiting factor. By using current desktop workstations it is not possible to perform large-scale real-time simulations. Optimizing ‘the researcher’s code’ can offer remarkable speed additions and parallel computing could provide improved possibilities in the near future.

8.5 References

[1] CAPE-OPEN: Thermodynamic and Physical Properties v1.1 (2006).

[2] Eriksson, G. Thermodynamic studies of high temperature equilibria. III. SOLGAS, a Computer Program for Calculating the Composition and Heat Condition of an Equilibrium Mixture. Acta Chemica Scandinavica 25(7), 1971, pp. 2651–2656.

[3] Eriksson, G., Hack, K. and Petersen, S. ChemApp – A programmable thermodynamic calculation interface. In: Werkstoffwoche '96, Symposium 8 Simulation, Modellierung, Informationssysteme (1997).

[4] Juslin, K. A Companion Model Approach to Modelling and Simulation of Industrial Processes. Dissertation, Helsinki University of Technology (2005).

[5] Kangas, P. Multi-Phase Chemistry in Process Simulation. Licentiate's thesis, Helsinki University of Technology (2009).

[6] Mathworks Ltd. Matlab R2007A User's Manual (2007).

[7] Pajarre, R., Koukkari, P. and Räsänen, E. Inclusion of the Donnan effect in Gibbs energy minimization. Journal of Molecular Liquids 125(1), 2006, pp. 58–61.

[8] Penttilä, K., Koukkari, P. and Pajarre, R. Thermochemical simulation of counter-current rotary drums. In: Proceedings of the 18th international conference of chemical thermodynamics (2004).

[9] Räsänen, E. Modelling Ion Exchange and Flow in Pulp Suspensions. Dissertation Helsinki University of Technology (2003).

[10] Towers, M. and Scallan, A. M. Predicting the ion-exchange of kraft pulps using Donnan theory. J. Pulp & Paper Sci. 22 (1996).

[11] Ylén, P. Measuring, Modelling and Controlling the pH Value and the Dynamic Chemical State. Dissertation, Helsinki University of Technology (2001).

[12] Viitikko, K. and Kalliola, A. Simulation of neutral conversion and water management in LWC paper making. Scandinavian Paper Symposium: Wet End Technology, Helsinki (2002).

[13] Kalliola, A. and Pakarinen, H. Experiences of pH buffering and calcium chemistry control in neutral papermaking. In: 15th PTS Symposium: Chemical Technology of Papermaking, Munich (2002).

[14] Kangas, P. and Ylén, J.-P. Modelling reaction kinetics in dynamic process simulator. In: 10th Mediterranean Congress of Chemical Engineering, Barcelona, Spain (2005).

[15] Koukkari, P., Penttilä, K., Salminen, J., Jutila, P., Komulainen, P., Maasalo, M. and Ylén, J.-P. Dynaaminen kemiallisen tilan mallintaminen paperikoneen yksikkö-operaatioista. CACTUS-projektin väliraportti (in Finnish), Espoo (1999).

[16] Koukkari, P. and Pajarre, R. Calculation of constrained equilibria by Gibbs energy minimization. Calphad 30(2006), pp. 18–26.

9. Multi-phase chemistry for boiler modelling

Petteri Kangas and Sakari Kaijaluoto, VTT

The multi-component boiler water chemistry and the desalination of sea water, both of importance in power production, were simulated by applying previously developed thermodynamic systems on concentrated aqueous solutions. The models were coupled with two different full-scale process simulators, APROS and BALAS. ChemApp was used as the multi-phase chemistry solver.

9.1 Background

The working principle of a MSF (Multistage Flash Evaporation) -process is shown in figure 1. The process is composed of a number of stages where the hot brine from the brine heater is cooled by flashing it stage by stage to reduced pressures. The released vapour is used to heat the incoming brine and the condensate formed is collected and led to the condensate pan of the next stage. Typically the total number of stages is between 20 and 30 and the number of heat rejection stages 3. The process simulated is the MFS desalination plant of the Al-Taweelah power plant in the Arabian Gulf area some 80 km NE of the city of Abu Dhabi [1].

The process of a standard boiler is described in the figures 42 and 43. Feed water is heated in the economizer before it is fed to the drum. Heat transfer to the aqueous phase occurs at the walls and bottom of the boiler. Released vapour is superheated before it is fed to the turbine. The Condensate from the turbine flows back to the feed water tank. If the boiler is used for producing steam as well as electricity and heat, part of the steam is used in the integrated processes. In such cases the condensates can be dirty and additional fresh water may be needed. Even when the boiler water is initially rather clean, the increasing

amounts of fresh water tend to accumulate various chemical species into the boiler. This accumulation can lead to formation of precipitates and corrosion inside the boiler or turbine. Controlling of the chemistry of boiler water is essential for a trouble free operation of boilers. The process model was developed for a typical standard boiler process but there were no correspondence between the model and a real operational system.

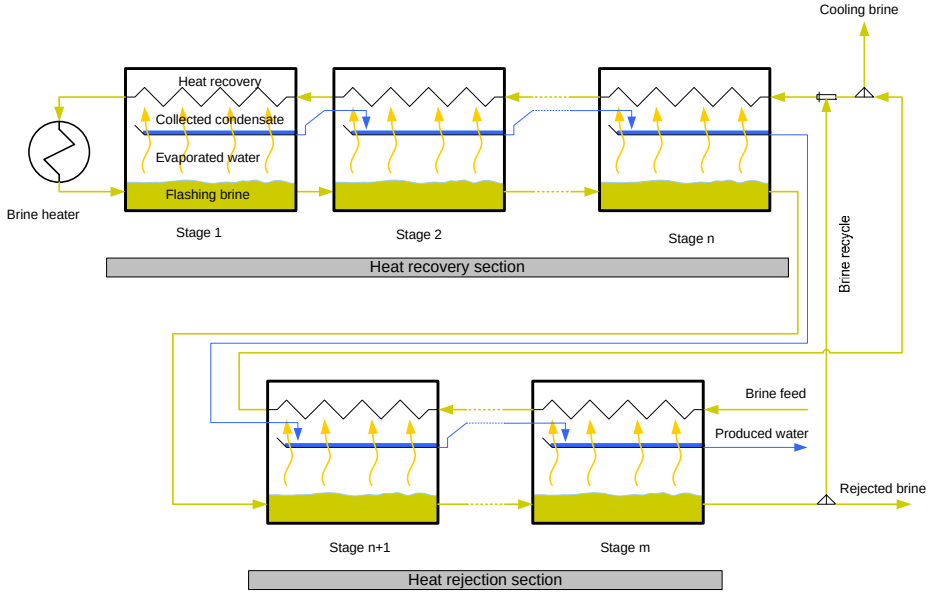

Figure 42. Schematic layout of desalination process.

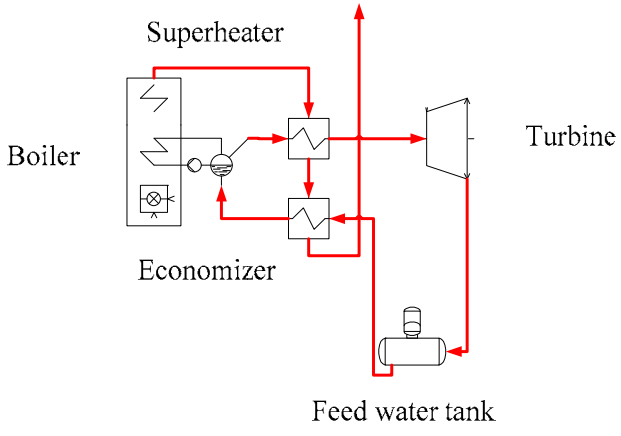

Figure 43. Schematic layout of boiler process.

The two processes were modelled using two different full scale process simulators earlier developed by VTT. The desalination process was modelled by BALAS [2], which is a steady-state process simulator for estimating, developing and sizing new and current process concepts. Main application area of the BALAS process simulator has been the modeling of different pulp and paper processes. The boiler water model was developed within APROS, which is a dynamic process simulator. It has been used for operator training and designing and tuning the process automation. The main application area of Apros is in different power production processes [3].

In both cases the rigorous multi-phase chemistry solver, ChemApp, was connected to the simulators as an external calculation engine. Additional interfaces were needed between the simulators and ChemApp. In BALAS the multi-phase chemistry was modelled as a unit process with a separate multi-phase reactor. In APROS, the multi-phase chemistry was connected to selected calculation volumes, e.g. tanks or points.

The two example cases were developed to test the applicability of multi-phase chemistry connected with the large-scale process simulators.

9.2 Methods

The multi-phase chemistry in both cases was modelled by minimizing the Gibbs free energy. Thermodynamic equilibrium was considered without kinetic constrains. Both multi-phase systems included an aqueous solution and Pitzer parameters were used for the constituent activities in the solutions.

For the desalination process, the chemical species considered in the equilibrium reactor were H_2O, N_2(g), O_2(g), H(+aq), OH(-aq), Ca(+2aq), CaC(+aq), $CaCl_2$(aq), $CaCO_3$(+aq), CaOH(+aq), $CaSO_4$(aq), Cl(-aq), CO2(aq), CO_3(-2aq), H_2SO_4(aq), HCO_3(-aq), HSO_4(-aq), K(+aq), KCl(aq), $KHSO_4$(aq), KOH(aq), KSO_4(-aq), Mg(+2aq), MgCl(+aq), $MgCO_3$(aq), MgOH(+aq), Na(+aq), NaCl(aq), NaOH(aq), SO_4(-2aq), $Ca(OH)_2$, $CaSO_4$, $CaSO_4$*0.5H_2O, $CaSO_4$*2H_2O, $Mg(OH)_2$, $CaHCO_3$(+aq), $CaHSO_4$, $MgHCO_3$(+aq), $MgHSO_4$(+aq), $MgSO_4$(aq), $NaHSO_4$(aq) and $NaSO_4$(aq).

For the boiler water chemistry, the chemical species considered were H_2O(g), CO_2(g), HCl(g), N_2(g), NH_3(g), NH_3(g) ja O_2(g), H_2O(aq), H+(aq), OH-(aq), Ca(+2aq), CaCl+(aq), $CaCl_2$(aq), $CaCO_3$(aq), Cl-(aq), CO_2(aq), CO_3(-2aq), HCO_3(-aq), HSO_4(-aq), K(+aq), KCl(aq), $KHSO_4$(aq), KOH(aq), KSO_4(-aq), Mg(+2aq), MgCl(+aq), $MgCO_3$(aq), $MgHCO_3$(+aq), $MgHSO_4$(+aq), MgOH(+aq),

$MgSO_4$(aq), N_2(aq), Na(+aq), NH_3(aq), NH_4(+aq), O_2(aq) ja SO_4(-2aq), $Ca(OH)_2$, $CaCl_2$, $CaCO_3$, $CaSO_4$, $CaSO_4$*0.5H_2O, $CaSO_4$*2H_2O, H_2SO_4, K_2CO_3, KCl, KOH, $Mg(OH)_2$, $Mg_2(OH)_2CO_3$*3H_2O, $MgCl_2$, $MgCO_3$, $MgCO_3$*3H_2O, $MgSO_4$, Na_2CO_3, Na_2SO_4, NaCl, $NaHCO_3$, NaOH and e-help (for electro-neutrality).

Both processes were modelled using the standard tools and methods of APROS and BALAS simulators. In the desalination model six multi-phase reactors were defined within BALAS. In the boiler water model, the multi-phase chemistry was calculated in four calculation volumes, which were selected to correspond the location of sample collection in the real process. In addition, the multi-phase chemistry was calculated for the boiler drum in order to model the fractionation of different chemical species between liquid and vapour.

Precipitation of carbonates was neglected as they have not been observed in scale analysis. The brine mixture was calculated as a ChemApp equilibrium reactor and then saturated with air in a flash tank. The brine pH was adjusted by the dosage of HCl and NaOH in the solution. As BALAS does not have a unit operation module for a flash evaporation stage, the simulation model was composed of two flash tanks, one for the brine and the other for condensate from previous stage, combined with a mixer and a condenser.

The condenser is an approach temperature module with following input parameters: approach temperature (temperature difference between condensation temperature and that of leaving cold fluid), vent fraction (fraction of incoming gas vented), undercooling of condensate and overall heat transfer coefficient. The necessary heat transfer surface area and the amount of condensing gas needed are among calculated parameters. Total back-mixing is assumed on the two-phase side. The flash tank module performs adiabatic flashing where the pressure is either given as a parameter or is set to the minimum pressure of incoming fluids.

9.3 Results

In general, the desalination model was able to predict the operational conditions reported from the Al-Taweelah power plant [1]. However, an interesting result of the multicomponent simulation is shown in the figure 44. It shows the concentration of non-condensable components in the evaporated vapour in stages 1 to 6. Solid lines show concentrations calculated using ChemApp whereas markers are used for the reference case where no multiphase modelling was applied.

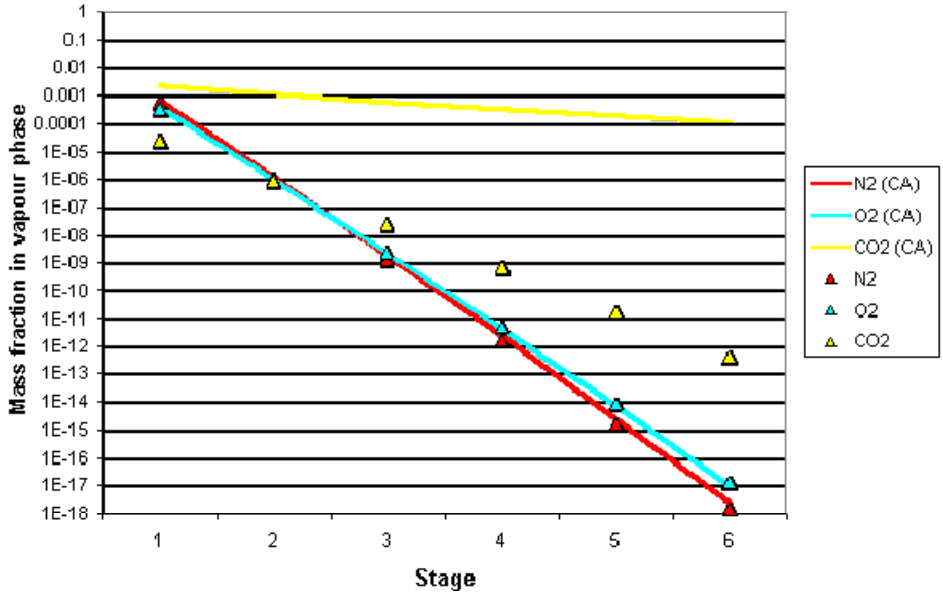

Figure 44. The non-condensable components in flashing vapour calculated by Balas (Henry's law) and by the Balas-Chemapp (multi-phase chemistry) -combination.

For N_2 and O_2 the standard Balas gas solubility model based on Henry's law agrees well with the ChemApp model. The standard Balas flash model can not, however, predict the release of CO_2 correctly, as most of the release is due to the chemical reactions of dissolved carbonates linked to the precipitation of $Mg(OH)_2$. In MSF plants the problems caused by the release of dissolved air and CO_2 are dealt with by venting a suitable amount of vapour to the vent gas system. The multicomponent model can be utilized for an improved design of the vent gas fractioning between stages, as it gives better accuracy with regard to the dissolved carbonates, which are finally released as CO_2 into the vapour phase.

9.4 Conclusions

The boiler water chemistry model has been qualitatively verified by plant observations [1] and it can be used for operator training. The main concern concurrently is the lack of silicates in its current multi-phase system. The future research also needs to be focused on improved property data in the elevated temperatures and pressures. The water temperature typically exceeds 250 °C and the pressure is over 60 bars in the characteristic boiler operation. The current thermodynamic parameters have been determined in much lower temperatures

and their extrapolation to such conditions is questionable. Thus further verification-validation studies on this topic should be performed.

9.5 References

[1] BALAS 2009. A steady-state process simulator developed by VTT. More information can be found at http//balas.vtt.fi.

[2] APROS 2009. A dynamic process simulator developed by VTT and Fortum. More information can be found at http://apros.vtt.fi.

[3] Shams, El Din A. M., El-Dahshan, M. E. and Mohammed, R. A. 2005. Scale formation in flash chambers of high-temperature MSF distillers. Desalination 177 (2005), pp. 241–258.

10. The scale-up of high temperature chemical reactors

Pertti Koukkari, VTT

Thermochemical simulation of reactive high temperature reaction mixtures has been performed by combining overall reaction kinetics with the multi-component Gibbs energy minimisation. The mass and heat transfer conditions of the reactor were combined with the enthalpy changes due to chemical reactions. Consequently, the change of temperature in the reactive system was calculated in terms of the extent of the overall reaction. ChemSheet was used as the modelling environment. The example shows simulation of a titanium(IV)chloride burner, known for its wide industrial use in TiO_2-pigment manufacture. The described method can be applied for several other multi-component reactors.

10.1 Background

Titanium dioxide, also known as titanium(IV)oxide, is the naturally occurring oxide of titanium metal. When used as a pigment, it is often called titania or titanium white. Titanium dioxide is the most widely used white pigment because of its brightness and very high refractive index (n = 2.7), in which it is surpassed only by a few other materials. TiO_2 is also an effective opacifier in powder form, where it is employed as a pigment to provide whiteness and opacity to products such as paints, coatings, plastics, papers, inks, foods, medicines etc. It is also used in cosmetics and for its UV absorbing properties as a UV-shield for both materials and human skin care products. Approximately 5 million tons of pigmentary TiO_2 are annually produced worldwide.

In the chloride process, crude ore (containing at least 90% TiO_2) is reduced with carbon, oxidized with chlorine to give titanium tetrachloride. This titanium tetrachloride is distilled, and re-oxidized with oxygen to give pure titanium dioxide. The oxidising reaction is spontaneous but its high activation energy (88 kJ/mol) requires the raw materials to be heated to ca. 900 °C. The chlorine gas, liberated in the oxidation is nearly 100 % recycled to the chlorination stage. To increase product throughput and to reduce unit energy consumption, a scale-up model of the oxidiser reactor was developed with ChemSheet.

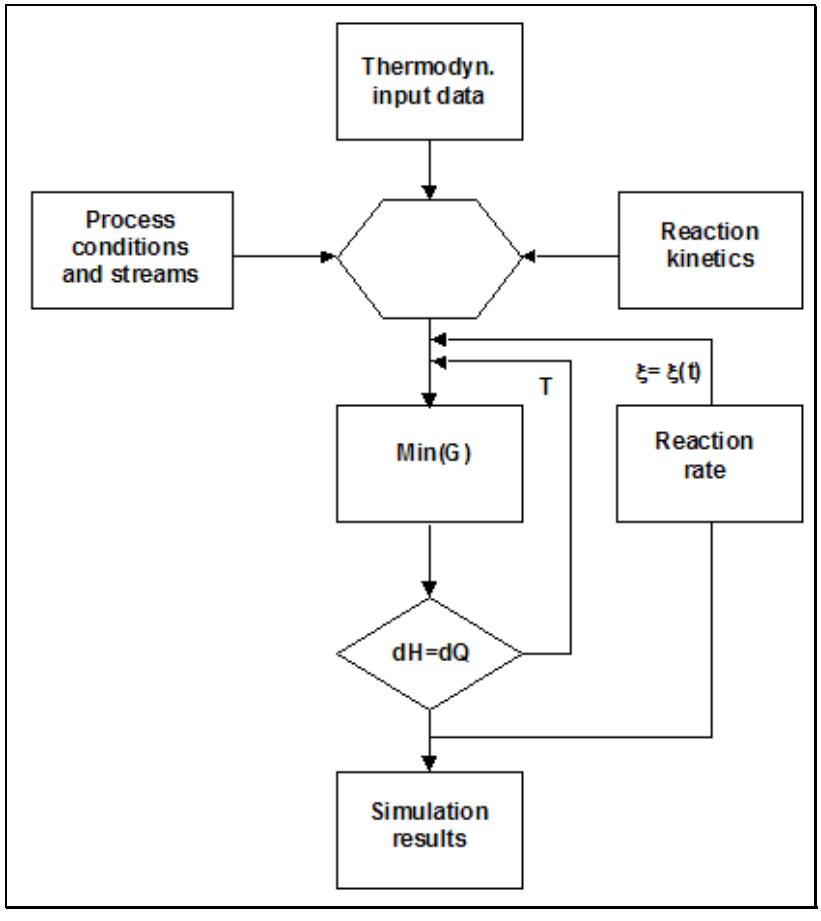

Figure 45. The Ratemix algorithm to calculate rate-controlled thermochemical states.

10.2 Methods

The key reactions in the oxidiser and their data (at ca. 1000 °C) are as follows [1]:

$$TiCl_4(g) + O_2(g) \leftrightarrow TiO_2(s) + 2Cl_2(g) \qquad (I)$$

$$Cl_2(g) \leftrightarrow 2Cl(g) \qquad (II)$$

Reaction	ΔH/kJmol^{-1}	ΔG/kJmol^{-1}	E_a/kJmol^{-1}
I	–177	–102	88
II	250	98	-

The reaction (I) is very exothermic (–177 kJ·mol^{-1}), while the important side reaction (II) is strongly endothermic (250 kJ·mol^{-1}). The local heat balance in the reactor depends on the mutual extents of these reactions. The reaction rate parameters for the consumption of $TiCl_4$ in the oxidation reaction were determined by Pratsinis et al [2] in the conventional Arrhenius expression:

$$\frac{d[TiCl_4]}{dt} = -\left(k + k'\sqrt{[O_2]}\right)[TiCl_4] \qquad k = A \cdot e^{-E_a/R \cdot T} \qquad k' = A' \cdot e^{-E_a/R \cdot T}$$

The activation energy E_a is deduced from the rate law of reaction (I) with $A = 8.26 \cdot 10^4$ s^{-1}. The rates for chlorine association-dissociation reactions and other side reactions such as oxychloride formation are not known for the burner conditions [3, 4]. For these homogeneous gas reactions the equilibrium assumption was then used, which enables the use of Gibbs free energy minimization. The combination of the kinetics of reaction (I) with the multi-component Gibbs energy minimization was performed with VTT's Ratemix algorithm (figure 45). Thus the reaction between titanium(IV)chloride and oxygen is calculated using the known rate equation and side reactions such as chlorine dissociation and oxychloride formation in the hot regions of the burner are assumed to be in local equilibrium.

The mass and heat transfer conditions are combined with the enthalpy changes due to chemical reactions. The conversion of the time-scale to 1-dimensional axial model in terms of the residence time is done using conventional steady state assumptions for plug flow. The heat transfer model covers the radial heat transfer from the tubular reactor volume to the inner surface of the reactor wall and from the outer surface of wall to the cooling water and is detailed according to any customised reactor.

10.3 Results

The model results with axial temperature and heat transfer profiles of the reactor, both of which also can be validated with direct process measurement [4]. In figure 46 the calculated and measured heat transfer of the reactor (left) and the calculated temperature and conversion profiles for the first 10 m section (right) are shown [5]. The O_2:$TiCl_4$-mole ratio was 1.1 and the initial mixing temperature ca. 950 °C. The temperature profile of the scouring sand (calculated with a separate heat transfer model) is included. The calculated yield of TiO_2 indicates that the reaction (I) appears slightly retarded due to thermodynamic conversion limit at peak temperatures. Additional heat transfer to cooling water allows the reaction to complete.

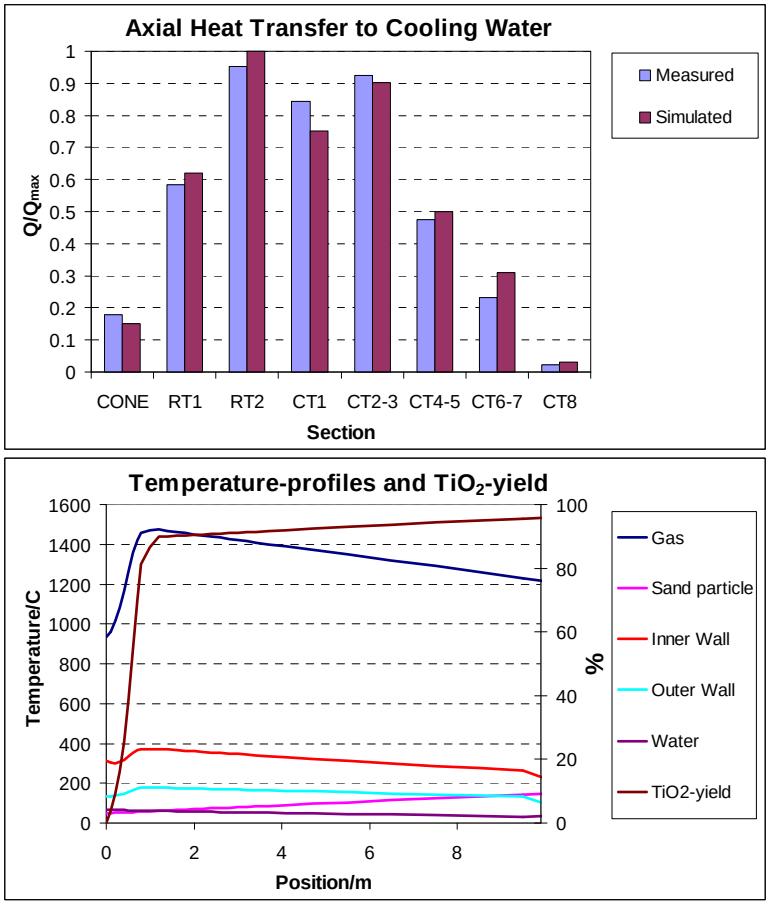

Figure 46. Results for the oxidizer calculation.

10.4 Conclusions

The Ratemix algorithm can be effectively used for combination of kinetics with multi-component Gibbs energy calculations. Within the inner loop, minimisation of Gibbs energy is combined with temperature target calculation with known heat exchange between the reactor and its surroundings. The outer loop controls rate-dependent chemical phenomena and is used to introduce necessary reaction kinetics. Thus the reactor is calculated in terms of its changing thermodynamic state, controlled either by heat transfer or chemical change, or both. The Ratemix algorithm can be directly used together with the Constrained Gibbs energy method [6].

The thermochemical model records the interdependence of chemical reactions and heat effects as function of retention time. The characteristic temperature and velocity profiles have been calculated and used for successful reactor scale-up. With the model, the peak exotherm can be easily located and the autogenic burner heat utilised for a secondary feed, which substantially increases reactor capacity without need of excess energy input. The thermochemical model also has served as a basis for the quantitative modelling of salient quality parameters, such as particle size and tint tone of the TiO_2 pigment, as well as for the development of new pigment grades based on these properties.

10.5 References

[1] Koukkari, P. A Physico-Chemical Method to Calculate Time-Dependent Reaction Mixtures, Computers & Chemical Engineering, Vol. 17, (1993), No. 12, pp. 1157–1165.

[2] Pratsinis, S. et al. J. Am. Ceram. Soc., 70, (1990), pp. 2158–2162.

[3] West, R.W. et al. Ind. Eng. Chem. Res., 46, (2007), pp. 6147–6156

[4] Koukkari, P. and Niemelä, J. Time-dependent reactor simulation by stationary state thermo-chemistry. Computers & Chemical Engineering, Vol. 21, (1997), No. 3, pp. 245–253.

[5] Koukkari, P., Penttilä, K. and Keegel, M. Coupled Thermodynamic and Kinetic Models for High-Temperature Processes. Proceedings of the 10th International IUPAC Conference on High Temperature Materials Chemistry, Part I, Forscungszentrum Julich, 2000. Pp. 253–256.

[6] Koukkari, P. and Pajarre, R. Introducing Mechanistic Kinetics to the Lagrangian Gibbs Energy Calculation. Computers and Chemical Engineering, Vol. 30, (2006), pp. 1189–1196.

11. Kilnsimu and its cement application

Karri Penttilä, VTT
Morihisa Yokota, Ube Industries

The rotary kiln remains in active use in several industries. The rotary kiln provides an efficient means for both heat and mass transfer in the processing of slurries and other condensed mixtures of particles. Pigment and cement manufacturing industries among others are using rotary drums for the thermal treatments of various materials. In the chemical recovery of kraft pulping rotary drums are applied for lime recycling. Other uses include manufacture of oxides (aluminium, zinc, lead), reduction of ores and waste incineration.

11.1 Background

There is increasing interest in the complex chemistry of the rotary drums, as many of the raw materials as well as the fuels used as heat sources vary in their chemical composition. This variation may lead to undesired emissions in the off gas or maintenance problems of the kiln. One common problem in lime and cement kiln is the formation of rings due to alkali compounds. An additional challenge is created by the size of the industrial kilns. Due to long residence times, which may exceed 10 hours, controlling and monitoring the kiln is difficult. Thus it is often beneficial to use a reliable simulation model to predict chemical and physical processes in the kiln.

11.2 Model

Most kilns operate in the counter-current mode, that is, the condensed material is fed into the kiln from the cold ‘feed end’, and is then processed to reacted product by heat transfer from the surrounding hot gas, which is introduced into the kiln from its hot ‘burner end’. The final material product is removed from the hot end. Fraction of exit gas can be circulated back to hot end to improve the heat transfer efficiency. As a heat source, a fuel burner operating with the primary air is typically used.

In KilnSimu there can be any number of bed and gas feed flows – but there must always be at least one bed feed at the ‘feed end’ and one gas feed at the ‘burner end’ of the kiln. If kiln operates in co-current mode then the ‘burner end’ and the ‘feed end’ coincides and the gas flow direction is reversed.

Schematically the rotary kiln can be divided into three zones according to reactions in the material bed [1]:

- drying zone
- heating zone
- reaction zone.

If there is moisture in the bed feed then it is removed in the drying zone. While drying the average temperature of the bed stays close to 100 ºC or increases slowly as the heat is consumed in the evaporation of the water. After all the water has been removed the temperature of the bed is raised quickly until it reaches the reaction temperature. Kiln may contain several reaction zones depending on the thermodynamic characteristics of the bed material.

Figure 47 shows the reaction zones and the simulated temperatures in TiO_2 calcination kiln. Example TiO_2 kiln has high moisture content in the bed feed and thus very long drying zone.

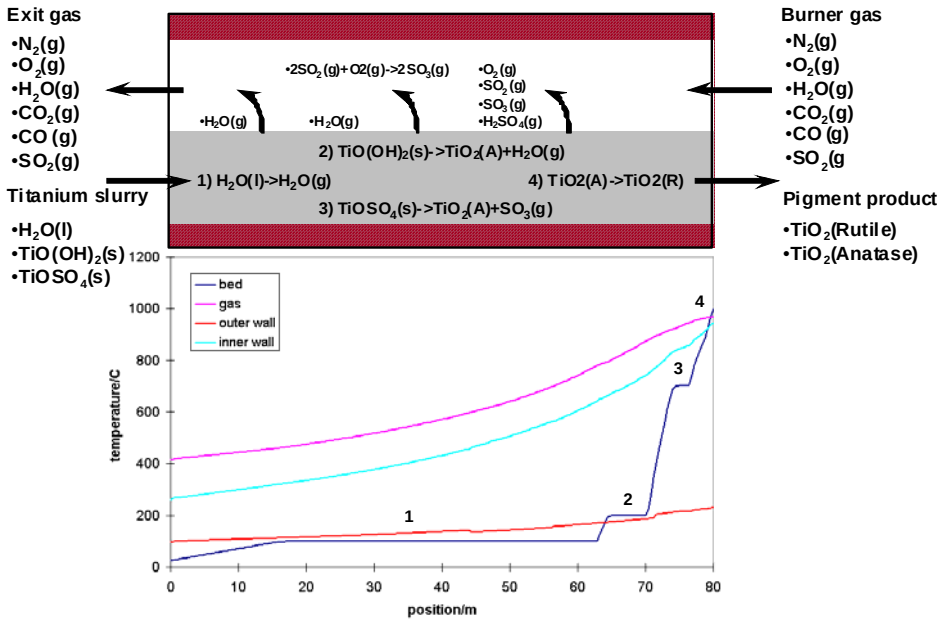

Figure 47. Reaction zones and simulated temperatures in TiO_2 calcination kiln.

11.2.1 The movement of the material bed

The radial movement of the bed depends on the holdup of the kiln, its angular velocity and the properties of the bed like its porosity, density and viscosity. Material that consists of dry particles behaves very differently than material that contains liquid phases like free water (at lower temperatures) or partly molten slag (formed at higher temperatures). Figure 48 shows the cross-section of the bed.

When the angular velocity of the drum is low the bed behaves as a solid object, which slides in place as the kiln rotates. The solid particles remain at rest with respect to each other. If the friction between the bed and the kiln wall is high enough, the bed starts moving along the wall as the bed gets stuck to it. When it reaches a point at which the gravitational force is greater than the frictional force it will slide back to the bottom of the kiln. If the friction between the bed and the wall is greater than the friction inside the bed then part of the bed will slump down. These slumping movements will start at the top of the free surface of the bed. When the angular velocity is increased the frequency of the slumping movement is increased. Eventually there is continuous rolling at the surface of the bed.

The axial velocity of the bed is proportional to inner diameter, rotational speed and inclination of the kiln and is inversely proportional to angle of repose of bed. In addition the bed velocity is inversely proportional to the holdup of the kiln [2]. If velocity is considered independent on the holdup (valid simplification for long industrial kiln), then generally the axial movement can be given as [3].

$$v_b = K \frac{d_i \omega f(\psi)}{f(\alpha)} \tag{1}$$

where $f(\psi)$ and $f(\alpha)$ are functions of inclination angle of kiln and angle of repose of bed.

11.2.2 The mass and heat balances

In KilnSimu the rotary kiln is divided into number of axial control volumes (see Figure 49). Each control volume consists of bed, gas, inner and outer wall regions, in which the temperatures and compositions of bed and gas flows and temperatures of inner and outer wall of the kiln are assumed constant.

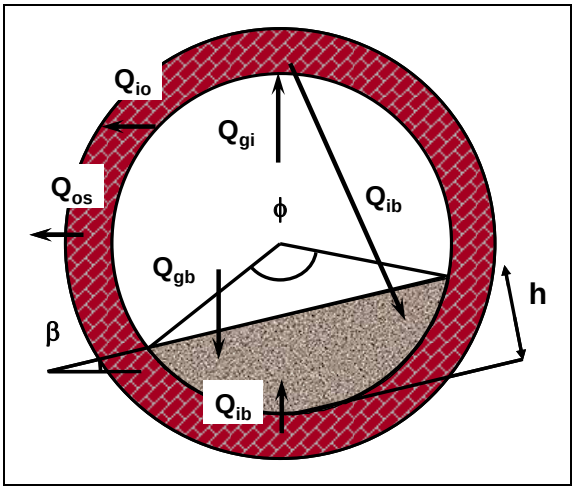

Figure 48. Radial heat flows and bed geometry in rotary kiln.

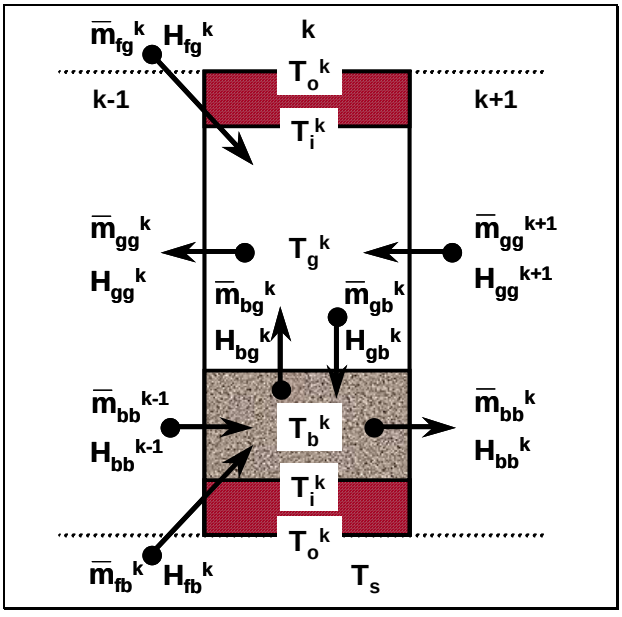

Figure 49. Axial and radial flows to and from a control volume and temperatures in it.

The differential mass and energy continuum equations are discretized accordingly. In steady state the mass and energy balances for the bed and the gas flows and energy balances for the inner and the outer wall in control volume k are given as:

$$\vec{m}_{bb}^{k-1} + \vec{m}_{gb}^{k} + \vec{m}_{fb}^{k} - \vec{m}_{bb}^{k} - \vec{m}_{bg}^{k} = 0 \tag{2}$$

$$\vec{m}_{gg}^{k-1} + \vec{m}_{bg}^{k} + \vec{m}_{fg}^{k} - \vec{m}_{gg}^{k} - \vec{m}_{gb}^{k} = 0 \tag{3}$$

$$H_{bb}^{k-1} + H_{fb}^{k} - H_{bb}^{k} + H_{gb}^{k} - H_{bg}^{k} + Q_{gb}^{k} + Q_{ib}^{k} = 0 \tag{4}$$

$$H_{gg}^{k-1} + H_{fg}^{k} - H_{gg}^{k} + H_{bg}^{k} - H_{gb}^{k} - Q_{gb}^{k} - Q_{gi}^{k} = 0 \tag{5}$$

$$Q_{gi}^{k} - Q_{ib}^{k} - Q_{io}^{k} = 0 \tag{6}$$

$$Q_{io}^{k} - Q_{os}^{k} = 0 \tag{7}$$

There is incoming axial bed flow from the previous control volume and incoming axial gas flow from the next control volume. There can be one or more feed flows from the surroundings to the bed and the gas regions. Outgoing flows have the same temperatures and the compositions as in their source regions.

There are also radial flows between the bed and the gas regions in the control volume. The flow from the bed consists of evaporated gas and solid dust carried away with gas flow. The flow to the bed is composed of the gas interacting with the bed surface and solid particles returning back to the bed. In the model the gas phase has a mixing coefficient that determines the fraction of gas interacting with the bed. Also each solid phase has a dusting and saltation coefficients that are used to calculate the mass fractions of the phase constituents transported from the bed to the gas $\vec{x}_{bg}^{k}$ and back to the bed $\vec{x}_{gb}^{k}$.

The bed and gas flows in the regions are described as thermodynamic systems, which transform mass and heat with each other and their surroundings. Thermodynamic system consists of gaseous and other mixture phases, and number of stoichiometric condensed phases. The equilibrium state of the system can be determined by minimizing its Gibbs energy at constant temperature and pressure. KilnSimu uses ChemApp programming library [4] to calculate the Gibbs energy minimum as well as the enthalpies and heat capacities of the bed and the gas flows.

Bed material consists of particles that are typically at meta-stable state. Most reactions in the bed are gas/solid or solid/solid reactions that are constrained by diffusion and mass transfer in the bed and inside the particles. The composition of the bed flow in a control volume is calculated by combining the equilibrium with time-dependent particle kinetics. The condensed phases in the bed are divided into reactive and inert subsystems by calculating the reaction rates of the phases. Equilibrium is then calculated for the mass flows of the reactive phase constituents only:

$$\vec{x}_{b}^{k} = \vec{A}_0 \exp(-\vec{E}_a / RT_b^k)\Delta t^k \tag{8}$$

$$\vec{m}_{b}^{k} = \vec{G}_{\min}\left(T_b^K, P_b^K, \vec{x}_b^k\left(\vec{m}_{bb}^{K-1} + \vec{m}_{fb}^{K} + \vec{m}_{gb}^{K}\right)\right) + \left(1 - \vec{x}_b^k\right)\left(\vec{m}_{bb}^{K-1} + \vec{m}_{fb}^{K} + \vec{m}_{gb}^{K}\right) \tag{9}$$

$$\vec{m}_{bg}^{k} = \vec{x}_{bg}^{k}\vec{m}_{b}^{k} \tag{10}$$

$$\vec{m}_{bb}^{k} = \left(1 - \vec{x}_{bg}^{k}\right)\vec{m}_{b}^{k} \tag{11}$$

where $\bar{x}_b^k$ are the mass fractions of reactive phase constituents calculated with first order reaction rate equations. Also more complex particle kinetics, like shrinking core model can be used. The composition of the gas flow is calculated in the same way.

The heat transfer flows in control volume k are calculated as follows:

$$Q_{gb}^k = h_{gb}^k A_{gb}^k \left(T_g^k - T_b^k\right) + \overline{GS_b}^k \sigma \left(T_g^{k4} - T_b^{k4}\right) \tag{12}$$

$$Q_{gi}^k = h_{gi}^k A_{gi}^k \left(T_g^k - T_i^k\right) + \overline{GS_i}^k \sigma \left(T_g^{k4} - T_i^{k4}\right) \tag{13}$$

$$Q_{ib}^k = h_{ib}^k A_{ib}^k \left(T_i^k - T_b^k\right) + \overline{S_i S_b}^k \sigma \left(T_i^{k4} - T_b^{k4}\right) \tag{14}$$

$$Q_{io}^k = 2\pi L^k \left(T_i^k - T_o^k\right) \Big/ \sum_l \frac{1}{k_l^k} \ln \frac{d_{l+1}^k}{d_l^k} = 2\pi L^k R^k \left(T_i^k - T_o^k\right) \tag{15}$$

$$Q_{os}^k = h_{os}^k A_{os}^k \left(T_o^k - T_s\right) + \overline{S_o S_s}^k \sigma \left(T_o^{k4} - T_s^{k4}\right) \tag{16}$$

Forced convective heat transfer takes place between the gas and the inner wall and the bed surface. There are many correlations in the literature [5, 6] that can be used to calculate the heat transfer coefficient as a function of gas flow properties, like its velocity, density, viscosity and thermal conductivity. KilnSimu also uses temperature dependent equations for gas species to calculate viscosity and thermal conductivity of the gas flow.

Conductive heat transfer takes place between the inner wall and the bed. So called penetration theory can be used to derive the conductive heat transfer coefficient between the inner wall and the bed [7]:

$$h_{ib} = \frac{2k_b}{\sqrt{\pi \alpha_b \tau_{ib}}} \tag{17}$$

Heat transfer is more efficient the shorter the contact time τ_{ib} between the inner wall and the bed is.

Radiation model consists of radial heat exchange between gray gas and reradiating bed and inner wall surfaces, i.e. radiation between the regions in the control volume. Total energy balance can be written over each region in terms of

the radiation arriving at it from all other regions in the control volume (axial radiation is neglected). Radiation equations are written in terms of total exchange factors, which are functions of emissivities and geometries of regions. Total exchange areas can be solved from the resulting system of linear, algebraic equations [8].

The measured emissivity and absorptivity of carbon dioxide and water vapour are tabularized as function of their partial pressures, temperature and mean path length. KilnSimu uses Leckner [9] correlation based on these tables to calculate the emissivity and absorptivity of the gas phase. Also emissivity of the soot particles is included.

11.3 Solution

The number of control volumes can be chosen freely but typically it should be between 40–80 for obtaining accurate prediction of the local temperatures and compositions in the kiln. Initially the temperatures and compositions in the control volumes are unknown, only the feed flows into the rotary kiln are known. Rotary kiln is divided into two sides: bed side consisting of bed, inner and outer wall regions and gas side consisting of gas regions. First the initial temperature and composition profiles are estimated for the gas flow. After that the temperatures and compositions of all incoming flows to the bed side in the first control volume are known, including the radial mass transfer from the gas side. Then the bed side temperatures are solved from equations (4), (6) and (7) by using appropriate solver (quasi-Newton method) for non-linear set of equations. Each time the solver changes the bed temperature equations (8) and (9) are calculated to obtain the bed flow composition and enthalpy. After solving the temperatures for the bed side in the first control volume all the flows to the bed side in the second control volume are known. Bed side temperatures and compositions in the second and in all the subsequent control volumes are solved in a similar manner. After that the gas side is calculated by using the previously calculated values for the bed side, including the radial mass transfer from the bed side. Gas flow temperature can be solved from equation (5) by using appropriate root-finding solver. Again each time the solver changes the gas temperature the gas flow composition and enthalpy are calculated. After solving both the bed and the gas side, the procedure is repeated until the temperatures in control volumes converge to their final values, which usually takes 10–20 iterations.

11.4 Application

Cement manufacturing is one of the most widely used industrial processes involving a rotary kiln unit operation. Cement process has two main variations: a wet process and a dry process. In the wet process a suitable mixture of raw materials is fed into the rotary kiln in the form of slurry, which may have water content of 30 to 40%. In the dry process this “raw meal” is first dried with exhaust gas from the rotary kiln and then heated in a precalciner system typically consisting of several cyclones and riser duct that is fuelled with coke to calcine the limestone. Cyclones collect dust from the kiln’s exhaust gas and mix that with partially calcined raw meal, which is then fed into the kiln at about 800 °C. The advantage of the dry process is its lower fuel consumption and thus it is the main choice for cement manufacturing today. Figure 50 shows an example of the dry process.

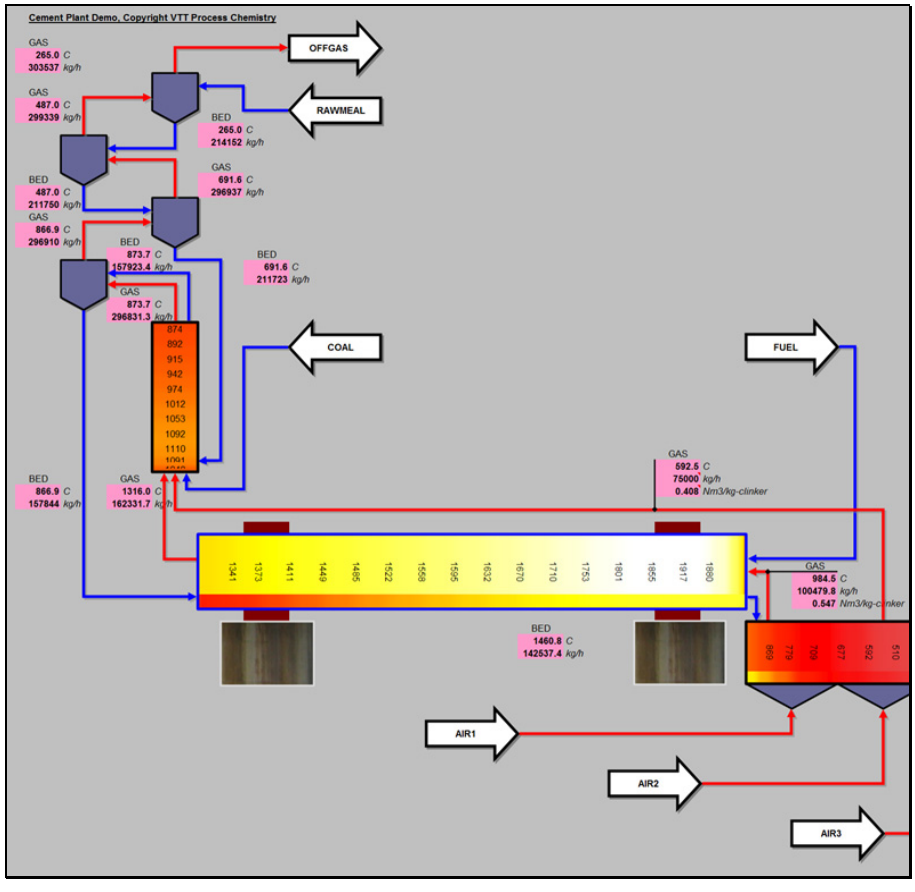

Figure 50. Cement process with a precalciner.

VTT has provided Ube Industries, a Japanese cement manufacturing company, with a KilnSimu model for rotary kiln and clinker cooler unit in the dry cement process. Ube Industries has three cement factories in Japan with combined production capacity of nine million tons of cement per year. Ube Process Technology Research Laboratory has combined KilnSimu with Aspen® flowsheet model to describe the whole cement manufacturing process.

There is interest of using alternative fuels in the cement process as additional heat sources and for waste incineration in the rotary kiln and the riser duct. Typical candidates in the Ube factories are waste plastics (including pachinko panels), oils, tyres and even tatami mats! These additional fuels may have a high content of volatile elements like sulphur and chlorine, which react with alkali metals to form sulphates and chlorides. These then accumulate to the process through alternate vaporization at the hot end and precipitation at cold end of the kiln and in the cyclones and cause cyclone clogging and ring formation and accelerated brick damage in the kiln.

KilnSimu cement model contains a full thermodynamic description of the phases and phase constituents in the cement system. These include gaseous species, liquid slag and solid mixtures and around 100 stoichiometric condensed phases. The mixture of raw materials consists of calcium carbonates, silicon oxides, aluminium oxides and iron oxides respectively occurring as limestone, sand, clay, bauxite, laterite, etc. In the precalciner most of the calcium carbonate is first calcined to calcium oxide or lime at 800–900 °C. Then in the kiln lime reacts with other raw materials at 1200–1450 °C to form calcium and iron silicates and aluminates that are the main components in the burned product called cement clinker.

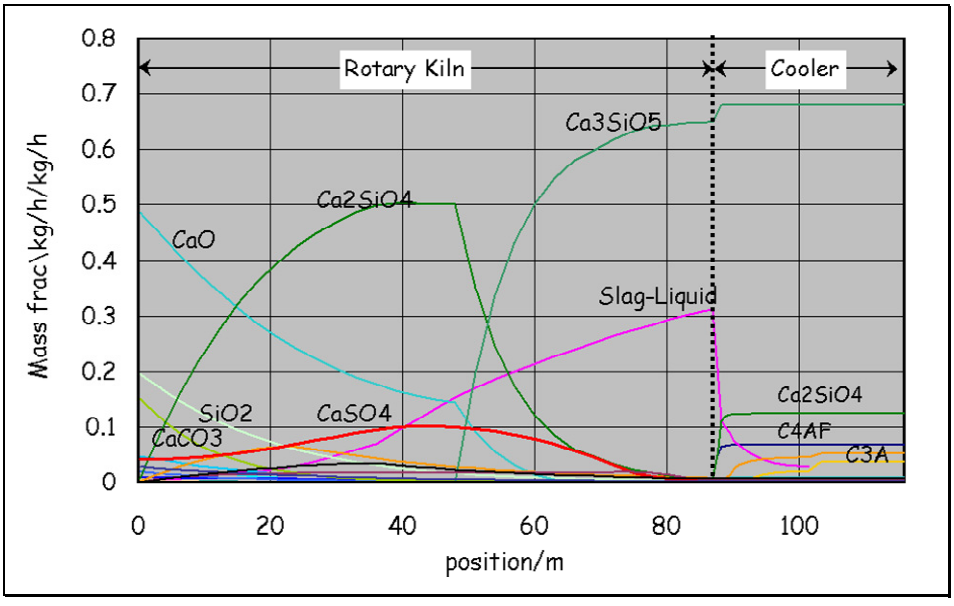

Figure 51. Simulated axial bed flow composition.

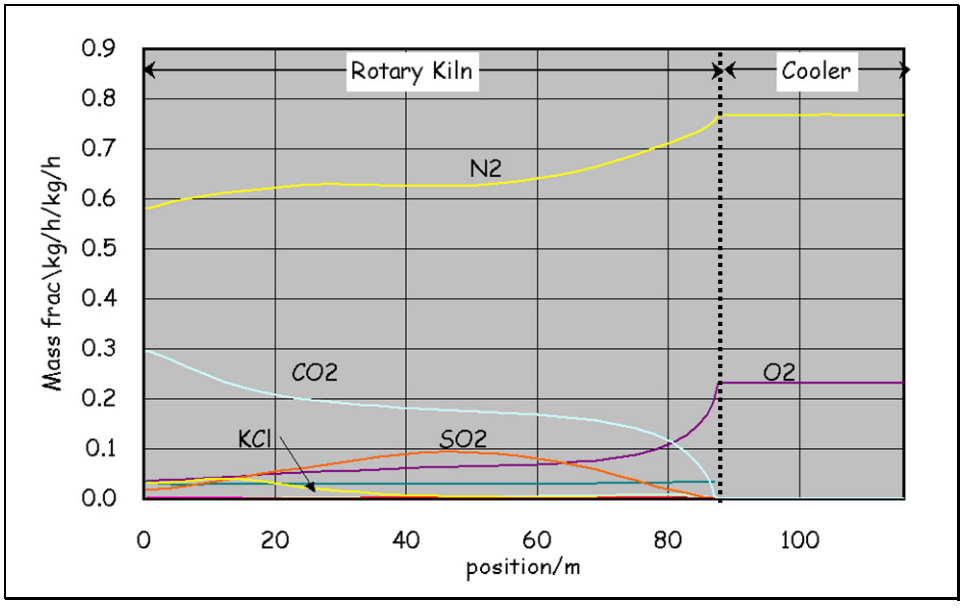

Figure 52. Simulated axial gas flow composition.

A special version of KilnSimu was prepared with a clinker cooler unit which is used for cooling the clinker from the rotary kiln and also for pre-heating the air going into the kiln and the riser duct. Cooler is typically a grate kiln where air is blown from the bottom of the cooler through the grates and the clinker in a cross current fashion. The clinker cooler is also divided into number of control volumes in a similar way as the rotary kiln.

Figure 51 shows simulated axial bed flow composition profile and Figure 52 shows simulated axial gas flow composition profile. Bed flow direction is from left to right and gas flow direction is from right to left. Figures include results for both the rotary kiln and the clinker cooler.

11.5 Conclusions

The simulation yields axial temperature profiles for the bed, the gas and the inner and outer walls. In addition, axial phase compositions of the bed and gas flows are calculated. Results can be used to optimize fuel consumptions with different material feed capacities and to study the effect of using various fuels. Other uses are optimizing the gas circulation and other energy factors including the kiln geometry. KilnSimu is also well suited for kiln scale-up.

In cement case KilnSimu model was successfully used to predict the cement clinker crystal formation and composition and to estimate the circulation of sulphate and chlorine species in the precalciner and rotary kiln. Results can be used for making a correlation between the brick damage rate and the behaviour of sulphates and chlorides.

11.6 Symbols

A	Heat transfer area.
$\vec{A}_0$	Vector of frequency factors of phase constituents, () 1/s.
d	Diameter, () m.
Δt	Residence time (L/v), () s.
$\vec{E}_a$	Vector of activation energies of phase constituents, () J/mol.
G	Gibbs energy, () J/mol.

$\bar{G}_{min}$	Function that returns vector of mass flows of phase constituents at equilibrium, () kg/s.
$\overline{GS}$	Total exchange area between gas and surface, () m^2.
h	Heat transfer coefficient, () W/m^2-K
H	Enthalpy flow, () W.
k	Thermal conductivity, () W/m-K
K	Proportionality constant, () 1/rad.
L	Length, () m.
$\vec{m}$	Vector of mass flows of phase constituents, () kg/s.
P	Pressure, () Pa.
Q	Heat flow, () W.
R	Thermal resistivity, () m-K/W.
R	Gas constant, () 8.314472 J/mol-K
$\overline{SS}$	Total exchange area between two surfaces, () m^2.
T	Temperature, () K.
v	Velocity, () m/s.
$\vec{x}$	Vector of mass fractions of phase constituents, ().

Greek symbols

α	Thermal diffusivity ($k/c_p\rho$), () m^2/s.
β	Angle of repose, () rad.
ϕ	Filling angle, () rad.
σ	Stefan-Bolzmann constant, () $5.67032 \cdot 10^{-8}$ W/m^2-K^4.
τ	Contact time (β/ω), () s.
ω	Angular velocity, () rad/s.
ψ	Inclination angle, () rad.

Subscripts and superscripts

b	Bed
f	Feed

g	Gas
i	Inner wall
o	Outer wall
s	Surroundings, surface
k	Control volume
l	Wall layer

11.7 References

[1] Dumont, G. and Belanger, P.R. Steady State Study of a Titanium Dioxide Rotary Kiln. Ind. Eng. Chem. Process Des. Dev., 17, (1978), pp. 107–114.

[2] Lebas, E. et al. Experimental Study of Residence Time, Particle Movement and Bed Depth Profile in Rotary Kilns. Can. J. Chem. Eng., 74 (1995), pp. 173–180.

[3] Manitius et al. Mathematical Model of the Aluminium Oxide Rotary Kiln. Ind. Eng. Chem. Process Des. Develop., 13, (1974), pp. 132–142.

[4] Eriksson, G., Hack, K. and Petersen, S. Werkstoffswoche ’96, Symposium 8: Simulation Modellierung, Informationsysteme, 1997, 47, DGM Informationsgesellschaft, mbH, Frankfurt, Germany. ISBN3-88355-236-4.

[5] Li, S. et al. A Mathematical Model of Heat Transfer in a Rotary Kiln Thermo-Reactor. Chem. Eng. Tech., 28, (2005), pp. 1480–1489.

[6] Tscheng, S. and Watkinson, A. Convective Heat Transfer in a Rotary Kiln. Can. J. Chem. Eng., 57 (1979), pp. 433–443

[7] Penttilä, K. A Simulation Model of TiO2-calcination Kiln. M.Sc. thesis, Helsinki University of Technology, Faculty of Process Engineering and Materials Science, 1996.

[8] Rhine, J. and Tucker, R. Modelling of Gas-Fired Furnaces and Boilers. 1991, McGraw-Hill England, p. 221.

[9] Leckner, B. Spectral and total emissivity of water vapor and carbon dioxide. Combustion And Flame, 19, (1972), pp. 33–48.

12. New dynamics for kiln chemistry

Pertti Koukkari and Karri Penttilä, VTT
Hannu Karema, Process Flow Oy

The technology of rotating drums has been available for over 100 years, yet it remains in active use in many of its traditional applications. The rotary drum provides efficient means for both heat and mass transfer in the processing of slurries and other condensed mixtures. The most well-known uses are lime, pigment and cement manufacture, as well as the lime sludge reburning in the recovery cycle of the wood pulping process. Other uses are in manufacture of oxides (zinc, lead), reduction of ores and waste incineration. With fostered pursuit for energy-efficiency everywhere in the industry, a new simulation tool, which combines computational fluid dynamics (CFD) with multiphase chemistry allows for improved insight on the kiln operation.

12.1 Background

Most kilns operate in the counter-current mode, that is, the condensed material is fed into the kiln from the cold ‘feed end’, and is then processed to the calcined or otherwise reacted product by heat transfer from the surrounding hot gas, which is introduced into the kiln from its hot ‘burner end’. The final product is removed from the burner end, e.g. as a solid oxide phase. The gas is usually circulated to a part to improve the heat transfer efficiency. As a heat source, a fuel burner operating with the primary incoming air is typically used. The chemistry of the kiln is often complicated, as coupled reactions and phase transformations occur in several stages, covering both gas, liquid and solid phases.

However, there is increasing interest to control the complex chemistry of the rotary drums, as many of the raw materials as well as the fuel mixtures vary in their chemical composition. These trends are emphasized by the endeavour to use biomass or waste as fuels, while simultaneously carbon dioxide emission are being minimised. Alternative fuels easily lead to undesired emissions in the offgas or maintenance problems of the kiln. On the other hand, if the operational conditions of the kilns remain sufficiently stable, their remote control and a centralised maintenance for several kilns can be achieved. Such arrangements may lead to significant savings in the operation cost of a production site. Both of the suggested trends would benefit from such simulation models, which include accurate description of the chemical and physical processes of the kiln.

12.2 Methods

The conventional models of rotary kilns typically cover equations of reaction kinetics with mass and heat balance equations which are solved numerically, supported with a number of algebraic expressions, describing the geometry of the furnace, the properties of reactant mixtures such as heat capacities, emissivities, viscosities and the like as well as the properties of the wall materials of the kiln, whose thermal conductivity is the most important factor [1]. The complexity of the problem requires simplification to calculation procedures based on mechanistic kinetics. In particular, the dominant bed reactions appear difficult to handle with mere reaction kinetic approach. The received equations for heat balances also become strongly non-linear in temperatures, and the mass balances become increasingly elaborate when complex chemistry of the reacting substances are taken into account.

Figure 53. Rotary drums remain among the best available technologies in the process industry.

The rotary kiln has also been modelled by using the multi-component thermodynamic technique, by presenting both the gas stream and the solids stream as a series of temperature-dependent thermodynamic equilibria [2, 3]. The solution is given in a series of successive thermodynamic equilibria, calculated by the Gibbs energy minimisation technique for such temperatures, which are characteristic for the operation range of the kiln. This treatment provides more comprehensive chemistry to be taken into account via the multi-phase calculation method. However, it is not certain that the global equilibrium conditions actually are reached in the practical rotary drum.

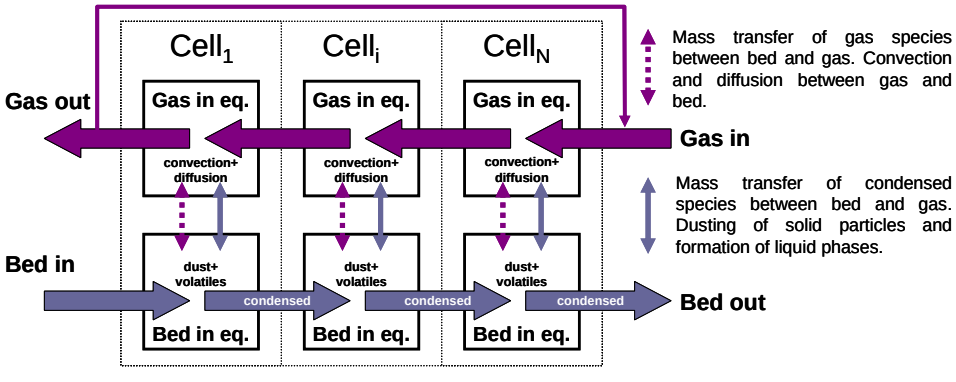

Figure 54. Kilnsimu model scheme.

Based on the multi-phase Gibbsian technique, VTT has developed KilnSimu software, which combines reaction kinetic and heat transfer equations with the thermodynamic multi-component calculation [4]. KilnSimu enables fast and easy access to the simulation of rotary kilns. Counter-current or co-current kiln operation with multi-phase chemistry and direct or indirect heating mechanisms can be simulated. The chemical system is defined in multi-phase format, and the thermodynamic composition is calculated by Gibbs energy minimisation, to which the necessary mass and heat transfer as well as reaction rate constraints can be appended. There are two solution domains; the gas volume and the feed volume. Both volumes are discretized axially (1D representation, see figure 54). Both volumes include corresponding parts of lining and drum.

KilnSimu has been applied with fair accuracy for e.g. lime kilns, titania pigment calcination, cement furnaces and various metallurgical kilns. Its strength is in the fairly accurate calculation of bed properties and composition, while one would wish to have a more accurate depiction of the gas reactions, including the interaction of the burner flame with the heat exchanging surfaces both from the reactive bed and kiln walls. The new calculation procedure was thus developed by combining the features of KilnSimu (bed calculation) to the powerful CFD (computational fluid dynamics) of ANSYS Fluent software.

ANSYS Fluent provides the full power of multi-phase CFD modeling combined with the leading selection of combustion sub-models. Chemical reaction modeling, especially in turbulent conditions, has been a hallmark of Fluent since its inception. ANSYS Fluent includes models for radiation, multi-phase flow, and chemical reactions. Gaseous, solid and liquid fuel combustion can be simulated. Models for the prediction of SOx formation and NOx formation and destruction are included in the package.

By combining the advanced capabilities of KilnSimu and ANSYS Fluent a new level in rotary kiln analysis was reached. The general analysis of kiln behavior and chemistry is handled by KilnSimu, while ANSYS Fluent simulates the gas volume including the combustion process. The solutions are coupled together via heat and mass transfer on interfaces (bed-gas and wall-gas). The aim is to achieve enhanced accuracy in estimating the gas volume phenomena combined with detailed description of the chemical states in the bed. The boundary conditions set by heat releasing and heat demanding zones can thus be deduced.

12.3 Results

The coupled Fluent-KilnSimu software has been successfully used to simulate Nordkalk's rotary lime kiln in Pargas [5]. The kiln is 73 m long with a diameter of 3.3 m, capacity being 210 tpd burned lime. Pulverized coal is used as fuel. The kiln is equipped with a 20 m cross-section for heat transfer in the upper end of the kiln. The feed is 20–40 mm fraction of Silurian limestone. After calcination the quick lime product is cooled in ten planetary coolers.

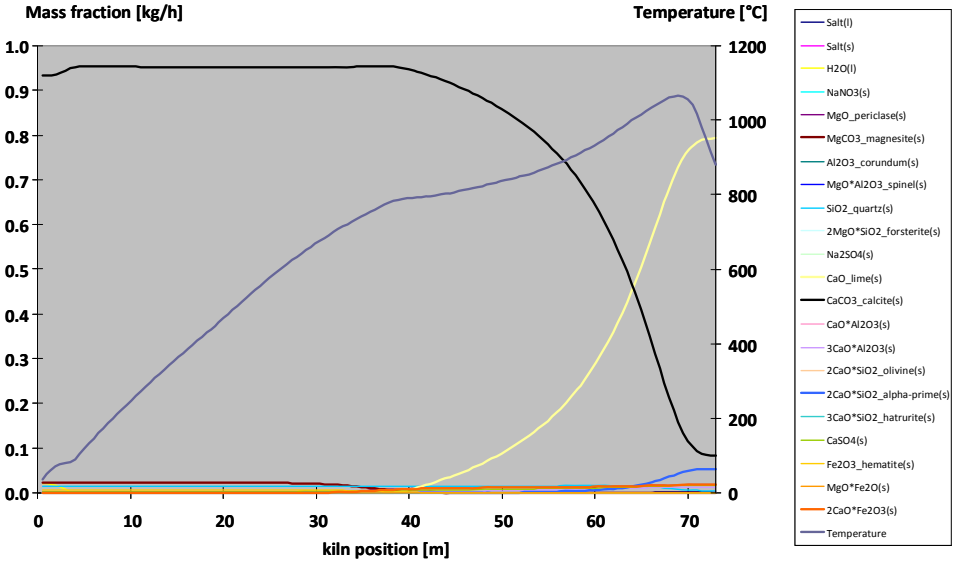

Figure 55. The bed composition profiles of a typical lime kiln as calculated by KilnSimu.

The limestone feed enters the kiln in its upper end. As shown in figure 55, the calcination process commences at ca 40 m and the bed temperature reaches its maximum at 70 m. The burned lime (CaO) exits the kiln in the lower end with a small content of residual calcium carbonate ($CaCO_3$). The results of KilnSimu for the temperature profile of the bed as well as the CO_2 release profile are used as boundary conditions for the ANSYS Fluent simulation of the gas stream.

Figure 56 shows the simulation of the burning of coal particles in Fluent. Coal particles enter the kilns with the primary air through the burner pipe. Various process configurations, e.g. in terms of the burner adjustment can be simulated for process optimisation. In figure 56, the upper case is with centered primary air directed along the near horizontal axis of the kiln, the lower case shows centered

primary air directed downward towards the bed. The red field behind the coal plume represents the bed material. The ‘touch area’ between the flame and bed becomes clearly visible in the simulation.

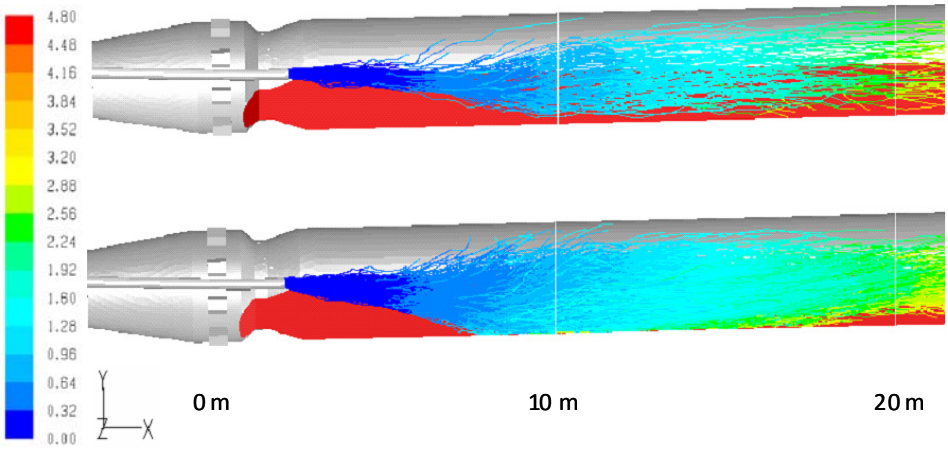

Figure 56. Example of Fluent-Kilnsimu combination with coal burning, horizontal (upper) and downward (lower) directed flames. The red field in the lower part of kilns shows the calcined bed.

The Fluent simulation of the gas phase allows for detailed studies of the flow patterns inside the kiln. Thus, e.g. the path lines for the secondary air used as oxygen source for the burner can be simulated in various settings for optimal efficiency of the kiln. When various mixed fuels are being used, not only the setting but also the composition of the gas phase will be of interest.

12.4 Conclusions

The simulations have contributed to a deeper understanding of various phenomena inside the kiln. The new approach can be used for improving material and energy efficiencies of the rotary drum processes as well as in reducing their CO_2-emissions.

Control of both the bed and gas compositions are of importance for smooth operations. The gas is often recirculated or used for preheating the bed material, while the enrichment of volatile impurities into the recirculating gas must be avoided. The bed simulation with advanced multi-phase model will include the formation of possible liquid slags, which typically are a source of maintenance breaks in particular in lime reburning kilns of the forest industry.

One further advantage of the new model is in its ability to connect the boundary conditions of the flame with the endothermic and exothermic reaction zones occurring in the bed of certain kilns. A proper connection with the bed exotherm may lead to significant savings in fuel consumption and thus also give much lower carbon dioxide emissions during operation.

12.5 References

[1] Manitius et al. Ind. Eng.Chem. Process Des. Develop., 13, No. 2, (1974), pp. 132–142.

[2] Kääntee, U., Zevenhoven, R. Backman, R. and Hupa, M. Modelling a Cement Manufacturing Process to Study Possible Impacts of Alternative Fuels, TMS Fall 2002 Extracting and Processing Division Meeting on Recycling and Waste Treatment in Mineral and Metal Processing, Luleaå, Sweden, June 16–20, 2002.

[3] Modigell, M. and Liebig, A. Thermochemical Process Modelling of Clinker Burning, GTT Product Presentation and Workshop, Aachen, Germany 6.–8.6. 2002.

[4] Ketonen M., Koukkari, P. and Penttilä, K. Simulation Studies of the Calcination Kiln Process, The European Control Conference, ECC 97, Brussels, Belgium 1–4 July, 1997.

[5] Eriksson, M., Karema, H., Boström, S., Koukkari, P. and Penttilä, K. Coupled Fluent-KilnSimu Simulation of a Rotary Lime Kiln, IFRF TOTeM 33 – Challenges in Rotary Kiln Combustion Processes, Pisa Italy, 11th–12th February, 2009, joint publication of Nordkalk Oy, Process Flow Oy and VTT.

13. Modelling of surface and interfacial properties

Risto Pajarre, VTT

Understanding of surface phenomena is of vital importance in such diverse areas as materials science and metallurgy, environmental and biological sciences and in aqueous chemistry. Surface and interfacial energies affect phenomena such as wetting and microstructure growth, while adsorption and surface compositions are determining factors in many mass transfer processes. There is a need for reliable computational methods to produce reliable numerical values for simulation, optimization and for search of new and improved materials.

13.1 Methods

The surface or interface is described as a series of one atom or molecule thick layers. In calculation of equilibrium properties, the total area of each surface or interfacial layer is set to constant by defining a new component for each constrained layer. The conjugate chemical potential in the constrained free energy (CFE) [1, 2] model is the surface or interfacial tension multiplied by the unit molar area. Both the interfacial compositions and energies are solved in a single equilibrium calculation that can be done using the ChemSheet program.

In interfacial layers between two condensed (liquid) phases, the normal thermochemical standard states of bulk liquids are used. On a gas-liquid surface, the standard state is adjusted based on experimental surface energies.

$$\mu_i^{0,surface} = \mu_i^{0,(bulk)} + A_i\sigma_i$$

For the calculation of excess energies of mixtures, adjusted bulk thermodynamic equations are used [1, 3]. Typically the energetic interactions are assumed to be governed by the same expressions as in bulk material, but scaled for the reduced coordination number of the surface, for example for metallic alloy in surface monolayer approximation.

$$\gamma_i^{bulk} = f\left(x_2^{bulk}, x_2^{bulk}, ...x_N^{bulk}\right) \Rightarrow \gamma_i^{surface} = 0.83 \cdot f\left(x_2^{surface}, x_2^{surface}, ...x_N^{surface}\right)$$

In interfacial layers the composition of the neighbouring layers is taken into account in a similar fashion by estimating the relative contributions to excess energies from the surrounding molecules in the same and neighbouring layers.

Adsorption of gaseous species can be modelled using a separate adsorption layer in a model. Different thermochemical descriptions of the adsorption layer lead to different adsorption isotherms such as

- Ideal solution => Langmuir Isotherm
- Regular solution => Frumkin isotherm
- Flory-Huggins model => Flory-Huggins isotherm

13.2 Results

The method is capable to predict surface tensions liquid mixtures based on the surface tension values of the pure components and the bulk thermodynamic data of the system [1]. The method then allows for the quantitative considerations of various surface systems, ranging from aqueous-organic in ambient temperatures to high temperature metallurgical melts. Some calculation examples are shown below in figures 57–60.

		Component(1)	Component(2)	...	Component(M)	Area(1)	Area(2)	...	Area(L)
bulk(1)	Species (1)	v_{11}	v_{12}	⋯	v_{1M}	0	0	⋯	0
	Species (2)	v_{21}	v_{22}	⋯	v_{2M}	0	0	⋯	0
	⋮	⋮	⋮	⋱	⋮	⋮	⋮		⋮
	Species (N)	v_{N1}	v_{N2}	⋯	v_{NM}	0	0	⋯	0
interface(1)	Species (1)	v_{11}	v_{12}	⋯	v_{1M}	A_1/A_0	0	⋯	0
	Species (2)	v_{21}	v_{22}	⋯	v_{2M}	A_2/A_0	0	⋯	0
	⋮	⋮	⋮	⋱	⋮	⋮	⋮		⋮
	Species (N)	v_{N1}	v_{N2}	⋯	v_{NM}	A_N/A_0	0	⋯	0
interface(2)	Species (1)	v_{11}	v_{12}	⋯	v_{1M}	0	A_1/A_0	⋯	0
	Species (2)	v_{21}	v_{22}	⋯	v_{2M}	0	A_2/A_0	⋯	0
	⋮	⋮	⋮	⋱	⋮	⋮	⋮		⋮
	Species (N)	v_{N1}	v_{N2}	⋯	v_{NM}	0	A_N/A_0	⋯	0
⋮	⋮	⋮	⋮	⋮	⋮	⋮	⋮		⋮
interface(L)	Species (1)	v_{11}	v_{12}	⋯	v_{1M}	0	0	⋯	A_1/A_0
	Species (2)	v_{21}	v_{22}	⋯	v_{2M}	0	0	⋯	A_2/A_0
	⋮	⋮	⋮	⋱	⋮	⋮	⋮		⋮
	Species (N)	v_{N1}	v_{N2}	⋯	v_{NM}	0	0	⋯	A_N/A_0
bulk(2)				⋯				⋯	
	Species (1)	v_{11}	v_{12}		v_{1M}	0	0		0
	Species (2)	v_{21}	v_{22}	⋯	v_{2M}	0	0	⋯	0
	⋮	⋮	⋮	⋱	⋮	⋮	⋮		⋮
	Species (N)	v_{N1}	v_{N2}	⋯	v_{NM}	0	0	⋯	0

Figure 57. Stoichiometric conservation matrix description of a layered interface model between two bulk phases. A new area component has been defined for each interfacial layer. The non-zero matrix elements (A_i/A_0) for interfacial constituents are derived from their molar surface areas (Ai), A_0 being a normalization constant.

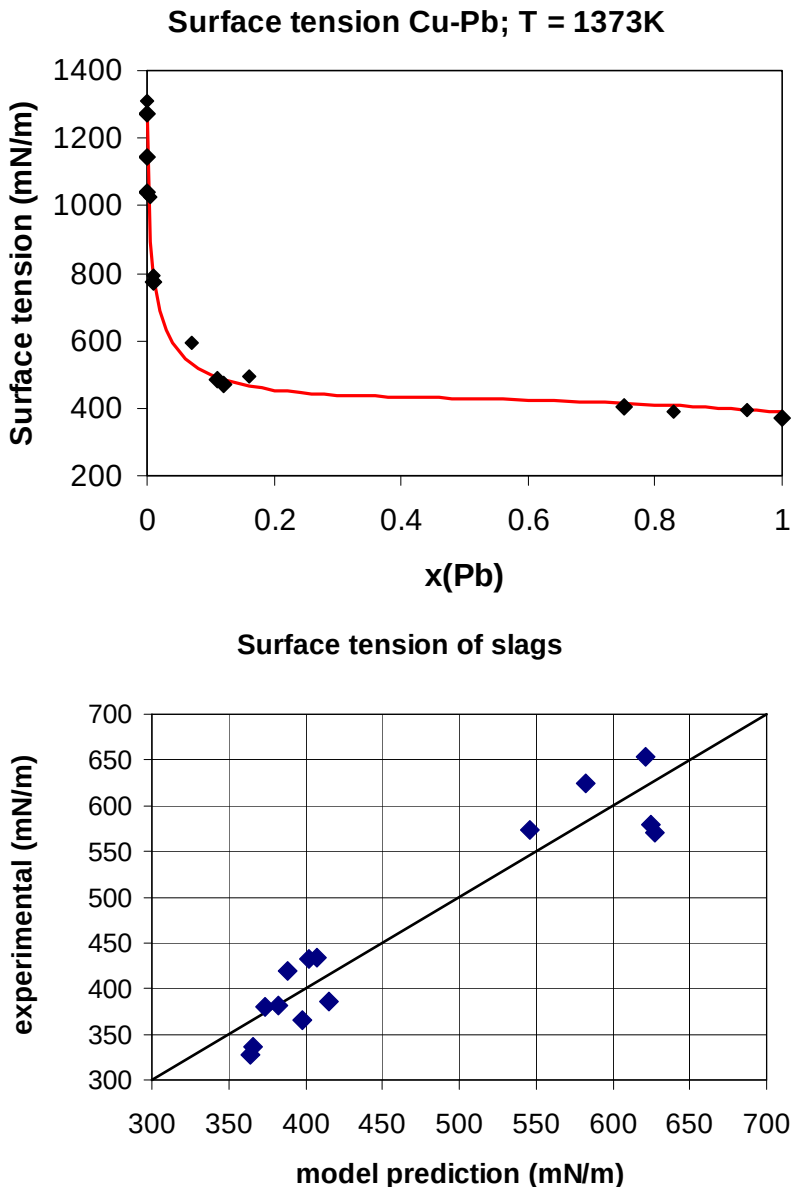

Figure 58. Surface tension of Cu-Pb alloy. Model curve and experimental data points (left); A comparison of experimental and modelled surface tensions of various molten slags [4] (right).

Likewise, the method can be used to estimate adsorption of surface active substances on a liquid surface.

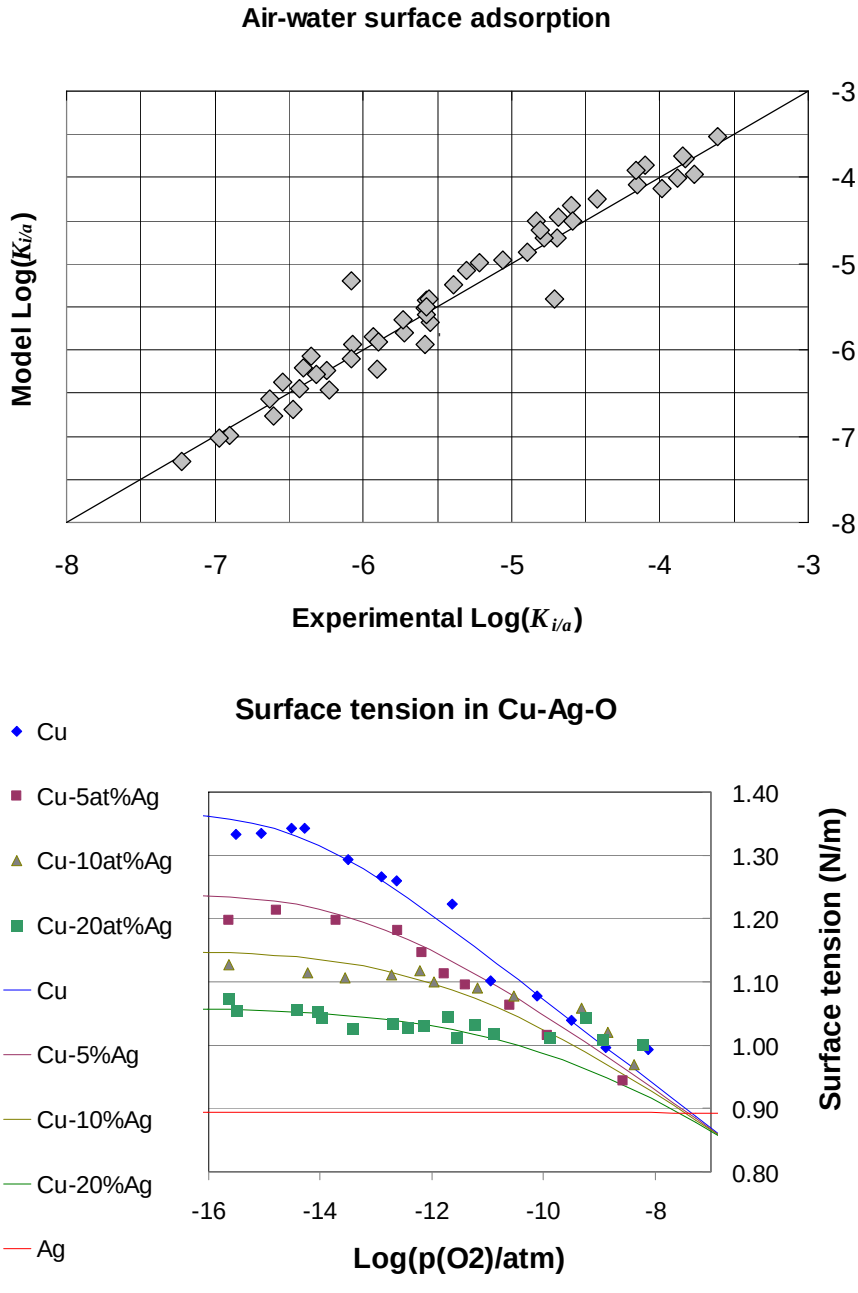

Figure 59. A comparison of experimental and modelled aqueous-air surface adsorption coefficients for 51 organic substances [3] (left); The effect of adsorbing oxygen on the surface tension of Cu-Ag alloys. Model curves and experimental measurements (right).

The constrained free energy method has also been promisingly applied for calculation of interfacial energies in a limited number of liquid-liquid mixtures.

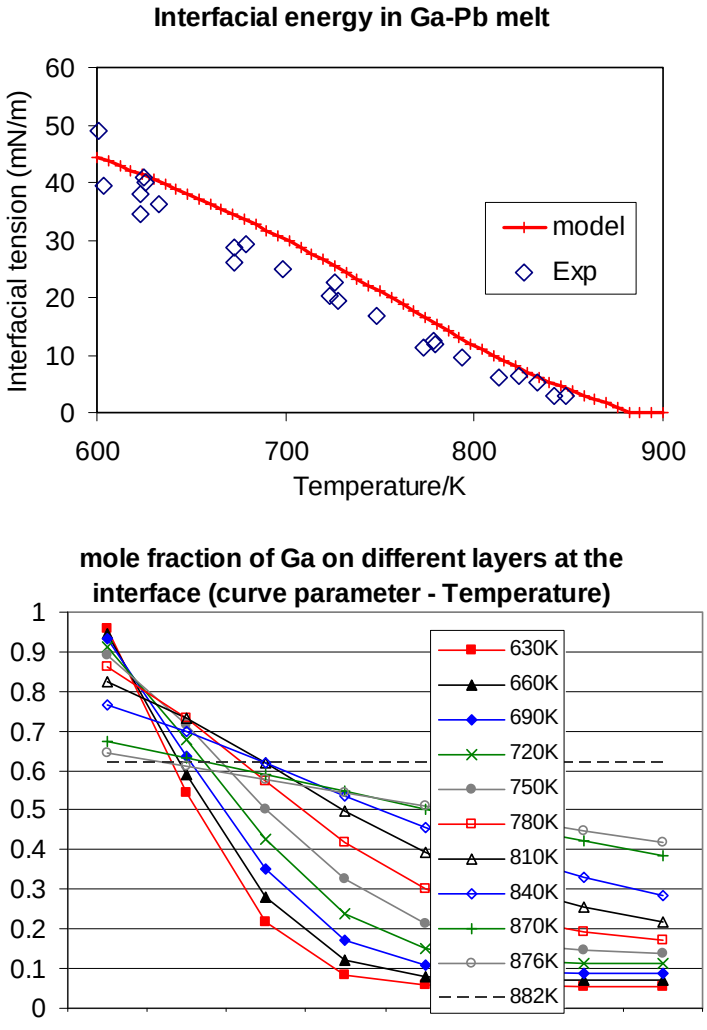

Figure 60. Interfacial energy (calculated results and experimental values) in a immiscible Ga-Pb melt (left). Model predictions of the interfacial layer composition (right).

Composition dependent surface energy affects also the melting point of alloy nanoparticles. This effect is due to the increasing proportion of surface energy on the Gibbs free energy of particulates with declining size. Consequently and as shown in figure 61 phase diagrams for such particles can be drawn and melting temperatures predicted based on the model [5].

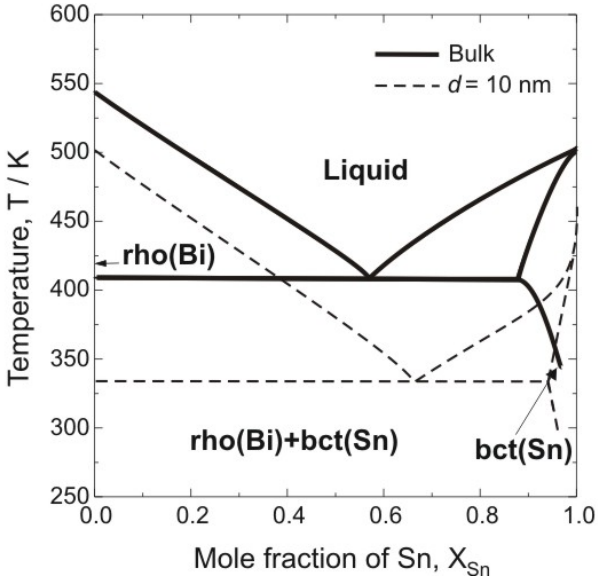

Figure 61. Phase diagram calculated for bulk and 5 nm nanoparticle for Bi-Sn alloy. Eutectic temperature would be expected to be lowered by about 40 degrees and shift towards higher Sn content, in general agreement with experimental results [5].

13.3 Conclusions

The constrained free energy method combined with mono- and multilayer models can be used to calculate surface energies and surface adsorption as a function of composition or bulk thermodynamic properties. The current application areas are mostly related to metallurgy, while potential application areas span a much wider range of systems.

13.4 References

[1] Pajarre, R., Koukkari, P., Tanaka, T. and Lee, J. Computing surface tensions of binary and ternary alloy systems with the Gibbsian method. CALPHAD: Comput. Coupl. Phase Diag. Thermochem. 30 (2006), p. 196.

[2] Koukkari, P. and Pajarre, R. Calculation of constrained equilibria by Gibbs energy minimization. CALPHAD: Comput. Coupling Phase Diagrams Thermochem. 30 (2006) 18.

[3] Pajarre, R. and Koukkari, P. Thermodynamics of adsorption at the aqueous-air interface. J. Colloid Interface Sci., accepted for publication, 2009.

[4] Heikkinen, E., Riipi, J., Fabritius, T., Pajarre, R. and Koukkari, P. Computational Modelling of Oxides' Surface Tensions in Secondary Metallurgy and Continuous Casting. VIII International Conference on Molten Slags, Fluxes and Salts – MOLTEN 2009, Santiago, Chile.

[5] Lee, J., Lee, J., Tanaka, T., Mori, H. and Penttilä, K. Phase Diagrams of Nanometer-sized Particles in Binary Systems. JOM, Vol. 57, No. 3 (2005), p. 56.

14. STEAMAX – Expert system for superheater design

Sonja Enestam, Metso Power
Pertti Koukkari, VTT

Increasing use of biomass and waste mixes as fuels in boiler combustion creates new opportunities for clean energy industries. Yet, the wide variety of fuel chemistry with numerous corrosive agents brings also new challenges in boiler design. Metso Power's novel expert system, based on ChemSheet, overcomes these difficulties and gives a fair competitive edge and economic reward to its developers.

14.1 Background

Environmental and climate concerns, as well as increasing economical pressures on the fossil fuel resources have in recent years increased the interest in the use of biomass and waste derived fuels for power production. Biomass and waste derived fuel can be attractive fuels for power production due to one or more of the following reasons:

- tightening landfill legislation
- green electricity benefits
- local availability
- low price of certain waste fractions.

Typical biomass and recovered fuels used in Europe today are forest residue, bark, demolition wood, municipal solid waste, industrial waste, agricultural residues and sludge.

Some of the biomass and waste fuel fractions can be burned as such, but very often mixtures of several fuel fractions are used. Fluidized bed combustion is a commonly used technique due to its flexibility and low emission levels. Co-combustion is a way of enabling the use of fuel fractions that are too difficult to burn on their own.

The demand for higher efficiency and reduced emissions, combined with the varying composition and quality of biomass and waste fuels, is however a big challenge. Biomass and waste fuels often contain high amounts of alkali metals and chlorine, often in combination with sulfur. The presence of these elements increases the risk for operational problems such as corrosion, fouling and bed sintering.

When designing and operating boilers for biomass and waste derived fuels thorough knowledge about the fuel composition and the behaviour of the fuel in the combustion process is needed. Also the interaction of different fuels in co-combustion is essential. As difficult fuel fractions are often cheap, the generation of a suitable fuel mixture is highly interesting from the point of view of process economy.

The wide variety of fuels and fuel mixtures burned today requires tools for optimization of combustion parameters, boiler design and superheater materials. For such needs, the STEAMAX expert system was developed by Metso Power [1]. The system is based on advanced multi-phase multi-component equilibrium calculations and uses the fuel composition as input. The system enables the optimization of steam parameters, prediction of corrosivity and selection of superheater materials in biomass fuel and waste combustion The STEAMAX tool has been verified with a large number of existing boilers and successfully used in the design of several new boilers and boiler re-builds.

14.2 The multi-phase chemistry method

The input for the calculation is given as the chemical analysis of the fuel or fuel mixture. The multi-component equilibrium calculation (figure 62) is performed in order to obtain the equilibrium composition of the combustion mixture, consisting of the flue gas, solid fly ash and molten ash, as a function of temperature and location in the boiler. The software used is a tailor made calculation routine based on VTT's thermochemical program ChemSheet [1, 2], which uses thermodynamic data from FACT [3]. The input data of STEAMAX concurrently includes 16 elements (C, H, N, O, S, Cl, Ca, Mg, Na, K, Al, Si, Fe,

P, Pb, Zn), the gas phase, 2 liquid solutions, 2 solid solutions, 12 pure liquid compounds and 269 pure solid compounds [4].

The ChemSheet calculation results with the expected equilibrium composition of the combustion mixture at a given temperature and pressure, which are representative to the boiler conditions. The equilibrium composition of the flue gas is calculated respectively. Thence, the model allows for determining the fraction of melt (molten slag) in the ash as function of temperature, as well as the chemical composition of the flue gas, including its minor constituents, which contain the potentially corrosive chlorine and sulphur compounds. The attached figure shows the amount of melt in the ash in a mixture of 50 e-% (% on energy base) stem wood and 50 e-% RDF as a function of temperature.

		Bark (Spruce)	Stem Wood Chips (Northern pine and spruce)	RDF
HHV, dry	*MJ/kg*	19,80	20,2	20,09
HHV, wet	*MJ/kg*	8,71	9,90	13,02
moisture	*wt-%*	56,0	51	35,2
volatiles	*wt-% (d.s.)*	75,0	n.a.	76,0
ash (815C)	*wt-% (d.s.)*	3,2	0,28	16,1
C	*wt-% (d.s.)*	49,1	50,1	44,3
H	*wt-% (d.s.)*	5,7	6,1	6,2
S	*wt-% (d.s.)*	0,03	0,01	0,28
O (diff.)	*wt-% (d.s.)*	41,7	43,4	31,2
N	*wt-% (d.s.)*	0,33	0,15	1,00
Cl	*wt-% (d.s.)*	0,02	0,01	0,89
Al	*g/kg (d.s.)*	1,35	0,01	10,00
Si	*g/kg (d.s.)*	2,98	0,01	31,10
Ti	*g/kg (d.s.)*	0,00	0,00	1,40
Na	*g/kg (d.s.)*	0,44	0,00	6,20
Mg	*g/kg (d.s.)*	0,60	0,22	4,40
K	*g/kg (d.s.)*	1,00	0,14	4,50
Ca	*g/kg (d.s.)*	8,26	0,75	19,60
Fe	*g/kg (d.s.)*	0,18	0,02	4,60
P	*g/kg (d.s.)*	0,13	0,04	1,10
Mn	*g/kg (d.s.)*	0,00	0,13	0,20
Pb	*mg/kg (d.s.)*	n.a.	n.a.	260,00
Zn	*mg/kg (d.s.)*	n.a.	n.a.	585,00

n.a. = not analysed

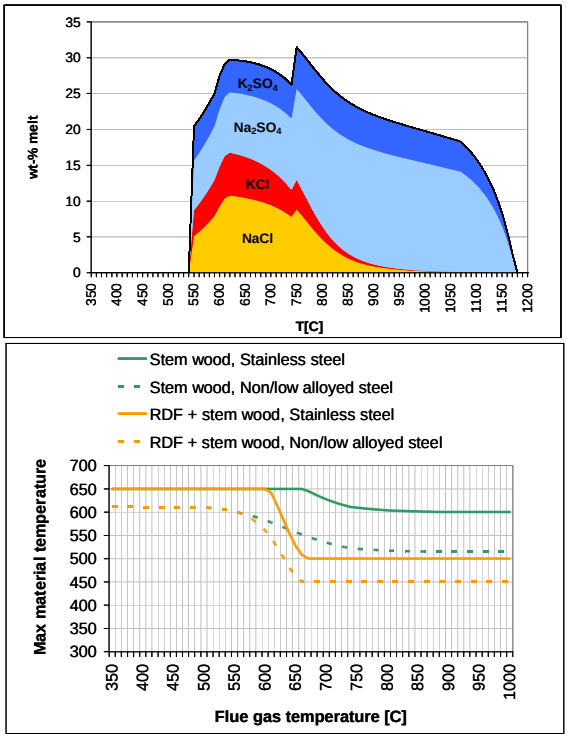

Figure 62. First melting point curves from the thermodynamic model and respective maximum allowed material temperatures as deduced from the fuel corrosivity index.

14.3 Model results: Index for corrosivity

The corrosivity of the fuel is related to the chlorine and sulfur content of the fuel and to the composition of the ash, particularly to its amount of potassium and sodium. Thus, a function related to the fraction of alkali chlorides formed during combustion could be developed to be used as a measure of fuel corrosivity. The index is estimated at different temperatures and locations in the boiler. Additionally, the risk of molten phase corrosion can be evaluated by calculating the melting curve for the fuel ash. The first melting point of the ash (T_0) is considered a threshold temperature for the onset of severe molten phase corrosion, and hence the material temperature of the superheaters must in all cases be kept below T_0. The calculation of the melting curve is performed with STEAMAX equilibrium data. The T_0 and relative corrosivity models as calculated for various fuel mixtures with their compositions are shown in the attached figure. For this fuel mixture T_0 and hence the maximum allowed material temperature is 540 °C. The melt consists of alkaline chlorides and sulphates. In the lower figure, calculated maximum material temperatures as a function of flue gas temperature for stainless steel (full lines) and non /low alloyed steel (dotted lines) for two fuel mixtures are shown for stem wood (green curves) and mixture of 50 e-% stem wood and 50 e-% RDF (yellow curves).

14.4 The use of STEAMAX

STEAMAX is today used at Metso Power as a tool in the design of new boilers for biomass fuel and waste combustion. When the fuel or fuel mixture to be burned in the boiler is known, STEAMAX is used for determining the maximum steam temperature and for selection of superheater materials and superheater locations. If, on the other hand, the required steam temperature is set, STEAMAX can be used to find the optimum fuel mixture for the boiler, e.g. to find the maximum allowed fraction of a high chlorine waste fraction.

STEAMAX is also a useful tool when the boiler operator wants to take into use new fuel fractions. Based on the fuel analysis estimations of the corrosivity can be made and suitable fuel mixtures can be chosen, without costly trials and errors. In the case of rebuilds, e.g. conversions of coal fired boilers to biomass fuel boilers, the corrosivity of the new fuel is often completely different from the old fuel. In such cases STEAMAX has been used to predict the corrosivity of the

new biomass fuel and to evaluate whether the old superheaters will work as such or whether changes have to be made in materials or operating temperatures.

STEAMAX has been verified with long term experience from a large number of full scale biomass, and waste boilers, such as that of Kymin Voima Oy in Kuusankoski (figure 63) and proven good reliability. The thermodynamic method offers a design platform, which is completely reproducible and verifiable. Its intermittent results combined with process monitoring provide a data-base, enabling the assessment of design parameters against verified experience.

14.5 Conclusions

The global equilibrium calculation together with empirical data thus provides a basis for an industrial expert system, which supports both design and operation of boiler superheaters. It also creates a viable method for a safe choice between stainless and low-alloyed steel in boiler design. As a typical superheater pack is constructed of ca 500 tonnes of steel, it is obvious that significant earnings can be won in reducing the consumption of up-scale construction material.

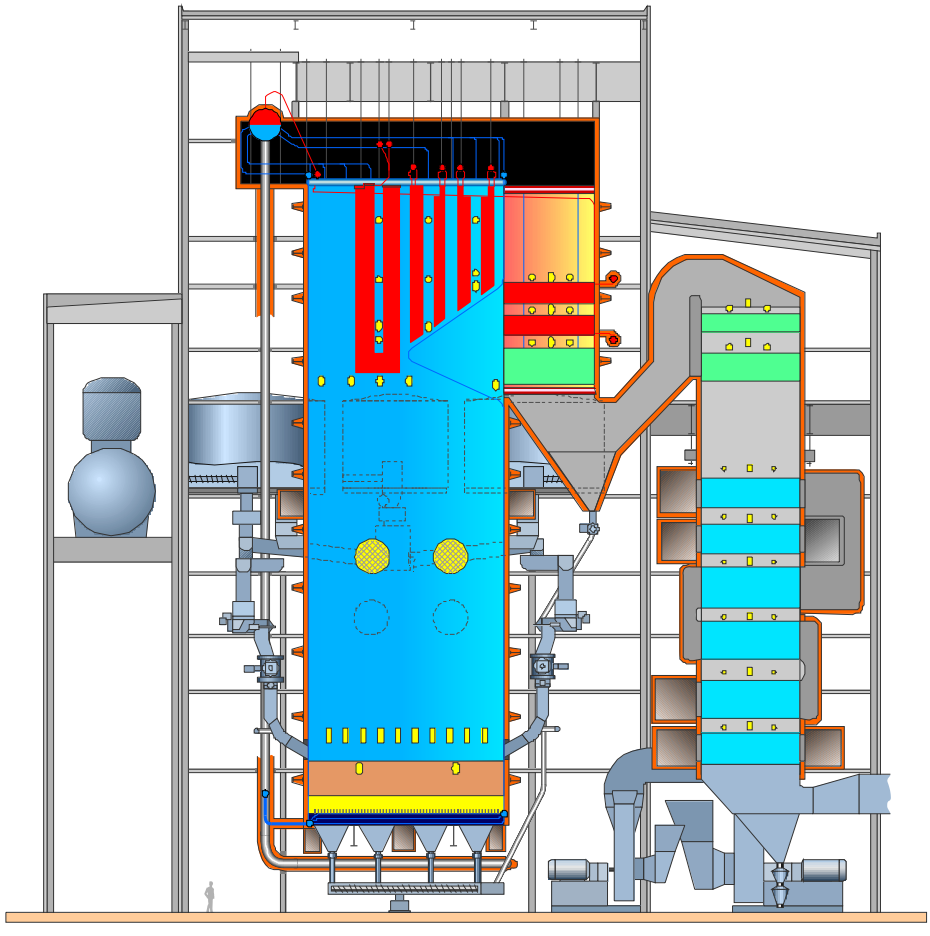

Figure 63. A schematic view of a fluidized bubbling bed boiler. (Kymin Voima Oy, Kuusankoski, Finland).

14.6 References

[1] http://www/chemsheet.com/.

[2] Koukkari, P., Penttilä, K., Hack, K. and Petersen, S. In: Brechet, Y. (ed.). Microstructures, Mechanical Properties and Processes, Euromat 99 – Vol. 3, Wiley-VCH Publishers, Weinheim, 2000. P. 323.

[3] Enestam, S., Niemi, J. and Mäkelä, K. The Clearwater Coal Conference, Clearwater, Florida, June 2008.

[4] Bale, C. W., Pelton, A. D., Thompson, W. T. “FACT-database”. CRCT École Polytechnique de Montréal, Quebec, Canada.

15. Modeling biochemical systems with constrained Gibbs energy minimization

Peter Blomberg, VTT

Rising costs of fossil resources and products based thereupon has launched a large-scale interest in processing green biomass into raw materials for the chemical industry. Environmental awareness and concern for the global community spur researchers towards seeking thermally efficient and minimally wasteful processes. Current and future biorefinery concepts will use microorganisms to convert lignocellulosic feeds into valuable platform chemicals. However, very few natural organisms produce the desired intermediates in suitable amounts for industrial scale production. The biochemical systems in metabolic engineering are rich in different types of chemical species, modestly reactive, and contain many distinct compartments. A novel method based on multicomponent multiphase Gibbs energy minimization with kinetic constraints and pertinent Legendre transforms has been developed to support thermodynamic modeling of biochemical systems.

15.1 Background

The potential of biosynthesis to produce value-added chemicals as intermediates for industrial biomaterials, commodities, and pharmaceuticals is generally regarded as promising. The number of such products, however, is small compared to the extensive domain of chemical compounds found in enzymatic systems. With the vast scope of optional pathways, computational research offers a means to select the most prospective reaction routes. The wide variety of chemicals makes purely reaction kinetic studies elaborate, as a great number of measured reaction rates would always be necessary [1]. Their significance as

predictive tools is thus less attractive. Instead, thermodynamic feasibility analysis based of the Gibbs free energy data has been proposed [2, 3].

If classical thermodynamics were applicable to biochemical pathways, all metabolites would spontaneously turn into carbon dioxide and water at a rate limited by oxygen uptake. We can tell from experience that oxygen reacts modestly with a large number of organic molecules due to high activation energies. This observation is not limited to oxygen; it is the hallmark of biochemical pathways to be very modestly reactive systems.

Local concentrations and from these deduced partial equilibria will have a significant role in the advancement of biochemical reactions. Despite large negative Gibbs energy of reaction, it is known that some enzyme-catalyzed reactions do not occur without sufficient concentrations of their respective substrates. Active enzymes locally deplete their supply of substrate if the distance between enzymes is larger than the average diffusion length. Effective substrate concentrations will thus depend on the flux through the pathway.

The reactions are subdued to both thermodynamic and kinetic constraints. Constrained Gibbs energy minimization [4] pursues to embrace both restrictions. Applications range from conceptual investigation of physical phenomena like ion partitioning inside a nanopore in a cell membrane to pathway analysis in relation to industrial bioconversion of lignocellulosic material.

15.2 Methods

Modern applications frequently include time constants of reaction that are comparable to the time constant accepted in the definition of equilibrium, which necessitates the inclusion of specific reactions into the description of the internal constraints of the system. Entity conservation in chemically reactive systems is found as either mass balance **Am** = **b** or flux balance **Sv** = **0**. These matrices are not only linked to each other by being each others left/right null spaces **AS** = **0**, but are special subsets of the generalized conservation matrix **C**.

The following mathematical program describes a typical constrained optimization formalism of a multiphase thermodynamic model. The objective function is the Gibbs energy of the system and includes the excess Gibbs energies of all phases (1). The molar amounts of conserved entities are stored in vector **d**. Vector **n** contains the molar amounts of each constituent in the system.

$$\min G \quad \text{s.t.} \quad \mathbf{Cn} = \mathbf{d} \quad , \quad \mathbf{n} \in \Re_+^N \quad \Rightarrow \quad \mathbf{g} \geq \mathbf{C}^{\mathrm{T}} \boldsymbol{\pi} \tag{1}$$

As an inherent thermodynamic property, the molar Gibbs energies of the constituents (**g**) are linear combinations of the component energy contributions (**π**). If a constituent is not in the equilibrium composition, its molar Gibbs energy is higher. This knowledge can be used to implement material reservoirs, dynamic Legendre transforms, and even group contribution estimation if need be [5].

All components used in the conservation matrix can be associated with structural, physical, chemical, and energetic attributes. Additional components, which constitute new rows in the conservation matrix, can be used to implement Donnan partitioning among other things. Time-dependent constraints usually involve the addition of one or more columns, which can be used to implement desired reaction kinetics [5] or metabolic networks.

The mass balance matrix of the pentose phosphate pathway in figure 64 was created with a new procedure that is guarantied to produce a mass balance matrix with only positive elements from any reaction network, including ones with cyclic and reversible reactions. This systematic method is a good tool for adding proper reaction constraints to any chemical system because constrained optimization is more stable if all elements are positive regardless of the numerical method in use.

	G6P	6PGL	6PGn	Ru5P	R5P	Xu5P	S7P	GAP	F6P	E4P	NADPH	$NADP^+$	H2O	CO2	R1	R2	R3	R4	R5	R6	R7	R8
v1		1	1											1	1							
v2			1											1		1						
v3														1			1					
v4					1			1		1								1				
v5						1	1		1										1			
v6								1		1										1		
v7									1	1											2	
v8	1	1	1	1	1	1	2		2													1
v9	1	1	1											1								
v10	1	1	1	1	1	1	1	1	1	1												
v11	1	1	1	1	1	1	2		2	1												
v12	2	1	1								1											
v13											1	1										
v14			1										1	1								

Figure 64. The labels and elements of a mass balance matrix for the pentose phosphate pathway demonstrate the use of a generalized approach to creating entity conservation matrices.

15.3 Kinetics

Equilibrium models on their own may not be sufficient to model transient systems. Similarly, there might not be enough parameters known for a purely kinetic model [1]. When mechanistic kinetics is incorporated into equilibrium models by the use of constrained Gibbs energies [6], the best of both worlds is combined. A maximum extent limitation can be set for a spontaneous chemical reaction by introducing a virtual component into the reaction. Here, R_1 and R_2 are virtual components set to limit the maximum forward extents of their respective reaction expressions (2).

$$\mathrm{Glu} + \mathrm{ATP} + \mathrm{R_1} \xrightarrow{k_1} \mathrm{G6P} + \mathrm{ADP} \quad , \quad \mathrm{ATP} + \mathrm{H_2O} + \mathrm{R_2} \xrightarrow{k_2} \mathrm{ADP} + \mathrm{Pi} \quad (2)$$

Figure 65 displays the conservation matrix augmented with two additional reaction constraints while figure 66 demonstrates results from the combination of reaction rates and thermodynamic equilibrium [5]. This sample system contains only one equilibrium reaction but could easily have contained hundreds. The equilibrium reaction is easily spotted by noticing the two identical columns denoting an isomerization reaction.

	Glu	H_2O	G6P	F6P	ATP	ADP	Pi	R1	R2
v1	1							-1	
v2		1							-1
v3	1		1	1					
v4					1	1			
v5	1	1				1			
v6		1					1		

Figure 65. The figure displays a conservation matrix augmented with two additional reaction constraints used to calculate the curves in figure 66. The rows denote the conservation of virtual components, most of which are linear combinations of atoms.

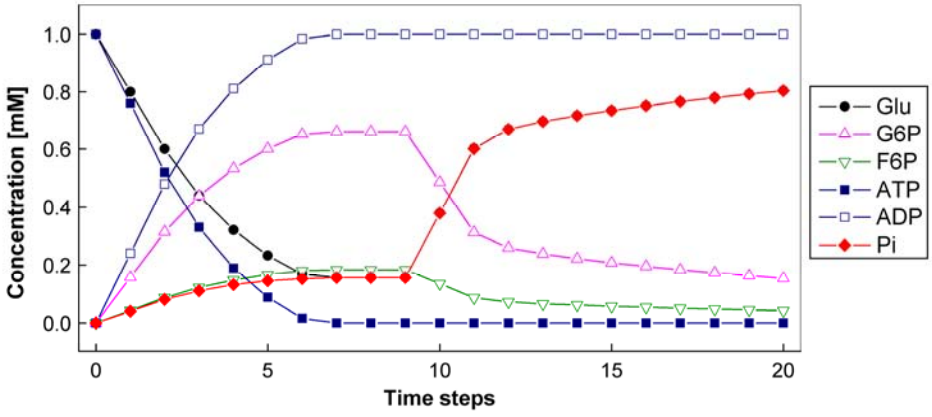

Figure 66. The figure depicts the composition in response to competing kinetics. A kinetic equilibrium is reached in the first eight time steps. Then the rate constant for ATP hydrolysis is amplified, which results in a burst phase and a subsequent steady state. These effects would not have been seen without constrained equilibrium.

15.4 Reaction networks

Bulk thermodynamics is characterized by having negative Gibbs energy changes for reactions in their forward direction. Therefore, the net flux through a reaction is always in the direction of lower Gibbs energy. If bulk thermodynamics i.e. compartment-wide average concentrations were applicable, all reactions in a biochemical pathway would have negative Gibbs energy changes. The above basic principle indicates that bulk thermodynamics is not sufficient for the analysis of enzyme-catalyzed reaction pathways. The result would falsely have been that glycolysis would not operate under the given conditions. Clearly, some other method of analysis is needed.

The idea of an energy diagram is to visualize the cumulative Gibbs energy change of reactions in a pathway similar to the Gibbs energy of a reactive system. The evolution in time is replaced by the evolution in nodes of the reaction network. Transformed Gibbs energies [7] can be combined with reaction kinetics enabled Gibbs energy minimization [6] to create energy diagrams similar in appearance to the cumulative reaction energies presented in [8]. The same information can alternatively be visualized by a histogram of reaction energy changes [9].

Cumulative reaction energies for standard state values have been published before. This method inadvertently assumes that every reaction goes to completion

while following a set of molecules moving from one node to the next. These curves are equivalent to the assumptions in bulk thermodynamics and they are marked with the word stepwise in figure 4. In the novel method, node specific energies are generated with the Constrained Gibbs Energy method by minimizing the energy of the local enzymatic system.

The stepwise cumulative reaction energies generally come in two flavors due to historical origins. One for values evaluated at 1 M and one for 1 mM standard state reference concentrations. The third curve represents what can be calculated based on measured concentrations. The graph uses physiological concentrations published in [10], which were obtained by kemostat cultivations. These calculations show that the standard state Gibbs energy change of a reaction is not the sole determining factor when pathway bottlenecks are sought. A larger positive energy change may be less restrictive if the mixing term is favorable as for the fourth reaction in figure 67. Reference [11] contains a more detailed analysis of this set of curves. The black curve accounts for local conditions, while the other assumes stepwise ideal behavior.

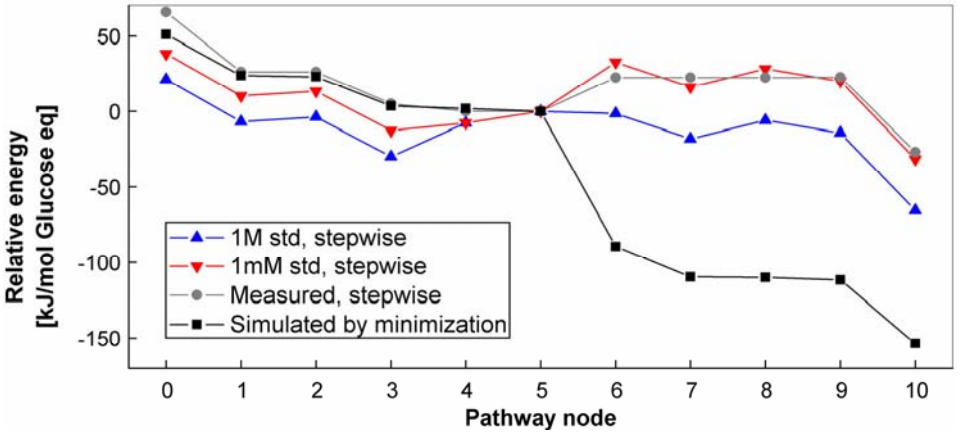

Figure 67. This figure contains energy diagrams of the ten reactions of glycolysis. The energy curves are aligned vertically at node 5, which serves as a convenient reference node. The first two curves show cumulative reaction energies for two standard states, while the third uses measured concentrations from Kümmel et al. [10]. The fourth curve represents the evolution of the local system as calculated by the novel method.

Knowing the composition makes it possible to predict which metabolites to look for in single knockout studies where a specific enzyme is missing since the last intermediate before the missing reaction might not be prevalent. It may also aid

in derivation of rate constants by mapping experimental measurements with computational quantities. Figure 68 shows the system composition at each node for the black curve in figure 4.

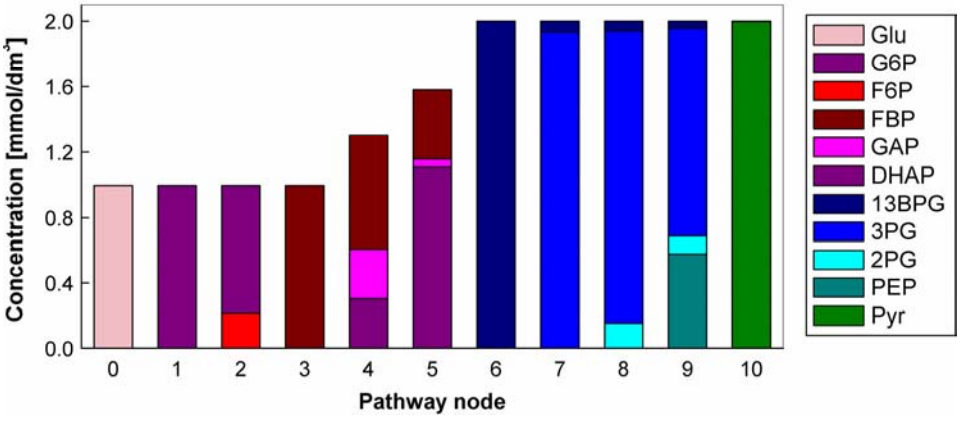

Figure 68. The figure shows the composition of the local system at each node in glycolysis at pH 6.5 and 0.2 M ionic strength. Nodes were calculated by assuming equilibrium of the first N reactions in the pathway. The black curve in figure 4 corresponds to these compositions.

15.5 Conclusions

Constrained Gibbs Energies offer a viable approach to model biochemical processes that involve enzyme catalysis, kinetically controlled reactions, and pH-buffered systems without sacrificing thermodynamic consistency.

Pathway energy diagrams are sequences of transformed Gibbs energies for subsystems evaluated at different nodes in the pathway. An energy diagram shows a monotonic non-increasing local Gibbs energy curve for feasible pathways. They can be used to choose pleasing pathways in metabolic engineering, or to find control points in metabolic control analysis.

A new computational approach for the analysis of biochemical pathways is proposed to help reach metabolic engineering goals. The novel method uses modern thermodynamics based on Gibbs energy minimization with entity constraints for assessing the thermodynamic feasibility of the flux-participating portion of the chemical composition.

15.6 References

[1] Teusink, B., Passarge, J., Reijenga, C. A., Esgalhado, E., Weijden, van der C. C., Schepper, M., Walsh, M. C., Bakker, B. M., Dam, K. van, Westerhoff, H. V. and Snoep, J. L. Can yeast glycolysis be understood in terms of in vitro kinetics of the constituent enzymes? Testing biochemistry, European Journal of Biochemistry 267, (2000), pp. 5313–5329.

[2] Li, C., Henry, C. S., Jankowski, M. D., Ionita, J. A., Hatzimanikatis, V. and Broadbelt, L. J. Computational discovery of biochemical routes to specialty chemicals. Chemical Engineering Science 59, (2004), pp. 5051–5060.

[3] Feist, A. M., Henry, C. S., Reed, J. L., Krummenacker, M., Joyce, A. R., Karp, P. D., Broadbelt, L. J., Hatzimanikatis, V. and Palsson, B. Ø. A genome-scale metabolic reconstruction for Escherichia coli K-12 MG1655 that accounts for 1260 ORFs and thermodynamic information, Molecular Systems Biology 3, (2007), Article number 121.

[4] Koukkari, P. and Pajarre, R. Calculation of constrained equilibria by Gibbs energy minimization. CALPHAD 30, (2006), pp. 18–26.

[5] Blomberg, P. B. A. and Koukkari, P. S. The combination of transformed and constrained Gibbs energies. Mathematical Biosciences 220, (2009), pp. 81–88.

[6] Koukkari, P. and Pajarre, R. Introducing mechanistic kinetics to the Lagrangian Gibbs energy calculation. Computers and Chemical Engineering 30, (2006), pp. 1189–1196.

[7] Recommendations for Nomenclature and Tables in Biochemical Thermodynamics (IUPAC Recommendations 1994). Prepared for publication by R. A. Alberty, Pure & Appl. Chem. 66 (8), (1994), pp. 1641–1666.

[8] Hatzimanikatis, V., Li, C., Ionita, J. A., Henry, C. S., Jankowski, M. D. and Broadbelt, L. J. Exploring the diversity of complex metabolic networks, Bioinformatics 21, (2005), pp. 1603–1609.

[9] Maskow, T. and Stockar, U. von How Reliable are Thermodynamic Feasibility Statements of Biochemical Pathways? Biotechnology and Bioengineering 92(2), (2005), pp. 223–230.

[10] Kümmel, A., Panke, S. and Heinemann, M. Putative regulatory sites unraveled by network-embedded thermodynamic analysis of metabolome data. Molecular Systems Biology 1 (2006), Article number 2006.0034.

[11] Blomberg, P. B. A. and Koukkari, P. S. Thermochemical Analysis of Reaction Pathways, Extended poster abstract for the 19th European Symposium on Computer Aided Process Engineering – ESCAPE19, Cracow, Poland 14–17 June 2009.

16. ChemSheet contact information

Germany:
GTT-Technologies
Kaiserststrasse 100
D-52134 Herzogenrath
Germany
info@gtt-technologies.de, www.gtt-technologies.de

Finland:
VTT Process Chemistry
Biologinkuja 7, Espoo, P. O. Box 1000
FI-02044 VTT Finland
www.vtt.fi, www.chemsheet.com

Japan:
RCCM
Research Center of Computational Mechanics, Inc.
7-1, Togoshi 1-chome
Shinagawa-ku, Tokyo
142-0041 Japan
nagano@rccm.co.jp, www.rccm.co.jp

USA:
Spencer Group International
P. O. Box 393
Trumansburg, New York 14886 USA
info@spencergroupintl.com, www.spencergroupintl.com

Series title, number and
report code of publication

VTT Research Notes 2506
VTT-TIED-2506

Author(s)
Pertti Koukkari (ed.)

Title

Advanced Gibbs Energy Methods for Functional Materials and Processes
ChemSheet 1999–2009

Abstract

ChemSheet is a thermochemical simulation tool, which combines the flexibility and practicality of spreadsheet operations with rigorous, multi-phase thermodynamic calculations. Customised applications are defined as independent worksheets in Excel® and simulations are run directly from the spreadsheet, taking advantage of its functional aspects and graphical features. A user-friendly dialog is available for model build-up.

ChemSheet was invented and published by VTT. It was commercialized in a joint venture with GTT Technologies GmbH of Herzogenrath, Germany. During the last decade, ChemSheet and its sister products have been adopted by both industrial users and active scientists worldwide. Due to the generic modelling principles based on Gibbs free energy minimization, the applications range from high temperature systems to biochemical analysis, including materials chemistry, corrosion, industrial reactor scale-up and process simulation. Practical models and expert systems have been developed e.g. in the chemical industry, pulp and paper, cement and lime manufacturing, metallurgy, steelmaking, power production and environmental technologies.

Within ChemSheet, the new Constrained Free Energy method allows immaterial constraints in the conservation matrix of the minimization problem, thereby enabling the association of constraint matrix properties with structural, physical, chemical or energetic attributes. Thus, the scope of free energy calculations can be extended well beyond the conventional studies of global chemical equilibria and phase diagrams. The most notable applications include surface and interfacial energies, electrochemical Donnan equilibria, calculation of paraequilibria and the introduction of mechanistic reaction kinetics to Gibbs'ian multiphase analysis. In biochemistry, the new method can be applied for efficient generation of energy diagrams for industrial production pathways within micro-organisms.

ISBN
978-951-38-7330-1 (soft back ed.)
978-951-38-7331-8 (URL: http://www.vtt.fi/publications/index.jsp)

Series title and ISSN
VTT Tiedotteita – Research Notes
1235-0605 (soft back ed.)
1455-0865 (URL: http://www.vtt.fi/publications/index.jsp)

Project number
26639

Date
November 2009

Language
English

Pages
146 p.

Name of project
DATAPOOL

Commissioned by
VTT

Keywords
Constrained Gibbs energy minimization, multi-phase systems, process simulation, reactor design, reaction rates, materials chemistry, fibre suspensions, surface energy, paraequilibrium, pathway energy diagrams

Publisher
VTT Technical Research Centre of Finland
P. O. Box 1000, FI-02044 VTT, Finland
Phone internat. +358 20 722 4520
Fax +358 20 722 4374

VTT Tiedotteita – Research Notes

2454 Toni Ahlqvist, Asta Bäck, Minna Halonen & Sirkka Heinonen. Social media roadmaps. Exploring the futures triggered by social media. 2008. 78 p. + app. 1 p.

2464 Antti Poteri. Solute transport and retention in fracture rock. 2009. 141. p.

2465 Krzysztof Klobut, Teemu Vesanen, Marja-Leena Pykälä, Kari Sipilä, Jari Kiviaho & Rolf Rosenberg. Handbook of SOFC system in buildings. Legislation, standards and requirements. 2009. 79 p.

2466 SAFIR2010. The Finnish Research Programme on Nuclear Power Plant Safety 2007–2010. Interim Report. Eija Karita Puska (Ed.). 2009. 535 p.

2470 Göran Koreneff, Maija Ruska, Juha Kiviluoma, Jari Shemeikka, Bettina Lemström, Raili Alanen & Tiina Koljonen. Future development trends in electricity demand. 2009. 79 p.

2472 Pertti Lahdenperä. Project alliance. The competitive single target-cost approach. 2009. 88 p.

2480 Sami Nousiainen, Jorma Kilpi, Paula Silvonen & Mikko Hiirsalmi. Anomaly detection from server log data. A case study. 2009. 39 p. + app. 1 p.

2482 Sampo Soimakallio, Riina Antikainen & Rabbe Thun (Eds.). Assessing the sustainability of liquid biofuels from evolving technologies. A Finnish approach. 2009. 220 p. + app. 41 p.

2486 Helena Järnström, Sirje Vares & Miimu Airaksinen. Semi volatile organic compounds and flame retardants. Occurence in indoor environments and risk assessment for indoor exposure. 2009. 58 p. + app. 8 p.

2491 Kirsi Aaltonen, Mervi Murtonen & Sampo Tukiainen. Three perspectives to global projects. Managing risks in multicultural project networks. 2009. 47 p. + app. 4 p.

2492 Tuomo Tuikka & Minna Isomursu (eds.). Touch the Future with a Smart Touch. 2009. 280 p.

2493 Hannele Holttinen, Peter Meibom, Antje Orths et al. Design and operation of power systems with large amounts of wind power. Final report, IEA WIND Task 25, Phase one 2006–2008. 2009. 200 p. + app. 29 p.

2496 Mona Arnold. Reduction and monitoring of biogas trace compounds. 2009. 75 p. + app. 5 p.

2497 Tuula Hakkarainen, Jukka Hietaniemi, Simo Hostikka, Teemu Karhula, Terhi Kling, Johan Mangs, Esko Mikkola & Tuuli Oksanen. Survivability for ships in case of fire. Final report of SURSHIP-FIRE project. 2009. 120 p. + app. 7 p.

2500 Esa Sipilä, Jürgen Vehlow, Pasi Vainikka, Carl Wilén & Kai Sipilä. 2009. Market potential of high efficiency CHP and waste based ethanol in Europan pulp and paper industry. 2009. 73 p.

2506 Pertti Koukkari (ed.). Advanced Gibbs Energy Methods for Functional Materials and Processes – ChemSheet 1999–2009. 2009. 145 p.

ISBN 978-951-38-7330-1 (nid.)
ISSN 1235-0605 (nid.)

ISBN 978-951-38-7331-8 (URL: http://www.vtt.fi/publications/index.jsp)
ISSN 1455-0873 (URL: http://www.vtt.fi/publications/index.jsp)